RADIOLOGY AND ONCOLOGY

1994
Vol. 28 No. 3
Ljubljana

ISSN 1318-2099
UDC 616-006

Ciprinol®

ciprofloxacin

***Antimicrobial spectrum**: gram-negative aerobes: E. coli, Citrobacter, Enterobacter, Klebsiella, Proteus, Salmonella, Shigella, Vibrio, Yersinia, Aeromonas, Pasteurella, Pseudomonas, Haemophilus, Neisseria, Acinetobacter, Campylobacter, Providencia, Serratia, Morganella, Legionella. Gram-positive aerobes: Staphylococci; variously susceptible are Streptococci. **Indications**: infections of the urinary tract, respiratory tract, ears, nose and throat, gastro-intestinal tract and abdomen, hepatobiliary tract, infections of the bones and joints and skin; gynecological infections and septicemia; treatment and prophylaxis of infections in immunocompromised patients. **Side effects**: gastrointestinal disturbances, dizziness, headache, fatigue, sensorial disorders, agitation, anxiety, rarely visual disturbances and convulsions; allergic reactions, decrease of blood pressure, paroxysmal tachycardia, pain in the joints, rarely photosensitivity, transient changes in some laboratory values. Risk of crystalluria with insufficient intake of liquid. **Interactions**: antacids with Al and Mg hydroxides, theophylline, barbiturate narcotics. **Note**: caution in elderly patients and CNS disorders, reduced reaction capacity (synergy with alcohol). **Contraindications**: hypersensitivity to quinolone chemotherapeutics, children in the age of growth, pregnancy and lactation. **Daily dosage**: infections of the lower respiratory tract (nosocomial) 2 x 500 to 750 mg orally, 2 x 200 to 400 mg iv; infections of the lower urinary tract 2 x 250 to 500 mg orally; uncomplicated infections of the upper urinary tract 2 x 250 to 500 mg orally, 2 x 100 to 200 mg iv; complicated infections of the upper urinary tract, bacteriemia, septicemia 2 x 500 to 750 mg orally, 2 x 200 to 400 mg iv; osteomyelitis 2 x 750 mg orally, 2 x 200 to 400 mg iv; other infections 2 x 500 to 750 mg orally, 2 x 200 to 400 mg iv; chronic salmonella carriers 4 x 250 mg orally; acute gonorrhea a single dose of 500 mg orally; in severe infections the oral dose can be increased to 3 x 750 mg, and intravenous dose to 3 x 400 mg daily; dose is reduced in elderly patients and in severe renal dysfunction. **Duration of therapy**: pyelonephritis at least 10 days, peritonitis (in combination with metronidazole) at least 14 days, osteomyelitis at least 6 weeks, other infections at least 3 days after disappearance of clinical signs. **Supply**: tablets: 250 mg 10 tabs; 500 mg 10 tabs; injection: 100 mg/10 ml 5 ampoules. All additional information can be obtained from the manufacturer.*

Suitable for the most severe hospital patients and also for out-patients

Systemic antimicrobial agent for both oral and parenteral use

Reaches high concentrations in body fluids, tissues and intracellular space.

KRKA
SLOVENIA

RADIOLOGY AND ONCOLOGY

Established in 1964 as ***Radiologia Iugoslavica*** *in Ljubljana, Slovenia.* ***Radiology and Oncology*** *is a journal devoted to publication of original contributions in diagnostic and interventional radiology, computerized tomography, ultrasound, magnetic resonance, nuclear medicine, radiotherapy, clinical and experimental oncology, radiophysics and radiation protection.*

Editor in chief

Tomaž Benulič
Ljubljana, Slovenia

Associate editors

Gregor Serša
Ljubljana, Slovenia

Viljem Kovač
Ljubljana, Slovenia

Editorial board

Marija Auersperg
Ljubljana, Slovenia

Matija Bistrović
Zagreb, Croatia

Haris Boko
Zagreb, Croatia

Malte Clausen
Kiel, Germany

Christoph Clemm
München, Germany

Mario Corsi
Udine, Italy

Christian Dittrich
Vienna, Austria

Ivan Drinković
Zagreb, Croatia

Gillian Duchesne
London, Great Britain

Béla Fornet
Budapest, Hungary

Tullio Giraldi
Udine, Italy

Andrija Hebrang
Zagreb, Croatia

Đurđa Horvat
Zagreb, Croatia

László Horváth
Pécs, Hungary

Berta Jereb
Ljubljana, Slovenia

Vladimir Jevtić
Ljubljana, Slovenia

H. Dieter Kogelnik
Salzburg, Austria

Ivan Lovasić
Rijeka, Croatia

Marijan Lovrenčić
Zagreb, Croatia

Luka Milas
Houston, USA

Maja Osmak
Zagreb, Croatia

Branko Palčič
Vancouver, Canada

Jurica Papa
Zagreb, Croatia

Dušan Pavčnik
Ljubljana, Slovenia

Stojan Plesničar
Ljubljana, Slovenia

Ervin B. Podgoršak
Montreal, Canada

Miran Porenta
Ljubljana, Slovenia

Jan C. Roos
Amsterdam, The Netherlands

Horst Sack
Essen, Germany

Slavko Šimunić
Zagreb, Croatia

Lojze Šmid
Ljubljana, Slovenia

Andrea Veronesi
Gorizia, Italy

Publishers
Slovenian Medical Society – Section of Radiology,
Croatian Medical Association – Croatian Society
of Radiology

Affiliated with
Societas Radiologorum Hungarorum
Friuli-Venezia Giulia regional groups of S.I.R.M.
(Italian Society of Medical Radiology)

Correspondence address
Radiology and Oncology
Institute of Oncology
Vrazov trg 4
61000 Ljubljana
Slovenia
Phone: + 386 61 1320 068
Fax: + 386 61 1314 180

Reader for English
Olga Shrestha

Design
Monika Fink-Serša

Key words und UDC
Eva Klemenčič

Secretaries
Milica Harisch
Betka Savski

Printed by
Tiskarna Tone Tomšič, Ljubljana, Slovenia

Published quarterly

Bank account number 50101 678 48454
Foreign currency account number
50100-620-133-27620-5130/6
Nova Ljubljanska banka d.d. – Ljubljana

Subscription fee for institutions 100 USD, individuals 50 USD.
Single issue for institutions 30 USD, individuals 20 USD.

According to the opinion of the Government of the Republic of Slovenia, Public Relation and Media Office, the journal RADIOLOGY AND ONCOLOGY is a publication of informative value, and as such subject to taxation by 5 % sales tax.

Indexed and abstracted by
BIOMEDICINA SLOVENICA
CHEMICAL ABSTRACTS
EXCERPTA MEDICA/ELECTRONIC PUBLISHING DIVISION

CONTENTS

ULTRASOUND

ONCOLOGY

RADIOPHYSICS

HISTORY

The publication of the journal is subsidized by the Ministry of Science and Technology of the Republic Slovenia.

Inštitut za diagnostično in intervencijsko radiologijo, KC Ljubljana; Klinika za otorinolaringologijo in maskilofacialno kirurgijo, KC Ljubljana; Klinički zavod za dijagnostičku interventnu radiologiju, KBC Rebro, Zagreb; Onkološki inštitut, Ljubljana

Radiol Oncol 1994; 28: 169-73.

Ultrasonography in diagnosis and folow-up of blunt renal injuries: A twelve-year's experience

Damir Miletić,[1] Željko Fučkar,[2] Miljenko Uravić,[2] Vladimir Mozetič,[2] Alan Šustić[3]

Clinical Hospital Center Rijeka, [1]Clinical Institute of Radiology, [2]Clinic for Surgery, [3]Department of Anesthesiology, Croatia

From January 1982 to January 1994, 103 blunt renal injuries were sonographically diagnosed in 1083 patients who sustained blunt abdominal trauma.
We have sonographically presented 46 (44,6 % of all renal lesions) contusions, 36 (35 %) intracapsular ruptures of the kidney, 17 (16,5 %) extracapsular ruptures and 4 (3,9 %) renal conquassations. Using ultrasound in the early diagnosis and follow-up, we have conservatively cured all contusions and intracapsular ruptures as well as 24 % of extracapsular ruptures, altogether 86 % of patients with diagnosed renal injury. Ultrasound achieved high sensitivity (97,2 %), specificity (99,9 %) and accuracy (99,6 %) in diagnosis of blunt renal injuries.

Key words: kidney-ultrasonography; wounds, nonpenetrating

Introduction

The most frequently exposed retroperitoneal organ in blunt abdominal injuries is the kidney. Common consequences of the retroperitoneal trauma are also retroperitoneal hematomas, while injuries of the great vessels, ureter, adrenal glands and pancreas occur rarely.

In 30–50 % of adults, abdominal trauma is followed by renal injury. High percentage of renal injuries is not caused by vulnerability of the renal parenchyma, but by sudden increase of the hydrostatic pressure.[1] The most frequent mechanism of renal injury is deceleration, and after that direct injury.

Correspondence to: mr. sc. dr. Damir Miletić, Klinički zavod za radiologiju, KBC Rijeka, Krešimirova 42, 51000 Rijeka, Croatia.

UDC: 616.61-001.42-07:534-8

The vast majority, precisely 75–85 % of blunt renal injuries are simple contusions or mild corticomedular and shallow surface lacerations. Such lesions are self-limited and require no specific treatment. About 10 % are deep parenchymal lacerations, which may or may not communicate with collecting system. Only about 5 % represent major parenchymal injuries ("shattered kidney") or serious vascular injuries such as avulsion of the vascular pedicle.[2]

In suspected renal injury intravenous urography (IVU) was an initial diagnostic method, followed by ultrasonography.[3] Basic ultrasound characteristics of injured kidney are the following:

1. enlargement of the kidney,
2. appearance of hypoechoic parenchymal zones with possible dislocation of pielocaliceal complex,
3. asymmetric account of kidneys and

4. detection of blood in perirenal space.[4]

The aim of this study was to evaluate the role of sonography not only in diagnosis of renal injury, but also in early indications for operative or conservative treatment, as well as in follow-up of injured patient.

Patients and methods

From January 1982 to January 1994 1083 patients who sustained blunt abdominal injury were examined at the Ultrasound Diagnostic Unit of the Clinical Hospital Center Rijeka, Croatia.

Sonographic approach to the kidney and perirenal space was paravertebral, lateral subcostal and occasionally intercostal (transhepatic or transsplenic).

Abdominal pansonography was performed by means of the following equipment: Fisher Emisonic, Bruel & Kjaer 1486, Aloka SSD 260 LS and Hitachi EUB 515 with sector, linear and convex transducers of 3,5 and 5 MHz.

Results

From 1083 sonographically examined patients who have sustained blunt abdominal injury, in 327 (30,2 %) of them we found traumatic intraabdominal lesion. The kidney was involved in 103 patients, which represents 31,5 % of all positive findings.

Blunt renal injuries can be classify into 4 categories with regard to clinical and patomorfologic criteria (Table 1).

Renal contusion (Table 1, Figure 1) was followed by hematuria in 72 % of patients (Table 2), microhematuria was present in 57 % and macrohematuria in other 15 % of patients. In this group we have detected the most of false negative IVU findings.

Intracapsular rupture of the kidney (Table 1, Figures 2 and 3) was frequently followed by significant laceration of the collecting system. That results in higher incidence of hematuria

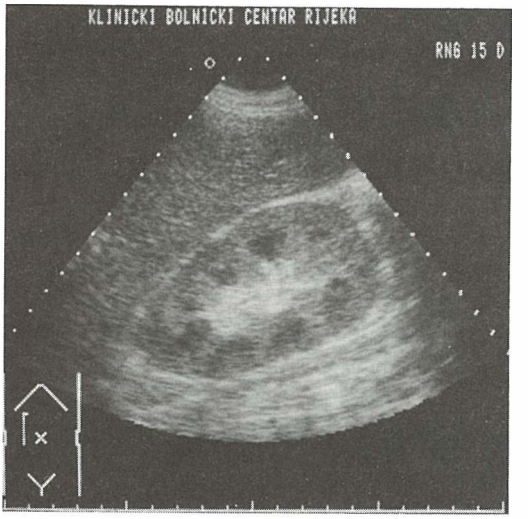

Figure 1. Intercostal sector scan of renal contusion.

Table 1. Sonography of blunt renal injuries.

Type of injury	Sonographic appearance	N°	%
Renal contusion	Unilateral organ enlargement, PPQ increase, hypoechoic renal medule	46	44,6
Intracapsular rupture of the kidney	a) Hypoehoic focal paranchymal lesion – fresh hematoma b) Hypoechoic sickle – like formation elevates renal capsule-subcapsular hematoma	36	35,0
Extracapsular rupture of the kidney	Intraparenchymal hypoechoic rupture linc involving renal capsule as well as perirenal hypocchoic collection	17	16,5
Renal conquassation	Thc whole organ (or most of it) enlarged, unclearly bordered from perirenal tissue, heterogeneous echostructure with hypoechoic bleeding foci	4	3,9
Total		103	100.0

Tabele 2. Clinical parameters of blunt renal injuries.

Type of injury	Hematuria	Positive IVU		Treatment
Contusion (46)	33 (72 %)	8/22 (36 %)		conservative
Intracapsular rupture (36)	31 (86 %)	26/35 (74 %)		conservative
Extracapsular rupture (17)	15 (88 %)	8/10 (80 %)	4 (24 %)	conservative
			9 (52 %)	renal sutures
			4 (24 %)	nephrectomy
Conquassation (4)	4 (100 %)	2/2 (100 %)		nephrectomy
Total (103)	83 (81 %)	44/69 (64 %)	86 (83 %)	conservative
			9 (9 %)	renal sutures
			8 (8 %)	nephrectomy

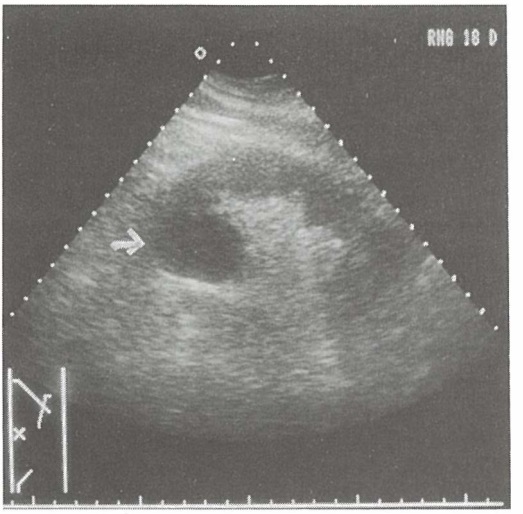

Figure 2. Subcostal sector scan of intracapsular rupture of the kidney (arrow).

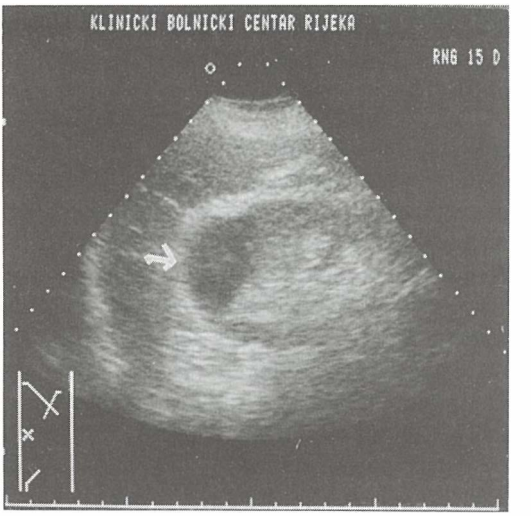

Figure 3. Subcostal sector scan of subcapsular hematoma of the kidney (arrow).

and positive IVU findings (Table 2). In 3 patients IVU presented an intrarenal extravasation of contrast medium, while ultrasound finding was negative. CT confirmed intracapsular renal rupture. It was false negative ultrasound result (0,5 % of all negative results). After initial volume compensation, all patients with renal contusion and intracapsular rupture were conservatively cured (Table 2) including sonographic follow-up. Ultrasound abnormalities regressed, except 2 residual cysts (1,9 % of renal injuries) and 3 posttraumatic scars (2,9 % of renal injuries, Figure 4).

Extracapsular ruptures of the kidney (Table 1, Figure 5) were serious renal lesions usually followed by hematuria and treated operatively (Table 2). Only 4 patients (24 % of this group)

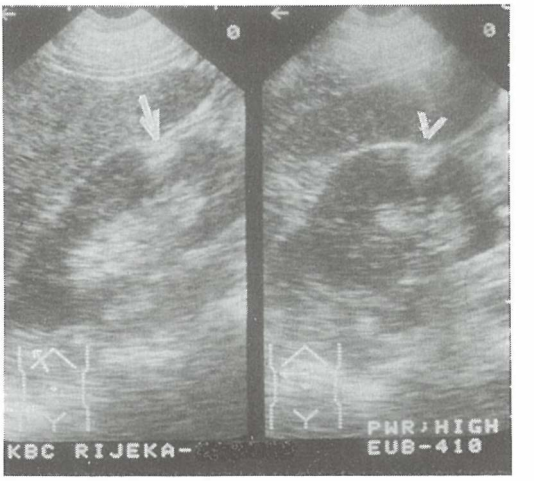

Figure 4. Intercostal sector scan of the posttraumatic scar in the renal cortex (arrow).

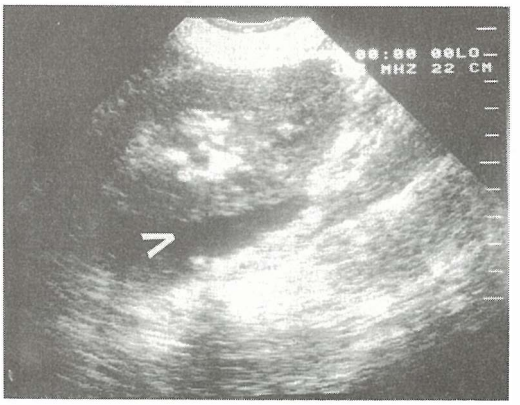

Figure 5. Subcostal sector scan of extracapsular rupture of the kidney (arrow).

were hemodynamically stable and two of them didn't have hematuria. Laceration of the renal parenchyma as well as perirenal collection was operatively confirmed in 13 patients. In 4 (24%) lumbotomized patients renal damage was so intensive that unilateral nephrectomy couldn't be avoided, while in other 9 (52%) the kidney was preserved (Table 2). In this group we also noted a rupture of an ectopic, unilaterally fused kidney, which was delivered by renal sutures.

Renal conquassation (Table 1, Figure 6) was always followed by hematuria and hypovolemia.

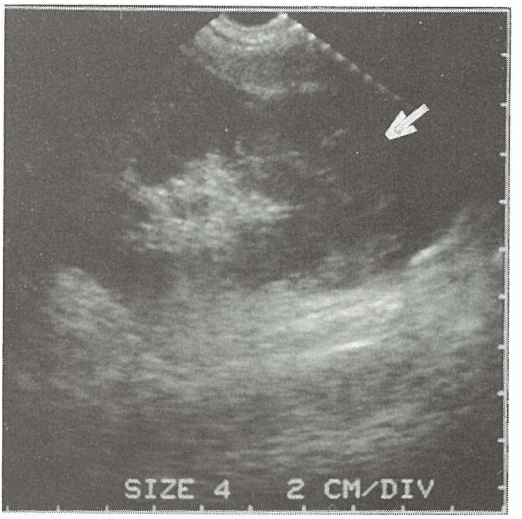

Figure 6. Intercostal sector scan of the partial renal conquassation (arrow).

All patients of this group were lumbotomized and unilateral nephrectomy was performed. In one injured patient sonographically was diagnosed renal conquassation due to enlargement of the kidney, heterogeneous echostructure with liquid foci. Large renal hypernephroma was found at explorative lumbotomy. We consider that ultrasound finding as false positive result, although the early indication for operative treatment was useful.

We had 103 real positive findings of traumatic renal lesion in total. They were proved with laboratory tests, intravenous urography, CT as well as explorative lumbotomy. We also had 977 real negative results, 1 false positive and 3 false negative results.

According to these results the following parameters of diagnostic value of ultrasound and intravenous urography in blunt real injuries are presented. (Table 3).

Table 3. Parameters of diagnostic value of ultrasound and intravenous urography in blunt renal injuries.

Parameters	Ultrasound	Intravenous urography
Sensitivity	97,2 %	63,8 %
Specificity	99,9 %	100,0 %
Accuracy	99,6 %	96,5 %

Discussion and conclusions

According to our results, the frequency of renal lesion in blunt abdominal trauma was 31,5%, which is adequate to results of Kimura et al.,[5] but notable higher than results of other authors.[6] It was probably due to routine ultrasound examination of every patient who sustained blunt flank trauma. Since the most frequent consequence of blunt renal trauma is simple contusion, if we rely on IVU and hematuria (Table 2), a significant number of such injuries could be misdiagnosed.

Our results show that 79,6% of all renal injuries (contusions and intracapsular ruptures) are light lesions requiring only conservative treatment and sonographic follow-up.

Extracapsular ruptures of the kidney are severe injuries, usually treated by explorative

lumbotomy with possible preservation of this organ. With help of ultrasound, even in this group we conservatively cured 24 % of patients. Two of non operated patients had no hematuria and IVU finding was normal (Table 2), because rupture of renal capsule wasn't followed by laceraton of collecting system. Leppaniemi et al.[7] consider that normal IVU finding excludes significant renal injury, which is opposite to our results (extracapsular rupture is certainly significant renal injury). Renal conquassation is a rare and severe injury, always requiring urgent nephrectomy.

According to our results, renal sonography must be performed in every blunt flank injury, regardless of negative IVU finding or absence of hematuria. Ultrasound is a technique capable to give reliable information of posttraumatic status of the kidney. Using ultrasound, we can assess the type and the degree of renal injury and follow-up the injured organ during conservative treatment. Ocult renal injuries can also be detected. Due to high sensitivity (97,2 %), specificity (99,9 %) and accuracy (99,6 %) of ultrasonography, we consider it as a method to be used in suspected renal injury.

Due to all mentioned characteristics of ultrasound in blunt renal injuries, it s necessary to point out the value of sonography in forensic medicine.

References

1. Fučkar Ž. *Sonografija urogenitalog sustava*. Ljubljana–Rijeka: Partizanska knjiga, 1987: 84–8.
2. Kassner EG, *Radiologic imaging*. New York-London: Gower Medical Publishing, 1989: 744–5.
3. Fučkar Ž, Peterković V, Dimec D. Uloga ehosonografije u dijagonostici tupih povreda bubrega. *Medicina* 1980; **17:** 184.
4. Fučkar Ž, Peterkovič V, Aničić M, Dimec D. Ehosonografska evaluacija tupih povreda bubrega. *Urol Arh* 1982; **19:** 36.
5. Kimura A, Toshibumi O. Emergency center ultrasonography in the evaluation of hematoperitoneum: a prospective study. *J Trauma* 1991; **31** (1): 20–3.
6. Wening JV. Evaluation of ultrasound, lavage and computed tomography in blunt abdominal trauma. *Surg Endosc* 1989; **3:** 152–8.
7. Leppaniemi AK, Haapianen RK, Lethonen IA. Diagnosis and treatment of patients with renal trauma. *Br J Urol* 1989; **64** (1): 13–7.

Radiol Oncol 1994; 28: 174-7.

Extracorporeal shock – wave lithotripsy in the management of bile duct stones

Alojz Pleskovič[1] and Franc Jelenc[2]

[1]Medical Faculty, Ljubljana, [2]Clinical Centre, Ljubljana, Slovenia

Extracorporeal shock – wave lithotripsy (ESWL) was undertaken in 16 patients with extra or intrahepatic bile duct stones which could not be removed endoscopically. Stone fragmentation was successful in 14 patients with stones in the biliary tract. Fragmentation failed in two patients with stones impacted in the pappila Vateri and had to be removed surgicaly. 14 of the 16 patients were free of stones after spontaneous passage (n = 9) or after endoscopic removal of the residual concrements (n = 5). Complications occurred in only three patients after ESWL (transitory hemobilia, transient hematuria). These data point to ESWL being clearly preferable to surgical intervention in bile duct stones refractory to endoscopic treatment, especially in the elderly with an increased perioperative risk.

Key words: cholelithiasis; lithotripsy

Introduction

The article by Sauerbuch et al. (1986), in which the autors describe their experience in Germany with the fragmentation of gallstones by means of extracorporeal shock waves (ESWL), generated a great deal of interest all over the world.[1-7] In our institution, most residual or primary bile duct stones after cholecystectomy are treated with basket extraction through an endoscopic spincterotomy. These technique may fail if the stones are large (>2 cm) or if they are in an unfavorable location (e. g., in an intrahepatic duct or beyond a stricture). The endoscopic approach may be impossible when the normal anatomic relationship between the bile duct and the duodenum is altered (e. g., periampullary diverticulum) or when the sphincter can not be reached because of previous gastrointestinal surgery.

Corespondence to: Alojz Pleskovič MD, Medical Faculty, Korytkova 4, 61105 Ljubljana, Slovenia.

UDC: 616.366-003.217.7-089.879

Material and methods

Between October 1988 and March 1992 we used ESWL to treat 16 patients who had residual or primary bile duct stones after cholecystectomy. The patients were divided into two groups, 11 patients with residual bile duct stones and 5 patients with primary bile duct stones after cholecystectomy. In both groups, the indication for treatment was the failure of or anticipated difficulty with basket extraction of the stone. In five of these 16 patients, basket extraction via endoscopic sphincterotomy either had failed or had not been attempted because of the large size of stones (>20 mm in three

patients) or the presence of an anatomic anomaly (periampulary diverticulum in two patients). Eleven patients had a T – tube in the bile duct, but basket extraction via an endoscopic sphincterotomy was impossible because the stones were in an unfavorable location (e. g., in an intrahepatic duct in six patients) or because of the large size of the stones (>20 mm in three patients) or because of a previous gastrointestial surgery (partial gastrectomy with Roux – en y anastomosis in two patients).

Baseline blood studies, including lactic dehydrogenase (LDH), aspartate transferase (AST), serum amylase, prothrombin time and partial tromboplastin time, and urinalysis were done less than 48 hr before ESWL and were repeated within 24 hr after the treatment. Abnormal tests were repeated until they returned to normal. Bile drainage was tested for blood. All patients had a coagulogram the day after the treatment and at least one more cholangiogram before discharged or treated further.

The study group included thirteen women and three men (age range, 27–84 years). Most of the patients were more than 65 years old. The treatments were performed by using Siemens-Lythrotripter equipment.

Results

All stones were fragmented successfully in 14 of the 16 patients. Fragmentation required one session in 12 patients, two sessions in one patient, four sessions in one patient. After ESWL, the stone fragments passed spontaneously in nine patients. In five patients the fragmented stones were removed by basket extraction through the endoscopic sphincterotomy. In two patients ESWL fragmentation failed and impacted stones in the pappila Vateri had to

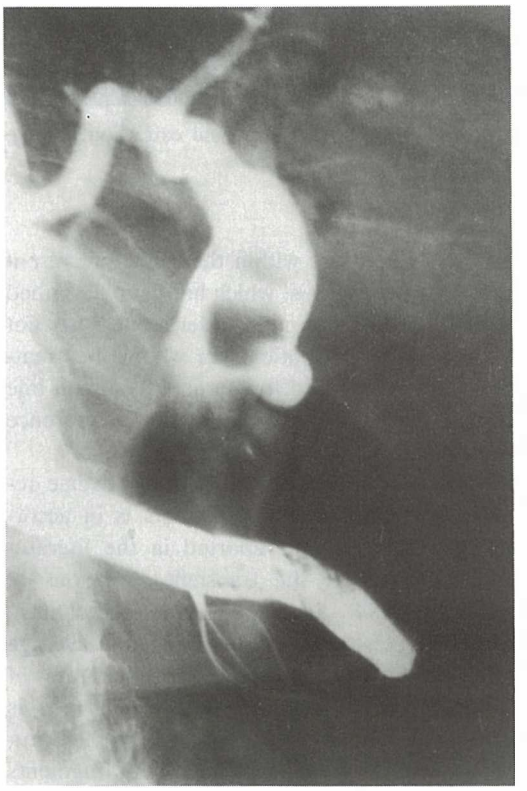

Figure 1. ERC showing a gallstone in the common bile duct.

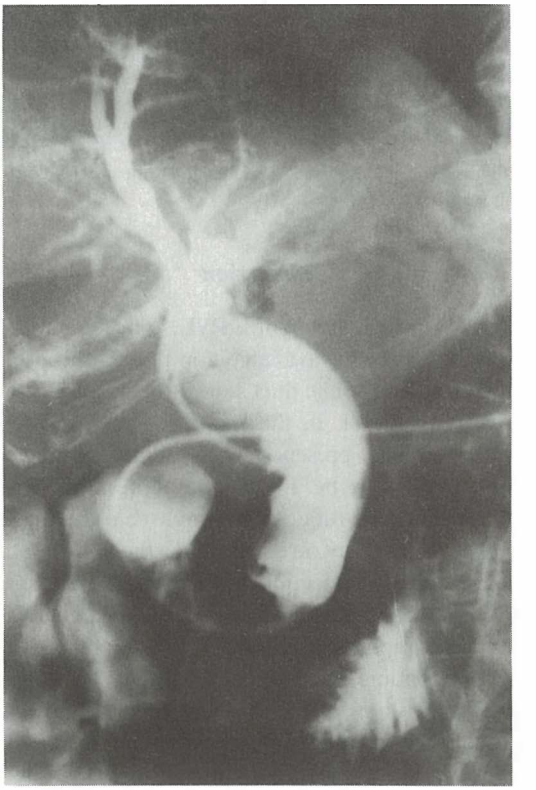

Figure 2. ERC after ESWL and spontaneous passage of fragments.

be removed surgicaly. The patients remained in the hospital from 2 to 14 days after the procedure, depending mainly on whether additional intervention was required. No clinically significant adverse reactions could be observed; in particular no evidence of pancreatitis was present. In two patients, transitory hemobilia developed. One patient had transient hematuria. Short – term elevations of LDS and AST were observed in most of the patients. Bruising of the skin was seen in four patients, but none had significant pain (Figure 1–4).

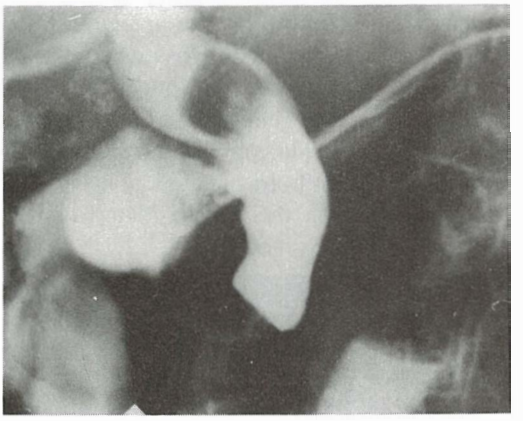

Figure 3. ERC showing a huge gallstone in the common bile duct.

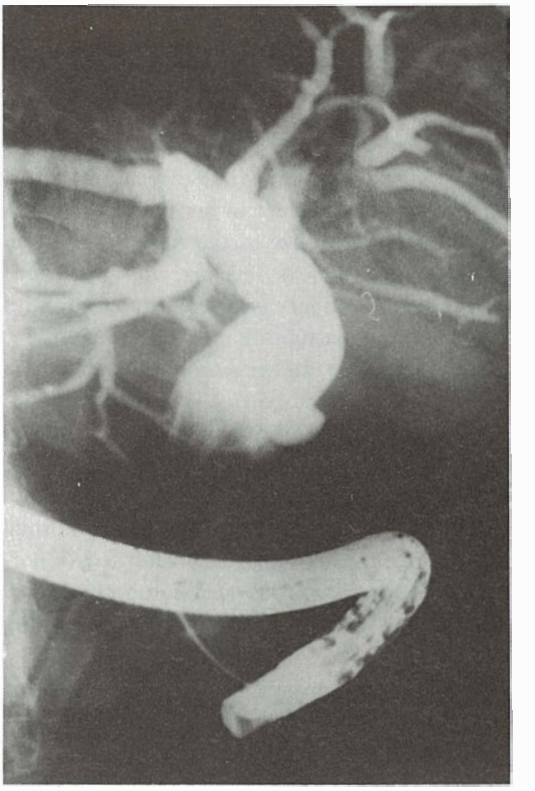

Figure 4. ERC after ESWL and extraction of fragments with Dormia basket.

Discussion

With the introduction of ESWL, another technique has become available for the nonsurgical management of bile duct stones.[1] A prerequisite for using ESWL in the treatment of bile duct stones is the presence of a biliary drainage tube. This may be a T – tube or a nasobiliary tube. Such a tube is indispensable because unless the stones are calcified, they must be visualized by injection of contrast material. Ductal stones rarely can be localized sufficiently by sonography.

The optimal or maximal number of shock waves has not yet been definitely established. Sauerbuch et. al. found that 500 – 1500 shocks were sufficient to fragment the stones. Other autors have reported the use of up to 3300 shocks.[8,9] Our use of between 1500 and 3000 shocks is therefore within the range of present practice. Pancreatitis, which has been described in the treatment of gallbladder stones, has not been reported in patients in whom the treatment was performed for retained common bile duct stones, possibly because of the presence indwelling drainage tube.

The lack of clinically significant adverse reactions to ESWL in our patients is in accordance with the data reported in the literature.[10,11] However, the transient elevations of LDH and AST – indicating liver – cell damage – may be related to the higher – than average number of shock waves used. Our rate of successful fragmentation of stones (88 %) is about the same as that reported in the literature, the rate of spontaneous passage of fragments (56 %) is also about the same as that found in other centres.[12-15]

Conclusion

ESWL a is successful method for the management of patients with bile duct stones when used in conjunction with other nonsurgical tehniques.

References

1. Sauerbruch T, Delins M, Paumgartner G, et. al. Fragmentation of gallstones by extracorporeal shock waves. *N Engl J Med* 1986; **314:** 818–22.
2. Mulley AG. Shock – wave lithotripsy: assessing a slam – hang technology. *N Engl J Med* 1986; **314:** 845–7.
3. Ferrucci JT. Biliary lithotripsy: what will the issues be? *A J R* 1987; **149:** 227–31.
4. Burthenne HJ. The promise of extracorporeal shock – wave lithotripsy for the treatment of gallstones. *A J R* 1987; **149:** 233–5.
5. Raskin JB. The continuing direct assault on the gallstone: enlightening, electrifying, and shocking. *Gastrointest Endosc* 1987; **33:** 262–3.
6. Nahrwold DL. Fragmentation of biliary tract stones by lithotripsy using local anesthesia. *Arch Surg* 1988; **123:** 91–3.
7. Van Sonnenberg E. Hofmann AF. Horizons in gallstone therapy – 1988. *A J R* 1988; **150:** 43–6.
8. Sauerbruch T, Stern M and the Study Group for Shock – wave Lithotripsy of Bile Duct Stones. Fragmentation of bile duct stones by extracorporeal shock waves. A new approach to biliary calculi after failure of routine endoscopic measures. *Gastroenterology* 1989; **96:** 146–52.
9. Brown BP, Loening SA, Johlin FC. Dayton MT, Maher JW. Fragmentation of biliary tract stones by lithotripsy using local anesthesia. *Arch Surg* 1988; **123:** 91–3.
10. Nicholson DA, Martin DF, Tweedle DEF, and Rao PN. Management of common bile duct stones using a second – generation extracorporeal shockwave lithotriptor. *B J Surg* 1992; **79:** 811-4.
11. Weber J, Adamek HE, Riemann JF. Extracorporeal piezoelectric lithotripsy for retained bile duct stones. *Endoscopy* 1992; **24:** 239–43.
12. Staritz M, Grosse A, Alkier R, Krzaska B und Meyer zum Buschenfelde KH. Terapie der Choledochlithiasis durch extrakorporale Stoswellenlithotripsie und adjuvante operative. Endoskopie. *Z Gastroenterol* 1992; **30:** 156–61.
13. Binmoeller KF, Bruckner M, Thonke F, Soehendra N. Treatment of difficult bile duct stones using mechanical, electohyraulic and extracorporeal shock wave lithotripsy. *Endoscopy* 1993; **25:** 201–6.
14. Lindstrom E, Borch K, Kullman EP, Tiselius HG, Ihse I. Extracorporeal shock wave lithotripsy of bile duct stones: a single institution experience. *Gut* 1992; **33:** 1416–20.
15. Adamek HE, Buttmann A, Hartmann CM, Jakobs R und Riemann F. Extracorporeal piczoelektrische lithotripsie von intra- und extahepatischen Gallengangssteinen. *Dtsch Med Wschr* 1993; **118:** 1053–9.

Radiol Oncol 1994; 28: 178-82.

Comparative assessment of three radiotherapy treatment protocols for inoperable cerebral metastases of non - small cell lung carcinoma

Liliane Demange,[1] Alison Franks,[2] Xavier Panis[1]

[1] *Department of Radiotherapy and Oncology, Institut Jean-Godinot, 1, rue du Général Koenig. 51056 Reims Cedex France*
[2] *Yorkshire Regional Centre For Cancer Treatment, Cookridge Hospital, Hospital Lane, Leeds LS16 62B*

Radiotherapy is often suggested in the treatment of inoperable brain metastases of non small cell lung carcinoma. This retrospective study of 83 cases has enabled us to assess the survival of irradiated and not irradiated patients as well as the predictive factors of better outcome from treatment.
Protocols delivering 30 Gy/10f/15d and 36 Gy/6f/25d lead to a significantly longer survival than the one delivering 20 Gy/5f/5d ($p < 0,0005$).
A Good initial neurological status and the improvement of neurological signs after radiotherapy are two factors of favourable prognosis. However, time of onset of metastasis, histology, existence and number of extracerebral metastases have no influence on survival.
We conclude that metastases must be irradiated early, as soon as the first neurological disorders appear. Treatment by irradiation of advanced metastases inducing major neurological disorders must be compared with the use of corticosteroids alone. Finally, we recommend the use of a dose greater than 20 Gy/5f/5d, with a fractionation adapted to the patient's neurological status.

Key words: brain neoplasms-radiotherapy; neoplasm metastasis; carcinoma, non small cell lung

Introduction

Prognosis of patients with brain metastases of non-small cell lung carcinoma (NSCLC) is poor and a majority of authors report a median survival of 3 to 6 months.[1, 2] In case of a single operable metastasis, a combined surgery and radiotherapy allows for a significant increase in survival; cases with a survival of more than 10 years have been reported.[3, 4] Unfortunately, routine practice shows that more than 75 % of cerebral metastases of non-small cell lung carcinoma cannot be removed by surgery. These patients are refered for consideration of radiotherapy.

In this study, we assess the survival results obtained by 3 different radiotherapy protocols among 83 patients with non-small cell lung carcinoma who were not suitable for surgery, in order to determine which patients will gain most from radiotherapy. The other aim of the study is to highlight the predictive factors of a better survival.

Correspondence to: Xavier Panis M. D., Institut Jean-Godinot, 1, rue du Général Koenig. 51056 Reims Cedex, France.

UDC: 616.831-006.6-033.2:615.849:614.24-006.6

Materials and methods

Patients

Eighty-three patients with brain metastases of non-small cell lung carcinoma were treated between January 1980 and December 1985. Median age of the 79 male and 4 female patients was 61 years (range 37–83 years).

Performance status according to Order's classification[5] (Table 1) showed 53 patients with minor neurological disorders (Order 1 and 2) and 30 patients with major neurological disorders (Order 3 and 4). In 5 patients, the brain metastasis was discovered before the lung carcinoma (revealing metastasis), in 37 simultaneously (synchronous metastasis) and in 41, several months after the end of the bronchogenic carcinoma treatment (secondary metastasis). Forty-four patients had an epidermoid carcinoma, 20 an adenocarcinoma, 13 an undifferentiated carcinoma. Forty patients had a single metastasis, 43 multiple metastases. Brain metastases were the only secondary location in 47 patients, while associated visceral metastases were present in 36 others.

Table 1. Order classification.

Neurological grade	Clinical condition
1	Normal physical and intellectual activity. Normal neurological condition.
2	Normal intellectual activity. Self-sufficient. Slight abnormalities at neurological examination.
3	Major neurological abnormalities necessitating hospital treatment and medical supervision.
4	Permanent hospitalisation. Serious physical and neurological condition

Treatment

No surgery was possible for the metastases, either because of their multiple locations, or because of the poor performance status of the patients. All patients received corticosteroids for at least one month.

Fifty-nine patients also had cranial irradiations.

In all patients, radiotherapy was given to the whole brain using two lateral opposing fields of 1.25 MeV photons (Cobalt 60). Three protocols were used, according to the individual choice of the radiotherapists:

- Protocol A: 20 Gy/5f/5d (5 fractions of 4 Gy in 5 days)
- Protocol B: 30 Gy/10f/15d (10 fractions of 3 Gy in 15 days)
- Protocol C: 36 Gy/6f/25d (2 courses of 3 fractions of 6 Gy in 3 days with an interval of 3 weeks).

Seventeen patients were treated with protocol A, 18 with protocol B, 24 with protocol C and 24 with corticosteroids only.

Evaluation

Response to the treatment has been evaluated in terms of neurological performance status and survival time.

Performance status according to Order's classification was assessed just before and three weeks after radiotherapy. Performance status was considered to have improved when it decreased at least one class, to have worsened when it increased at least one class, and to have been stable when its class did not change.

Survival time was assessed from the diagnosis of brain metastasis, and survival curves were drawn up using the Kaplan-Meier method. Predictive factors were studied and distributional comparisons were made by the use of the log-rank and chi-square tests.[6]

Results

All patients died, the majority from their brain metastasis. Overall median survival was 95 days, 25 days for those treated with corticosteroids alone and 105 days for those treated by radiotherapy.

Quality of response to radiotherapy

After radiotherapy, neurological status improved in 32 patients (54%), was stable in 22 patients (38%) and worsened in 5 patients (8%).

Median survival was 150 days for patients whose condition improved, 60 days for patients whose condition was stable and 30 days for patients whose condition worsened.

The difference in survival between patients whose condition improved and the others (those whose condition was stable or worsened) was statistically significant ($p < 0,025$).

Radiotherapy protocols

Median survival was 60 days for patients treated with protocol A (20 Gy/5f/5d), 99 days for those treated with protocol B (30 Gy/10f/15d) and 125 days for those trated with protocol C (36 Gy/6f/25d) (Table 2). Whilst difference in survival is not statistically significant between the two protocols that resulted in the longer survivals (B and C), it is statistically significant between protocol A and the other two (B and C) ($p < 0,0005$).

We did not find any statistically significant survival difference between patients treated with corticosteroids alone (25 days) and those treated with protocol A (60 days).

Moreover, radiotherapy is most efficient in patients with a good neurological condition. Thus, median survival for Order 1 and 2 patients was 25 days when untreated and 125 and 150 days respectively when treated with 30 Gy/10f/15d and 36 Gy/6f/25d. While médian survival with, or without, radiotherapy was 25 days for Order 3 and 4 patients.

Other factors that influence the quality of response to treatment

Factors such as time between discovery of metastasis and that of lung cancer (time of onset of metastasis), histological status, number of metastases, presence or absence of extracerebral metastases did not result in any statistically significant difference. However, difference in survival was significantly greater in patients with a good neurological condition (Order 1 and 2) compared to others (Order 3 and 4) (Table 2).

Table 2. Study of predictive factors of the quality of response to radiotherapy according to median survival.

Factors studied	Median survival	
Protocol of radiotherapy		
– 20 Gy/5f/15d	60 days	
– 30 Gy/10f/15d	99 days	$p < 0,0005$
– 36 Gy/6f/25d	125 days	
Time of onset of metastasis		
– revelatory	150 days	
– synchronous	90 days	NS
– secondary	25 days	
Histology		
– epidermoid carcinoma	90 days	
– adenocarcinoma	70 days	NS
– undiffentiated carcinoma	70 days	
Number of metastases		
– one	99 days	NS
– several	70 days	
Extracerebral metastases (EM)		
– without EM	30 days	NS
– with EM	98 days	
Neurological status at diagnosis		
– Order 1 and 2	95 days	$p < 0,025$
– Order 3 and 4	25 days	

NS = non significant

Discussion

Use of radiotherapy for the treatment of non operable cerebral metastases of NSCLC allows for better survival than use of corticosteroids alone. In our study, the conditions required for obtaining a better result were the use of a dose greater than 20 Gy/5f/5d and a neurological status which was not seriously impaired.

In the literature, most of the series published analyze the results of a radiotherapy treatment on cerebral metastases whatever their origin. One of the characteristics of our study is that we examined a group of patients with cerebral metastases of an homogeneous origin (NSCLC)

to determine the predictive factors of a better response to treatment. Moreover, each of the radiotherapists in our team followed invariably his own protocol in the treatment of cerebral metastases, a habit which facilitated our comparison of the results of the three protocols.

Improvement of survival by radiotherapy treatment of non operable metastases of NSCLC has been reported by several authors with median survivals of 3 to 4 months from discovery of cerebral metastasis,[5, 7–10] close to the figures determined by our study. It is also found in the literature that radiotherapy induces longer survivals in patients with a good neurological status (Order 1 and 2).[5, 7–10] Our study, and those of Newman[7] and Franchin,[9] conclude that best results occur when radiotherapy allows the patients to maintain or to recover a good neurologic status (Order 1 and 2).

Median survival is, in our study, influenced by the radiotherapy dose. An analysis of the results of the three protocols we used (20 Gy/5f/5d, 30 Gy/10f/15d, 36 Gy/6f/25d) confirms a significantly longer median survival for the protocols using 30 Gy/10f/15d and 36 Gy/6f/25d. Improvement of survival when using higher doses for cerebral metastases of NSCLC has been analyzed by other authors.[7, 8, 10] Newman[7] reports a better survival when the dose used is greater than 40 Gy/20f/28d. Chatani,[8] in a randomized study, found a significantly improved survival ($p < 0,05$) when applying 50 Gy/20f/28d than when applying 30 Gy/10f/15d. Egawa[10] observes a correlation between the dose applied and the median survival: 0.6 month with doses lower than 30 Gy, 1.7 months for doses in the 30–50 Gy range and 4 months for doses of more than 50 Gy. Improvement of survival for higher doses has led to the accrual of a series of 44 patients requiring re-irradiation (among whom 15 had metastases from NSCLC).[11] After a first treatment with 30 Gy, the patients received a second course of irradiation resulting in a total dose of 60 Gy. Unfortunately, the additional treatment was seldom advantageous; survival after irradiation being generally short, and rarely improved in quality. Finally, a significant number of survivors after reirradiation died from cerebral necrosis. Therefore, the authors conclude in suggesting that a higher total dose with a conventional fractionation be used for the initial treatment of cerebral metastases. Similarly, it should be noted that the addition of a chemotherapy to radiotherapy[12] in the treatment of cerebral metastases of bronchogenic carcinoma results in a higher tumour regression rate than that obtained with radiotherapy alone, although survival is not improved.

The analysis of other parameters that could have an influence on survival of inoperable metastases of NSCLC shows no difference according to relative times of onset of metastasis and bronchogenic tumour, histology and number of metastases. These results are found as a recurring feature in the literature.[3, 5, 7–10, 13, 14] It must be emphasised that the longest survivals of patients with a single metastasis, found by Deviri,[15] benefit from the fact that those single metastases could be treated by surgery. The lack of influence on survival of the presence of extracerebral metastases associated with cerebral metastases is consistent with the results of other studies;[5] however, it must be said that in his conclusions, Robin[14] found a better survival for cerebral only metastases.

Finally, it appears that the radiotherapy treatment of inoperable metastases of NSCLC must not be fixed and must firstly take into account the patient's neurological status. The dose delivered must be high enough to be effective. One could recommend a high and concentrated dose (e. g. 36 Gy/gf/25d) for patients with a bad neurological status, and a high but fractionated dose (e. g. 30 Gy/6f/15d) for those with a better neurological status. In patients with a very poor performance status, radiotherapy must be considered versus steroids alone. However, when radiotherapy is used, metastases should be irradiated as soon as possible when neurological symptoms develop.

References

1. Ballantine HT, Byron FR. Carcinoma of the lung with intracranial metastasis. *Arch Surg* 1942; **57:** 849–54.

2. Perese DM. Prognosis in metastatic tumors of the brain and the skull. An analysis of 16 operative and 162 autopsied cases. *Cancer* 1959; **12:** 609–13.

3. Galichich JH, Sundaresan N, Arbit E and al. Surgical treatment of single brain metastasis: factors associated with survival. *Cancer* 1980; **45:** 381–86.

4. Mussi A, Janni A, Pistolesi M, Ravelli V, Buonaguidi R, Angeletti CA. Surgical treatment of primary lung cancer and solitary brain metastasis. *Thorax* 1985; **40:** 191–93.

5. Posner JB. Management of central nervous system metastases. *Semin Oncol* 1977; **4:** 81–91.

6. Kaplan EL, Meier P. Non parametric estimation from incomplete observation. *J Amer Stat Assoc* 1958; **53:** 457.

7. Newman SJ, Hansen HH. Frequency, diagnosis and treatment of brain metastases in 247 consecutive patients with bronchogenic carcinoma. *Cancer* 1974, **33:** 492–96.

8. Chatani M, Teshima T; Hata K, Inouet T, Suzuki T. Whole brain irradiation for metastases from lung carcinoma. *Acta Radiologica Oncology* 1985, **24:** 311–14.

9. Franchin G, Minatel E, Roncadin M, Trovo M, et al. Accelerated split course regimen in the treatment of brain metastases. *Radiother Oncol* 1988, **12:** 39–44.

10. Egawa S, Tukiyama I, Akine Y, Kajivra Y, et al. Radiotherapy of brain metastases. *Int J Radiat Oncol Biol Phys* 1986, **12:** 1621–25.

11. Hazuka MH, Kinzie JJ. Brain metastases: results and effects of re-irradiation. *Int J Radiat Oncol Biol Phys* 1988; **15:** 433–37.

12. Ushioy, Aritan, Hayakawa T. Chemotherapy of brain metastasis from lung carcinoma: a controlled randomized study. *Neurosurgery* 1991, **28:** 201–10.

13. Sundaresan H, Galichich JH, Beattie EJ. Surgical treatment of brain metastasis from lung cancer. *J Neurosurg* 1983, **58:** 66–71.

14. Robin E, Bitran JD, Golombs HM, et al. Prognostic factors in patients with non small cell bronchogenic carcinoma and brain metastasis. *Cancer* 1982, **49.** 1916–19.

15. Deviri E, Schachner A, Havely Y, Shalit M, Levy MJ. Carcinoma of lung with a solitary cerebral metastasis. Surgical management and review of the literature. *Cancer* 1983, **52:** 1507–09.

Radiol Oncol 1994; 28: 183-7.

Adjuvant treatment of malignant melanoma with interferon after radical surgery – part II. Effect of recombinant alpha interferon

Zvonimir Rudolf

Institute of Oncology, Ljubljana, Slovenia

In our randomized prospective study, patients with malignant melanoma were treated with both human leukocyte interferon alpha (HuIFN) and recombinant interferon alpha 2b (Intron) after surgical removal of primary tumor (Clark level of invasion IV, V and/or thickness exceeding 1.5 mm). They were randomized into two arms: (1) those treated with HuIFN• or with Intron; and (2) a control group with no immediate treatment. Interferon was applied through 30 weeks. Cumulative dose for HuIFN was 6×10^7 U (2×10^6 U weekly), and for Intron 9×10^7 U (3×10^6 U weekly). Both arms of the study included altogether 421 patients: 161 in the control group, 160 in the HuIFN group, and 100 patients in Intron group. The results of 5-year analysis showed significant differences in the disease-free interval as well as in survival between both arms in favour of interferon (both HuIFN and Intron) treated patients ($p < 0.005$). According to stratification by sex, the difference was significant also between female as well as male patients, of both groups ($p < 0.005$). In a majority of patients interferon application caused a flu-like syndrome, whereas adverse effects on blood count and chemistry could not be established. The treatment (given in the reported dose) was not toxic and was applied on an out-patients basis.

Key words: melanoma-drug therapy; interferon-alpha; interferon alfa, recombinant

Introduction

In the world, patients with malignant melanoma of the skin represent approximately 1 % of all cancer patients. The incidence of melanoma has been rapidly increasing, doubling its value every 6–10 years, and likewise, also melanoma-related mortality has been exhibiting a trend of constant increase.[1, 2]

Correspondence to: Prof. Zvonimir Rudolf, MD, PhD, Institute of Oncology, Zaloška 2, 61105 Ljubljana, Slovenija, Tel. +386 61 1314225, Fax +386 61 1314180.

UDC: 616.5-006.81-085

Considering the high mortality rates observed in patients with malignant melanoma (with deep level of invasion) as well as ineffective treatment of advanced disease, many studies have been investigating the potential of various treatment modalities.

Since the results of malignant melanoma treatment are still unsatisfactory, especially in advanced stages of disease, an effort should be directed to earlier treatment. Unfortunately, the results of adjuvant treatment in the early stage of the disease with chemotherapy[3] have also not confirmed the effectiveness of treatment so far.

During the last decade a number of clinical studies have been performed to investigate the therapeutic potential of interferons in the treatment of various malignant diseases.[4] Although partial and occasional complete regressions have been observed in some cancer patients,[5] the overall results of single-agent interferon treatment point out the need for further clinical and laboratory research in order to establish the role of interferon in cancer treatment, particularly in solid tumors.

In view of the previously mentioned facts, we decided to established the role of interferon as an adjunct to surgical treatment of primary malignant melanoma. A prospective randomized trial[6] was commenced in 1988 in patients with malignant melanoma stage IIA and B according to the AJCC classification.[7]

In our randomized prospective study, patients with malignant melanoma were treated with human leukocyte interferon alpha (HuIFN) after surgical removal of primary tumor (Clark level of invasion IV, V and/or thickness exceeding 1.5 mm). They were randomized into two groups: (1) those treated with HuIFN and (2) a control group with no immediate treatment. HuIFN was applied through 30 weeks in cummulative dose 6×10^7 U, and 2×10^6 U weekly. Both arms of the study included altogether 321 patients.[8]

The results of general analysis showed significant differences in the disease-free interval as well as in survival between both groups in favour of HuIFN treated patients ($p < 0.005$).

Later in the study, a group of patients treated with recombinant alpha interferon was added. In this report the analysis and comparison of various treatment modalities is presented.

Patients and methods

In the protocol only patients with histologically proven primary tumor after radical surgery were included. As mentioned previously, all the patients were in Stage IIA and IIB of the disease which means that the primary tumors were classified as Clark IV, V level of invasion and/or tumor thickness exceeding 1.5 mm. The patients were randomized into two protocol arms – those treated with HuIFN or Intron and control group with no immediate treatment after radical surgery (Controls).

All patients in both arms were on regular clinical follow-up. Complete bloods counts, blood chemistry, renal and liver functin tests were taken each check; these were performed monthly in the first 2 years, and later on in 2 month intervals. Complete evaluation of patients was done before and after therapy. Patients with relapse (in both groups) were further treated as necessary (with surgery, radiotherapy, chemotherapy) and were afterward also on regular follow-up.

Treatment – Treatment in the first group of patients consisted of i/m paplication of crude human leukocyte interferon (Imunološki zavod, Zagreb, Croatia) and started within the first month after surgical excision. Interferon was applied for 30 weeks in cumulative dose of 6×10^7 units. Each patient received 2×10^6 units of interferon weekly.

Similar regimen was applied in the second group of the treatment arm. In this group the treatment consisted of i/m application of Intron; the drug was applied for 30 weeks in cumulative dose of 9×10^7 units and each patient received 3×10^6 units of intron weekly.

HuIFN group – A total of 160 patients, 70 males and 90 females, have been entered into the HuIFN group. The mean age of patients was 48 years (48 ± 14 years, range 20–78 years). The patients were distributed according to the primary tumor site as follows: head and neck region (HN) – 15; trunk (T) – 79; limbs (L) – 66. Primary tumors were determined as superficialy spreading type (SSM) in 31 cases, nodular type (NM) in 127 cases and *lentigo maligna* type (LMM) in two cases. The level of invasion was Clark IV in 109 cases, and Clark V in 12 cases. In 39 cases the level of invasion was Clark III, but tumor thickness exceeded 1.5 mm, which was in accordance with the protocol criteria.

Intron group – A total of 100 patients were included in this group, 45 males and 55 females. Mean age of patients was 48 years (48 ± 14 years, range 20–73 years). The patients were distributed according to the primary site as follows: HN – 6; T – 54; L – 40. Primary tumors were determined as SSM type in 19 cases, NM in 79 cases and LMM in two cases. The level of invasion was Clark IV in 66 cases and Clark V in 5 cases. In 29 cases the level of invasion was Clark III, but tumor thickness exceeded 1.5 mm.

Control arm – The control arm comprised 161 randomly selected patients (71 males and 90 females) in the mean age of 52 years (52 ± 13 years, range 21–84 years). As to the primary tumor site, lesions were located in head and neck region in 16 cases, on the limbs in 70 and on the trunk in 75 cases. In 92 patients tumors were assessed as SSM type, in 3 patients as LMM and in 66 patients as NM type. The level of invasion was Clark III in 23 cases (but thickness more than 1.5 mm), Clark IV in 101 cases, and Clark V in 12 cases.

Patient distribution by various potential prognostic factors is presented in Table 1. Our analysis showed that all protocol groups, i. e. HuIFN, Intron and Controls, were similar as to their sex and age distribution. Also, there was no major difference in the site and type of primary tumor, and neither in its level of invasion.

Table 1. Comparison of HuIFN, Intron and Control groups according to the sex and age distribution, type and site of primary tumor and the level of invasion.

		HuIFN		Intron		Controls	
		No.	%	No.	%	No.	%
Sex	M	70	44	45	45	71	44
	F	90	56	55	55	90	56
Age	< 53	100	63	64	64	81	50
	> 53	60	37	36	36	80	50
Type	NM	127	79	79	79	66	41
	SSM	31	20	19	19	92	57
	LM	2	1	2	2	3	2
Local.	Trunk	79	49	54	54	75	47
	HNeck	15	9	6	6	16	10
	Limbs	68	41	40	40	70	43
Clark	III	39	24	29	29	38	23
	IV	109	68	66	66	101	62
	V	12	8	5	5	12	7
Total		160	100	100	100	161	100

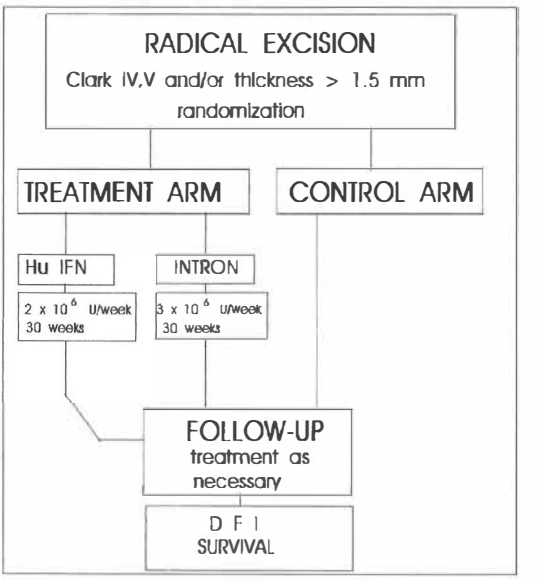

Figure 1. Protocol summary.

Statistical analysis – The statistical analysis was done using the Kaplan-Meier product-limit method[9, 10] which is a non-parametrical method to estimate the probability of an event occuring during a given time-interval. Statistical significance of graphed survival curves was tested using logrank program which performs a chi-square-like analysis.[11, 12, 13]

Results

Survival analysis

The analysis of survival in both protocol arms is presented in Fig. 2. The difference between both treated groups and the controls is significant (Intron curve vs. Controls curve and HuIFN curve vs. Controls curve, $p < 0.01$). There was no difference between both treatment groups, i. e. Intron and HuIFN.

Since the localization of primary tumor could influence the survival, the patients were analyzed by grouping according to the primary site.

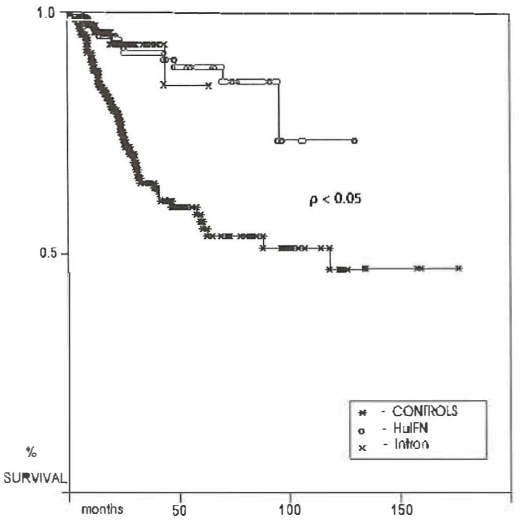

Figure 2. The comparison of survival between patients in control group, patients treated with human leukocyte interferon alpha and patients treated with recombinant interferon alpha 2b.
(Controls – control group, HuIFN – patients treated with human leukocyte interferon alpha, Intron – patients treated with recombinant interferon alpha 2b; the difference between HuIFN and controls as well as between Intron group and controls is significant, $p < 0.05$).

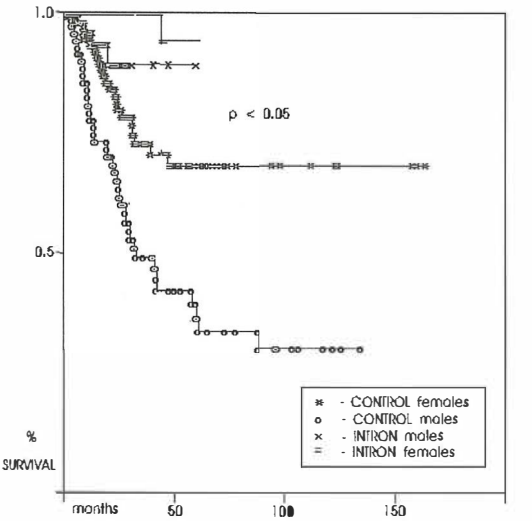

Figure 3. The comparison of survivals between Intron group and controls by sex stratification.
(Control females – female controls, CONTROL males – male controls, Intron females – female patients treated with recombinant interferon alpha 2b, Intron males – male patients treated with recombinant interferon alpha 2b).

No difference could be established between patients with primary tumor in head and neck region, limbs, or trunk.

The possible influence of age on survival was analyzed. Between the groups of patients treated with Intron age more and less then 53 years no diference could be noted.

Analysis of survival according to stratification by tumor type was performed, and there was no difference in survival between patients with nodular, lentiginous or superficial spreading type.

The difference between patients treated with intron and control patients was significant also by sex stratification (Fig. 3). Females in the treated group had better survival than female controls; likewise, male patients treated with intron survived longer than male patients in the control group (Intron females curve vs. Control females curve, and Intron males curve vs. Control males curve; $p \leqq 0.05$).

Interferon treatment was well tolerated by the majority of patients and no patient refused it because of toxic side effects. In all patients the application of interferon was followed by mild up to moderate fever (less than 39° C) which was transient. The patients also experienced flulike syndrom, which was anticipated. The application of interferon in the stated dosage exerted no effect on blood count and chemistry. In one case, as reported previously,[14] a moderate allergic reaction manifested with urticaria followed the second course of treatment in the HuIFN group. Since the fever and flu-like syndroma were transient, after pilot study it was decided that the regimen should be applied on an out-patients basis.

Discussion

The increasing incidence of melanoma and its tendency to affect younger adults, as well as relative ineffectiveness of treatment in advanced stages, point out the need for an effective adjuvant therapy.

In our study, both treatment regimens (i. e. HuIFN and Intron) resulted in prolongation of the survival of patients, since the difference between both protocol groups when compared with the controls (HuIFN vs. Controls as well as Intron vs. Controls) was significant. In addition, the difference between male as well as female patients of both groups was also significant. According to these results, it can be postulated that the interferon (both HuIFN and recombinant alpha interferon) treatment prolonged the survival of patients in treated groups.

Also, the treatment was not associated with significant toxic side effects.

Possible mechanisms of interferon action have not been fully explained yet. Theoretically, interferons could exert their antitumor effects in three ways: (1) via the host immune system; (2) by altering some non-immune host/tumor cell interactions; or (3) by direct effects on the tumor cells. Data from laboratory animal experiments suggest that interferon act best when tumor load is low, such as was the situation in our study.[6, 8] Interferons are also an important part of lymphokine cascade. It is reasonable to conclude, that interferon could act as a biological response modifier through many yet uknown mechanisms including lymphokine cascade.

According to our results, the adjuvant interferon (both HuIFN and Intron) treatment can be advised in cases with prognostically unfavourable melanoma, i. e. primary melanoma tumors with Clark IV, V level of invasion and/or a thickness more than 1.5 mm.

Acknowledgement

The financial support by grant No. C3-0563-302/27-40/B of the Ministry of Science and Technology of Slovenia is gratefully acknowledged.

References

1. Cancer incidence in Slovenia, 1980, 1981, 1982, 1983, 1984, 1985, 1986. Ljubljana: Institute of Oncology-Cancer Registry of Slovenia, 1984, 1985, 1986, 1987, 1988, 1989, 1990.
2. Rudolf Z, Roš-Opaškar T. Survival and disease-free interval of malignant melanoma patients in relation to the prognostic factors. *Radiol Oncol* 1992; **26:** 45–55.
3. Koh HK, Sober AJ, Harmon DC, Lew RA, Carey RW. Adjuvant therapy of cutaneous malignant melanoma – a critical review. *Medical and Pediatric Oncol* 1989; **13:** 244–60.
4. Baron S, Tyrring SK, Fleischmann R, Coppenhaver DH, Niesel DW, Klimpel GR, Stanton JG, Hughest TK. The interferons – mechanisms of action and clinical applications. *JAMA* 1991; **266(10):** 1375–83.
5. Kirchner H. Update on interferons. *Progress in Oncology* 1988; **7:** 5–62.
6. Rudolf Z, Furlan L. Adjuvant treatment of malignant melanoma with human leukocyte interferon. *Period Biol* 1990; **92(1):** 141–2.
7. American Joint Committee on Cancer: *Manual for staging of cancer,* 3rd ed. Philadelphia: JB Lippincott, 1987.
8. Rudolf Z. Adjuvant treatment of malignant melanoma with human leukocyte interferon after radical surgery: I. general analysis. *Radiol Oncol* 1993; **27:** 332–8.
9. Kaplan EL, Meier P. Nonparametric estimation from incomplete observations. *J American Statistical Association* 1958; **53:** 457–81.
10. Matthews DE, Farewell VT. *Using and understanding medical statistics.* Karger, 1988, 67–78.
11. Peto R, Pike MC. Design and analysis of randomized clinical trials requiring prolonged observation of each patient: I. Introduction and design. *Br J Cancer* 1976; **34:** 585–612.
12. Peto R, Pike MC. Design and analysis of randomized clinical trials requiring prolonged observation of each patient: II. Analysis and examples. *Br J Cancer* 1977; **35:** 1–39.
13. Anderson S, Auquier A, Hauck WW. *Statistical methods for comparative studies.* J Wiley, 1980, 199–234.
14. Rudolf Z. Treatment of malignant melanoma with human leukocyte interferon – preliminary results of randomized trial. Filipič B(ed): Yugoslave colloquium on interferon. Ljubljana, Slovenian Microbiological Society 1986, 129–33.

Radiol Oncol 1994; 28: 188-93.

Oromandibular reconstruction with microvascular osteocutaneous free flap (report of twenty cases)

Marijan Car,[1] Mirna Juretič,[1] Hrvoje Štalekar,[2] Zoran Žgaljardić,[1] Žarko Tomljanović,[2] Ivo Rakulić,[2] Ivan Luštica[3]

Clinical Hospital Center Rijeka, [1] Department of Maksillofacial Surgery, [2] Department of Traumatology, [3] Department of Otorhinolaryngology, Croatia

Twenty patients with oral cancer who undervent Commando operation and postoperative reconstruction of the oromandibular defect with microvascular osteocutaneous free flap have been reported. Eight metatarsal, seven radial and five fibular microvascular osteocutaneous free flaps were used, being successfully performed in 18 (90%) patients.

Each of the tree flaps used, was characterized by some advantages and disadvantages. Fibular microvascular osteocutaneous free flap has been the best for the mandibular reconstruction at any rate, because of the posibility of taking a great part of the bone and reconstruction of the largest defects and even the whole mandible.

Use of metatarsal microvascular osteocutaneous free flap has been limited to smaller mandibular defects only, while the radial microvascular osteocutaneous free flap developed very severe and a long – term morbidity of the donor site.

Key words: oral cancer; mandibular neoplasms-surgery; surgical flaps; microvascular osteocutaneous free flaps

Introduction

Primary reconstruction of partial mandibular defect has not been considered to be necessary for years. Later, the defects have been reconstructed in different ways and with various success.

Using various plates (A–O system, Thorp and others), the reconstruction was successful in 73% to 100%, ranging from 40% to 70% with nonvascularized bones, bone grafts or pedicled osteomiocutaneous flap.[1]

Urken[1] reports data showing 96% of success at partial mandibular defect reconstruction with vascularized osseous composite free flaps in 322 published cases between 1986 and 1990.

Primary oromandibular defect reconstruction following radical tumour excision leads to the most rapid healing and recovery of the patient to a normal life.

The increased number of the surviving patients after reconstructions in the oral cavity with the microvascular osteocutaneous free flaps has been accompanied by significant functional improvements and aesthetic results.[1]

Correspondence to: Doc dr. sci. Marijan Car, 5126 Crikvenica, Basaričekova 2, Croatia. Tel.: (051) 781 538.

UDC: 616.716.4-006.6-089.843

Good vascularization, sufficient three – dimensional bone size, similarity to the mandibular shape, facility of forming and transfering of the flap without compromised vascularization, as well as minimal donor site morbidity and the possibility of two medical teams (maxillofacial and microsurgical) working at the same time to shorten the operation time, are the greatest advantages of vascularized osseous composite free flaps.

The purpose of this paper is to present our experience with oromandibular defect reconstructions with microvascular osteocutaneous free flaps from foot, lower leg and foream, the osseous parts of which are the second metatarsal bone, the fibula and the radius.

Materials and methods

From January 1990 to December 1991, twenty previously untreated patients with oral cancer were operated at Department of Maxillofacial-Surgery, Clinical Hospital Center in Rijeka.

All treated patients were males, 40 to 70 year old. Fourteen of them were smokers consuming more then twenty cigarettes per day; five patients gave up smoking, while one of them was a non smoker. Nine of them were alcoholics, nine patients consumed alcohol occasionaly, and two of them were abstinents.

Half of them suffered from hypertension and various cardiac disturbances; two patients sufferred from obstructive chronic respiratory disturbances and one from mild form of diabetes.

All tumors were histologically confirmed as planocellular carcinomas.

Out of twenty operated patients, fifteen were classified as T4 N1 M0, four as T4 N2 M0 and one as T4 N3 M0.

Tumors were localised on the floor of the mouth and the tongue in nine cases, the flooer of the mouth and the mandibular gingiva in six, retromolary in four, and on the buccal mucosa, floor of the mouth and the mandibular gingiva in one.

All tumours involved the mandibular bone. Ablative part of operation was performed by maxillofacial surgeons, while the primary reconstruction was carried out by team of microvascular surgeons.

All patients underwent Commando operation, i.e., the radical tumor excision, partial resection of mandible and the radical neck dissection together with neck blood vessels (arteries and veins) preparation for microsurgical anastomosis. A part of mandibular corpus was resected in all 20 patients; in two of them, resection was extended to the mandibular ramus and in one nearly whole was resected. Seven patients underwent tracheotomy.

Microvascular osteocutaneous free flaps were taken from feet – second metatarsal bone (Figure 2) in eight patients, from lower leg – fibula (Figure 3) in five and from the forearm – radius

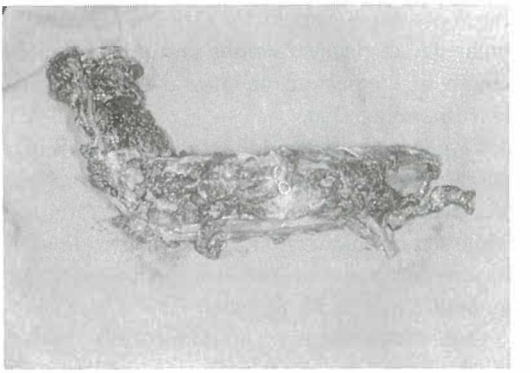

Figure 1. Bone angulation of the microvascular osteocutaneous free flap.

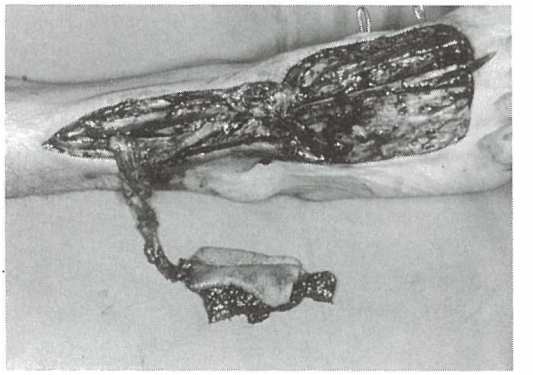

Figure 2. Metatarsal microvascular ostcocutaneous free flap.

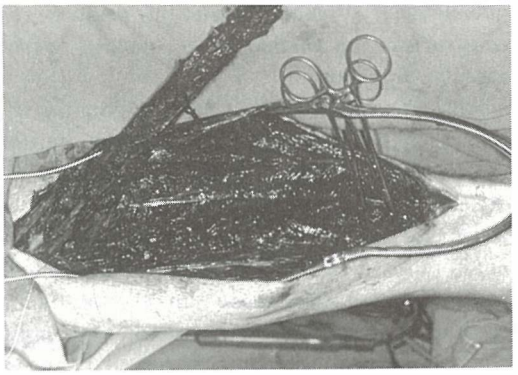

Figure 3. Fibular microvascular osteocutaneous free flap.

(Figure 4) in seven patients. Selection of particular flap depended on the extent of the oromandibular defect.

Microvascular osteocutaneous free flap from the foot usually served for the smallest mandibular defect reconstructions because of limited length of the second metatarsal bone and the corresponding skin.

Larger mandibular defects were reconstructed with radial microvascular osteocutaneous free flaps usually taken from the left forearm, while fibular microvascular free flaps were used for reconstruction of defects when almost whole mandible had to be replaced.

Osteosynthesis was predominantly carried out by a wire or a plate with screws. Seventeen patients underwent bone angulation (Figure 1) in order to from the angle of mandibule and chin. It was done by a traiangular osteotomy, and the angulation achieved, was fixed by two wires. Intermaxillary fixation was set in these cases.

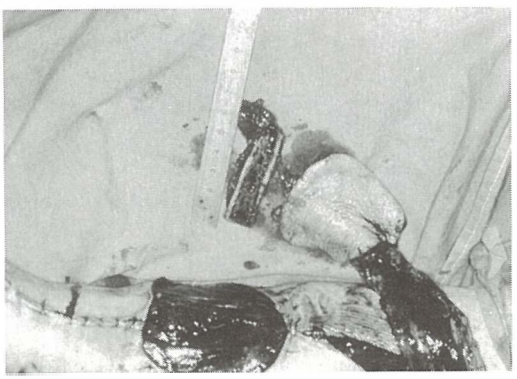

Figure 4. Radial microvascular osteocutaneous free flap.

Soft tissue defect in the oral cavity was covered with the skin from the microvascular osteocutaneous free flap.

Anastomoses were carried out to the superior thyroid and the facial arteries and the external jugular and the facial veins (Table 1).

Two patients underwent double vein anastomosis. Anastomoses to arteries and facial veins were always performed at the opposite side of the neck from the postoperative defect.

Donor site skin defects were covered with Thiersch grafts. Forearm defects were successfully closed with local flaps.[2] Immobilization was performed each time using a plaster splint and the Kirschner wire splint on the foot.

All the flaps were followed up regularly in the course of the first five consecutive days. Further controls were done by maxillofacial surgeons.

Table 1. Recipient blood vessels of the neck.

Blood vessels	Number	%
Arteries		
thyreoidea superior	16	80
facialis	4	20
Total	20	100
Veins		
jugularis externa	16	73
facialis	4	18
transversa colli	2	9
Total	22	100

Table 2. Eficiency of microvascular osteocutaneous free flap transfers.

Flap	Successful reconstruction – accepted flap		Ineffectual reconstruction – rejacted flap	
	Number	%	Number	%
Metatarsal (n = 8)	8	100	0	0
Radial (n = 7)	6	86	1	14
Fibular (n = 5)	4	80	1	20
Total (n = 20)	18	90	2	10

Results

Out of 20 microvascular osteocutaneous free flap transfers, 18 (90 %) were successfully done while two of them (10 %) failed (Table 2).

Microvascular osteocutaneous free flap transfers were followed by various complications (Table 3).

Except partial dehiscence at the flap border the most frequent complications during the postoperative course were neck infections and fistulae appearing in connection with them.

Dehiscences at the flap border were refreshed and sutured. Infections were successfully treated by high doses of antibiotics. Fistulae were closed with local flaps in five patients, while the pedicled flap (latissimus dorsi) was used once for the fistula closure.

Intraorally exposed bone or osteosynthetic material was covered by local mucous membrane flap under local anestesia.

All operated patients were monitored for blood circulation in the flap. Revision of microvascular anastomosis during the 24 hours was needed in four patients.

Two flaps falied and were taken away while the defects were covered with pedicled flaps (pectoralis major – myocutaneous flap).

Superficial marginal necrosis, which occured in three patients, healed secondarily without any consequences.

We had more donor site complications, especially on the forearm after the radial microvascular osteocutaneous free flap transfer, including three fractures of the radius. These fractures occurred as the consequence of the specific osteotomy, the ischemic changes in the remaining radius, the age of patients and poor postoperative immobilization. Decay of skin cover with Thiersch graf at the same donor site during the postoperative course led to denudation of tendons in four patients. Shrivelling, weakened mobility and impaired finger grip occurred. Denuded tendons were covered with new Thiersch graf. We tried to slove the defect of soft tissues of the forearm with local flaps, after the flap had been taken. In this way better results were obtained.[2]

The aforementioned complications in our series resulted in weakened mobility, grip and pressure of fingers up to 50 % in six patients after the radial microvascular osteocutaneous free flap had been transferred. Eight patients developed gait disturbances; four of them after the fibular microvascular osteocutaneous free flap transfers and the remaining four who underwent the transfer of the metatarsal microvascular osteocutaneous free flap. These disturbances appeared as the consequence of ischemia in the foot after removal of peroneal and dorsal metatarsal arteries.

The opertion lasted from 6 to 10 hours and was followed by several microvascular revisions and postoperative complications. Two medical teams always worked together.

The time of hospitalization depended on the operation efficiency and postoperative complications. Other factors influencing the duration of hospitalization were age, general condition and other diseases of the operated. The shortest hospitalization time among the patients who underwent Commando operation and the primary reconstruction, was 10 days.

All the presented patients have been regu-

Table 3. Postoperative complications following microvascular osteocutaneous free flap transfers.

Complications	Number	%
At the recipient site		
Partial dehiscence at the flap border	9	45
Neck infection	6	30
Fistula	6	30
Intraoral bone exposure	2	10
Intraoral plate exposure or the wire of osteosynthesis	3	15
Microvascular		
Revision of microvascular anastomoses	4	20
Partially failed flap	3	15
Completely failed flap	2	10
At the donor site		
Haematoma	2	10
Seroma	2	10
Infection	4	20
Gait disturbances	8	40
Denuded arm tendons	4	20
Fracture of the radial bone	3	15

larly controlled, being all alive. In two of them with microvascular osteocutaneous free flaps (radial and fibular), where the defect was subsequently reconstructed by pedicled flaps, functional and cosmetic results were poor.

In the remaining 18 patients, the appearance, speech and swallowing were satisfying.

Four of them have been wearing lower protheses accompanied by more or less disturbances.

Metastases were found on the opposite side of neck in three patients in the time interval from 6 to 12 months. Two of them underwent functional and one radical neck dissection.

Discussion

When malignant aggressive disease, such as the oral cancer, is in question, the progressive invasion and erosion of the face represent the worst problem.

Radical resection and reconstruction of the defect is the best choice for the patient.[3]

Reconstruction of the anterior mandibular part has been considered to be necessary by majority of head and neck surgeons from the esthetic and functional point of view. Considerations about the lateral defect reconstruction differ.[1]

Comparing results of performed reconstruction of the defect with those without it, better function has been shown in patients with primary reconstruction of the mandibular defect with microvascular osteocutaneous free flap.[4]

The second metatarsal bone, the radius and the fibula have been used for the mandibular reconstruction, always together with a part of skin for a defect reconstruction in the oral cavity in our series of microvascular ostecutaneous free flaps.

Drawing a parellel among those tree aforementioned flaps regarding the quality of the bone and skin, the length and vessel diameter of the pedicle, donor site complications and the possibility of two medical teams working together, the following can be concluded: Fibular microvascular free flap provides the highest and the best quality in all tree dimensions, longitudinally especially. This flap is the best for the mandibular bone defect reconstruction only[5] while the skin is of poorer quality compared to the remaining two flaps described. Complications and morbidity of the donor site are less frequent than in the remaining two.

Radial microvascular osteocutaneous free flap has been frequently used in oromandibular reconstruction.[6, 7]

A bone of 10 to 12 cm is of low quality and insufficiently shaped in all three dimension, being therefore bad for the mandibular reconstruction. The skin is of high quality, thin and suitable for reconstrucion of the soft tissue defects in the oral cavity.

Donor site complications after the radial flap transfer are the severest, being caracterized with frequent fractures of the radius. Of seven presented patients in our series in three of them developed a radial fracture (43 %); Soutar and Widdowson[5] 14 %; Boorman et al.[8] 31 % and Urken[1] 23 %.

Metatarsal microvascular ostecutaneous free flap is one of the first that has been used for the oromandibular reconstruction (Rosen et al., 1979)[9] providing the shortest bone (7 to 10 cm) of satisfying dimensions. The skin is of high quality, convenient for soft tissue defect reconstruction in the oral cavity.

Donor site morbidity is significant and of long duration. Fifty percent of patients from our series developed gait disturbances. Problems connected with this flap are greater than benefits.

All the three vascular osteocutaneous free flaps observed, have been equally suitable regarding the length and blood supply of the pedicled flap and the possibility of two medical teams working at the same time.

References

1. Urken ML. Composite free flap in oromandibular reconstruction. *Arch Otolaryngol Head Surg* 1991; **117:** 724–32.

2. Juretić M, Car M, Zambelli M. The radial free flap: our experience in solving donor site problems. *J Cranio Maxillo Facial Surg* 1992; **20:** 184–6.

3. Vaughan E. The radial forearm free flap in orofacial reconstruction: personal experience in 120 consecutive cases. *J Cranio Maxillo Facial Surg* 1990; **18:** 2–7.

4. Urken ML, Weinberg H, Viskery C, Buchbinder D, Lawson W, Biller F. Oromandibular reconstruction using microvascular composite free flaps. *Arch Otolaryngol Head Neck Surg* 1991; **117:** 733–44.

5. Hidalgo D. Fibula free flap: a new method of mandible reconstruction. *Past Reconstr Surg* 1989; **84:** 71–9.

6. Soutar D, Widdowson WP. Immediate reconstruction of the mandible using a vasculared segment of radius. *Head Neck Surg* 1986; **8:** 232–46.

7. Swanson E, Bovd JB, Mankelow R. The radial forearm flap: Reconstructive applicationes and donor site defects in 35 consccutive patiens. *Plast Reconstr Surg* 1990; **85:** 258–66.

8. Boorman JG, Brown JA, Sykes PJ. Morbidity in the forearm flap donor arm. *Br J Plast Surg* 1982; **40:** 207–12.

9. Roscn I, Bell M, Barron P, Zuker R, Manketelow R. Use of microvascular flaps including free osteocutaneous flaps in reconstruction after composite resection for radiation – recurrent oral carcinoma. *Am J Surg* 1979; **138:** 544–9.

Radiol Oncol 1994; 28: 194-9.

Diagnosis and treatment of malignant mesothelioma of the peritoneum

Erika Brenčič,[1] Marjeta Stanovnik,[2] A. Višnar-Perović[1]

[1]Institute of Diagnostic and Interventional Radiology, Clinical Center, Ljubljana, [2]Institute of Oncology, Ljubljana, Slovenia

Six patients with malignant mesothelioma of the peritoneum (MMP) diagnosed by US and CT between 1982 and 1992 are presented. MMP was suspected on the basis of diffuse changes in the peritoneum, omentum and mesenterium. The diagnosis was confirmed by cytological and histological examinations. The very suspicion of MMP based on US and CT alone, without the presence of typical symptoms, may shorten the time to definitive pathomorphological diagnosis.
All patients were treated by combined chemotherapy (ChT), whereas four also underwent surgery and irradiation (RT). Four patients have died and two are alive with disease. A relatively prolonged survival was achieved only in two patients receiving multimodal therapy; this was probably influenced by the patients' youth, good performance status at the beginning of therapy and prognostically favourable MMP subtype.

Key words: mesothelioma, peritoneal neoplasms

Introduction

Malignant mesothelioma of the peritoneum (MMP) is a rare primary malignant disease. The disease may affect the peritoneum, though its pleural invasion is more common.[1, 2] Men exposed to a contact with asbestos are affected in a greater percentage. It can be expected that the expanding development of asbestos industry will result in an increased number of new cases of this disease. The latent period from the exposure to asbestos and the onset of disease is know to be very long. The mechanism of asbestos action upon the peritoneum has not been explained yet.[3]

Symptoms of this disease show great diversity, ranging from colic pains to loss of body weight. Clinical examination may reveal ascites with or without palpable tumor masses.

The diagnosis of MMP is often established only after explorative laparotomy or on autopsy.

Classical radiological methods are insufficient as they can image different stages of changes in the intestinal mucosis, without actually being able to explain the organic cause of obstruction. The establishing of correct diagnosis is rendered very difficult as the disease closely resembles the clinical picture of abdominal carcinomatosis and carcinoid involvement.[4, 5]

Correspondence to: Erika Brenčič, MD, PhD, Institute of Diagnostic and Interventional Radiology, Clinical Center, Zaloška c. 7, 61105 Ljubljana, Slovenia. Fax: + 38 61-13-10-44.

UDC: 616.381-006.32-07-08

US and CT are noninvasive diagnostic methods able to present small or diffuse peritoneal, omental and mesenterial changes, with exclusion of a metastatic involvement. US- and CT-guided aspiration biopsies for cytological examination help to provide fast and accurate diagnosis.[6, 7, 8]

Systemic or intraperitoneal (IP) ChT in combination with surgery or radiotherapy (RT) resulted in a prolonged survival in a selected group of patiens.[9, 10, 11] According to the experieuces of other centers[9, 12] longer survival can be attributed to the following factors: sex, early stage of disease, younger age, histological subtype of MMP and good performance status at the beginning of treatment.

Materials and methods

In the period from 1982 to 1988, 51 patients with malignant mesothelioma were registered by the Cancer Registry of Slovenia at the Institute of Oncology in Ljubljana.[13]

The success of treatment and diagnosis was reviewed in 6 patients with MMP treated during the years 1982–1992 at the Institute of Oncology.

Table 1. Basic data on the six studied patients.

Pat. No.	Age Sex	Asbestos exposure	Mode of biopsy and finding	Site
1	32/M	possible	Biopsy on lapt. tubulopapillary MMP subtype	Peritoneum
2	49/M	yes	Biopsy on laps. epithelioid MMP subtype	Peritoneum
3	56/M	no	Aspir. biopsy of the inguin. lgl	Peritoneum, pleura, lung, inguin. lgl
4	27/M	no data	Biopsy on lapt. multicentric MMP subtype	Peritoneum inguin. lgl
5	56/M	yes	Aspir. biopsy of the ascites	Peritoneum
6	47/M	yes	Aspir. biopsy of the ascites	Peritoneum

Abbreviations: lapt. – laparotomy; laps. – laparoscopy

All patients were males in the mean age of 44 years. Exposure to asbestos was confirmed in 3 of 6 patients. In one patient such exposure was possible whereas in another one it was excluded. No data on possible exposure to asbestos were available for one patient (Table 1).

In Pat. 1 and Pat. 4 the histologic diagnosis was confirmed by biopsy on laparotomy, and in two patients by aspiration biopsy of the ascites. Pat. 3 underwent aspiration biopsy of the inguinal lymph nodes, whereas Pat. 2 had the diagnosis confirmed by biopsy on laparoscopy (Table 1).

Epithelial subtype of MMP was established in Pat. 1 and Pat. 2. Multicystic subtype of MMP was histologically confirmed in Pat. 4. In the remaining three patients aspiration biopsy failed to identify the histologic subtype. The diagnosis of MMP was confirmed by autopsy in all four deceased patients.

In five patients the initial CT examination was carried out at the time of diagnosis, whereas Pat. 1 had CT performed only on the follow up after the initial therapy.

CT examination was always performed with 5-sec. exposure time and 16 mm distance between individual sections through the entire abdominal cavity. Intestinal loops were imaged by means of Gastrografin, a contrast medium for oral application. For exclusion of metastases, the results of investigations for the assessment of peritoneal, omental and mesenterial involvement, possible presence of ascites and changes in other organs were considered.

Separate CT examinations of the thorax were not performed, though the pleural space above the diaphragm was imaged in all patients.

Peritoneal involvement was found in all cases; in Pat. 3 and Pat. 4 the disease was present in the inguinal lymph nodes, whereas in the former patient pleural and pulmonary involvement was found as well (Table 1).

Debulking surgery was performed in Pats 1, 2, 4 and 5. Two patients were not subjected to surgery, one because of pulmonary and pleural dissemination, and the other because of numerous peritoneal tumor infiltrations (Table 2).

Table 2. Treatment sequence and outcome.

Pat. No.	Treatment sequence	No. of surg.	Interval(mos) From dg to death	Interval(mos) From compl. th to last follow-up	Outcome
1	lapt (bx)iv.ChT > RT > iv.Cht > lapt(ex) > ip.ChT > lapt > lapt	4	90	10	dead
2	laps(bx) > iv.ChT > RT	1	4	1	dead
3	iv.ChT	0	10	7	dead
4	lapt(deb) > iv.ChT > RT > iv.ChT	1	33	15	alive with disease
5	iv.ChT > lapt(deb) > iv.ChT > RT	1	21	11	dead
6	iv.ChT	0	5	–	alive with disease

Abbreviations:
lapt – laparotomy; laps – laparoscopy; iv.ChT – intravenous chemotherapy; ip.ChT – intraperitoneal chemotherapy; RT – radiotherapy; bx – biopsy; deb – debulking surgery; ex – explorative surgery; > – followed by

Table 3. No. of cycles, combination of drugs and irradiation.

Pat. No.	No. of cycles and drug. comb. iv.ChT	ip.ChT	Abdom. RT TD-cGy	Fract. cGy	Duration (days)
1	11/ADM, CTX, CDDP 7/ADM, VP16, CDDP 6/CDDP, MIT, IFO	1/ADM CDDP	2.980	80/100	11/21
2	2/MIT, 5-FU	0	3.000	100	30
3	5/ADM, CTX, CDDP	0	0	0	0
4	6/ADM, CTX, CDDP 5/MIT, C	0	3.000 only pelvis	300	10
5	3/VLB 3/ADM, CTX, IFO	0	3.450	150	23
6	2/MIT, CDDP, VCR	0	0	0	0

Abbreviations:
ADM – doxorubicin, CTX – cyclophosphamide, CDDP – cis-platin, VP16 – etoposide, MIT – mitomycin, 5-FU – fluorouracil, C – carboplatin, VLB – vinblastine, VCR – vincristine, IFO – ifosfamide

All 6 patients were given a systemic chemotherapy (ChT). Pat. 1 received a single intraperitoneal (i. p.) application of ChT which was ineffective (Table 3).

Different combinations of cytostatics and different numbers of cycles were used (Table 3).

Four patients were also irradiated. Three of these received TD 2980–3450 cGy to the whole abdomen, whereas in Pat. 4 the irradiation field was restricted to pelvis alone (Table 3).

Follow up included chest X-ray, US, CT of the abdomen and cytologic examination of the ascites. US-guided aspiration biopsy was used in order to evaluate possible progression of the disease.

Results

The initial CT examination revealed peritoneal involvement in 5 patients by imaging the thickening and irregular contours of the peritoneum. Pat. 1 had the initial CT performed only on the first follow-up examination after therapy. The thickened peritoneum found on that occasion (Figure 1) persisted throughout the follow-up of 90-month lasting course of disease. When comparing the results of all follow-up examinations, only the quantity of ascites was found to have varied. Tumor masses that appeared occasionally did not exceed 5 cm of size (Figure 2) and were located in different sites, most fre-

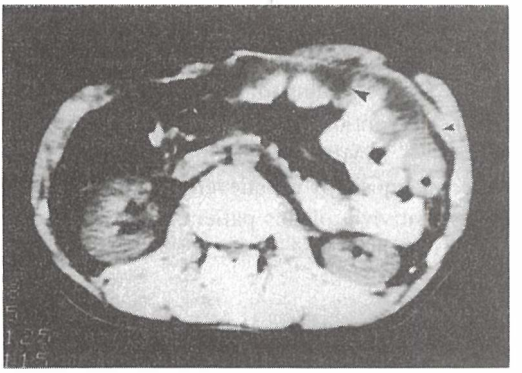

Figure 1. CT image of peritoneal thickening (small arrow), ascites, and minor tumors (big arrow).

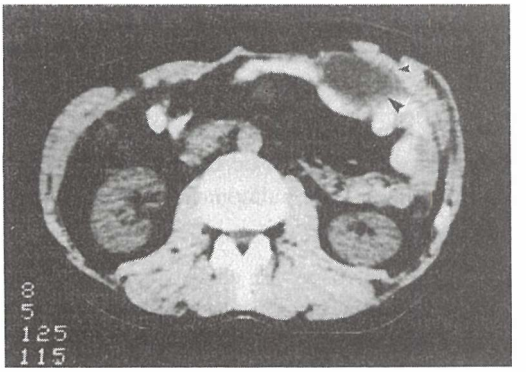

Figure 2. CT image of a soft-tissue tumor (big arrow) situated between the intestinal loops and the abdominal wall; thickened peritoneum (small arrow).

quently between intestinal loops. Associated with further progression of the disease, these tumors obstructed the intestinal loops and consequently caused the patient's death.

On the first examination in three patients tumors larger than 5 cm and the density of 20–30 HE were found. At that time, ascites was present in 5 patients, its density ranging between 10–20 HE (Figure 3). In five patients increased distance between the anterior abdominal wall and intestinal loops could be seen due to ascites and omental changes (Figure 4).

Thickened mesenterium was found in all patients. In two of them this could be ascribed to the stellate mesenterial changes caused by the presence of small tumors and their consequential obstruction of blood supply. None of the patients had any pleural outflow at the time of the first CT examination. Pat. 3 and Pat. 4 showed evidence of lymph node involvement (Table 1), whereas changes in the pleura and lung of Pat. 3 appeared soon after the beginning of therapy.

In Pat. 1 a combination of different treatment modalities (Table 3) resulted in a 90 month survival. The patient died because of progressing disease and ileus. Pat. 5 died 21 months after the diagnosis, despite the combined therapy. Only a short-lasting remission was achieved in 2 patients who survived 4 and 10 months respectively. Two patients are still alive, one of them with palpable tumors in the peritoneum and inguinal lymph nodes. His disease, however, shows tendency of stagnation, and the patient has been off the specific treatment for

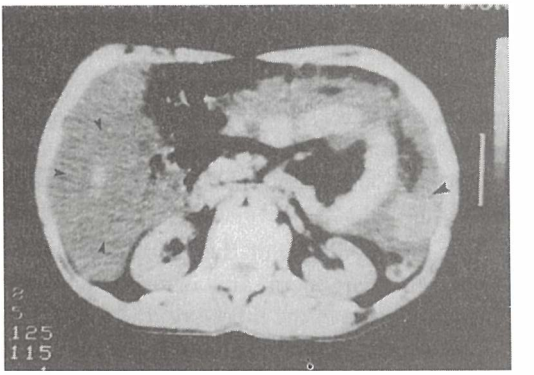

Figure 3. CT image of a soft-tissue tumor (big arrow) and ascites (small arrow).

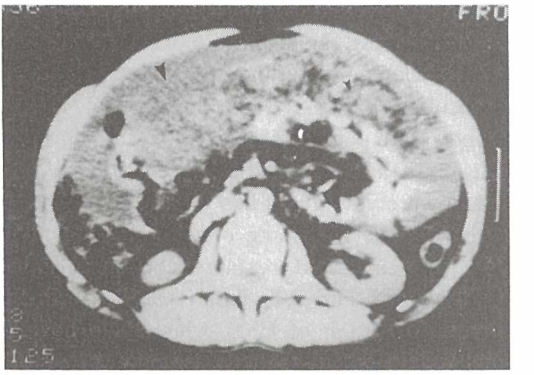

Figure 4. Ascites (big arrow) and changed omentum (small arrow) imaged on CT examination.

15 months already. The other patient had been receiving ChT for 5 months, but the only therapeutic effect achieved was a decrease of ascites (Table 3).

Toxic side effects after ChT and RT were moderate. No life-threatening adverse reactions occurred during therapy.

Discussion

MMP can be successfully diagnosed by US and CT, when these are complemented with aspiration biopsy. The diagnosis or suspicion for MMP is based on the presence of ascites, and peritoneal, omental and mesenterial changes which can be imaged on CT. CT examination speeds up the diagnostic procedure and helps to provide the final diagnosis of MMP.

In some of our patients follow-up by means of CT was able to confirm the presence of disease (tumors and ascites) during therapy. In others, however, CT failed to evidence the disease, though microscopic peritoneal changes detectable only by aspiration biopsy might have been present.

Treatment results of the presented patients with MMP are poor and in agreement with those reported in the literature: the duration of survival is 2, 12 and 18 months after diagnosis.[3, 8, 14]

Patients with well differentiated papillary MMP and cystic form of MMP were found to have a longer survival even without treatment.[14]

Considering the small number of studied patients, the combined therapy in Pat. 1 and Pat. 4 resulted in 33 and 90 month survival, respectively. Both patients had prognostically favourable epithelial and multicentric MMP subtype. They were young and had a good performance status at the beginning of treatment. In both cases the combined treatment comprised debulking surgery and RT. Pat. 1 received a single i. p. application of ChT, which could not be continued owing to ileus. The patient died 90 months after the beginning of treatment. Pat. 4 has been without a specific therapy for 15 months, and is alive with evidence of disease 33 months after diagnosis.

At the beginning of treatment, Pat. 5 was over 40 years old, and had a residual tumor of unknown MMP subtype; he died 21 months after diagnosis. It is believed that the relatively longer survival of this patient could be attributed to undiagnosed, possibly favourable MMP subtype.

In two of six patients, short survival (4 and 10 months respectively) was due to their rapid course of disease. Combined therapy was ineffective also because of unfavourable prognostic factors at the beginning of therapy, though one of them had the epitheloid MMP subtype. Pat. 6 has been only receiving ChT for 5 months now.

It is interesting to note that one of the patients was not exposed to asbestos, and died with pleural and pulmonary involvement 10 months after diagnosis.

Owing to unspecific clinical symptoms and late establishment of correct diagnosis, the patients with MMP are generally admitted for treatment with highly advanced stages of the disease.[3] Therefore, the treatment intent is often limited to palliation.

In their study, though it was carried out on a smaller number of patients, Lederman et al. reported that a longer survival had been achieved by combined therapy.[10, 11] The survival of patients with combined radical therapy is longer than that of patients receiving palliative treatment only. Based on the correlation of our findings with the results of other studies,[14] we believe that MMP is possibly curable in patients with favourable prognostic factors.

Considering that this is a rare disease, the number of patients in individual studies is generally small. Though being rather low, the number of patients with longer survival points out the need for multicentric studies to be carried out, so that the optimum treatment for MMP could be determined on a larger population of patients.

References

1. Haskell CM. *Cancer Treatment,* 3rd Edition, W. B. Company 1990; **188:** 300.
2. Suzuki Y. Pathology of Human Malignant Mesothelioma. *Seminars in Oncology* 1981; **81:** 268.
3. Plaus WJ. Peritoneal Mesothelioma. *Arch Surg* 1988; **123:** 763.
4. Whitley NO, Brenner DE, Antman KH, Grant D, Aisner J: CT of Peritoneal Mesothelioma. Analysis of Eight Cases. *AJR* 1982; **138:** 531.
5. Granke SD, Ellis JH, Richmond DB. CT Findings of Hipervascular Malignant Peritoneal Mesothelioma. *Computerized Radiol* 1987; **11:** 91.
6. Reuter K, Raptopoulos F, Krolikowski FJ, D'Orsi CJ, Graham S, Smith EH: Diagnosis of Peritoneal Mesothelioma. Computed Tomography, Sonography and Fine-needle Apsorption Biopsy. *AJR* 1983; **140:** 1189.
7. O'Neil JD, Ros PR, Storm BL, Buck JL, Wilkinson EJ. Cystic Mesothelioma of the Peritoneum. *Radiology* 1989; **170:** 333.
8. Pui-Li Y, Guico R, Parikh S, Chin S. Cystic Mesothelioma of the Retroperitoneum. *J Clin Ultrasound* 1992; **20:** 65.
9. Antman KH, Klegar KL, Pomfret EA, Osteen RT, Amato DA, Larson DA, Corson JM. Early Peritoneal Mesothelioma. A Treatable Malignancy. *Lancet* 1985; **2:** 977.
10. Lederman GS, Recht A, Herman T, Osteen R, Corson J, Antman KH. Long-term Survival in Peritoneal Mesothelioma, The Role of Radiotherapy and Combined Modality Treatment. *Cancer* 1987; **59:** 1882.
11. Lederman GS, Recht A, Herman T, Osteen R, Corson J, Antman KH: Combined Modality Treatment of Peritoneal Mesotheliomas. *NCI Monogr* 1988; **6:** 321.
12. Antman KH, Shemin R, Ryan L, Klegar K, Osteen R, Herman T, Lederman G, Carson J. Malignant Mesothelioma. Prognostic Variables in a Registry of 180 Patients, the Dana-Farber Cancer Institute and Brigham and Women's Hospital Experience over Two Decades, 1965–1985. *J Clin Oncol* 1988; **6:** 147.
13. Cancer Incidence in Slovenia 1988. Institute of Oncology, Ljubljana, Report No. 30, Ljubljana, 1992.
14. Antman KH, Pass HI, Recht A. Benign and Malignant Mesothelioma. Cancer: *Principles and Practise of Oncology.* Third edition. De Vita V. T. Jr. et al., Ed.: Philadelphia, Lippincott 1989: 1399.

Radiol Oncol 1994; 28: 200-4.

Human papilloma viruses 16 and 18 in patients under 40 years of age with operable squamous cancer of the uterine cervix

Marjetka Uršič-Vrščaj,[1] Jurij Lindtner,[1] Jožica Marin[2]

[1]Institute of Oncology, [2]Institute of Microbiology, Ljubljana, Slovenia

Numerous investigations support the belief that human papilloma viruses (HPV) play an important role in the etiology of cervical cancer. Our study carried out in 31 patients with operable squamous cervical carcinoma (SCC), who were under 40 years of age, was aimed to investigate the incidence of HPV 16 and 18 infection in this group of patients, their sexual behavior as well as the efficacy of Slovene gynecological service in cervical cancer detection. HPV 16 was found in 67% and HPV 18 in 22% of our patients, which is consistent with the data reported by other authors.

Key words: human papilloma viruses cervix neoplasms-etiology

Introduction

In the majority of western countries the incidence as well as the mortality of SCC have been gradually decreasing since 1950, as a result of their carefully planned and systematically practised strategy for early detection of this disease. On the other hand, the facts that cervical cancer related deaths are the most frequent in women under 40 years of age, and that an increasing trend in SCC incidence has been reported in some areas in that particular age group, should not be ignored.[1,2] A prerequsite for a successful mass screening for precancerous conditions of the uterine cervix and non-invasive cancer is certainly the simple and painless method of cervical smear taking at the time of gynecological checkup. Papanicolaou test, or shortly "Pap test" (PT) was introduced in 1941 by Papanicolaou and Traut, and it has become a synonym for a complete gynecological examination. Though the value of PT is indisputable, some drawback of this diagnostic method nevertheless need to be pointed out. The most relevant is certainly the fact that cytomorphology is unable to foretell which of the seemingly indistinguishable (identical) precancerous changes will sooner or later turn into intraepithelial or invasive carcinoma.

The changes caused on cells by papilloma viruses were described already in 1933. Due to the lack of suitable cultures (growth media) and some serological tests, it was only after 1970 that a possible correlation between HPV and cervical cancer became apparent on the basis of several experimental, clinical and epidemiological studies. Advances in molecular biology, particularly the discovery of polymerase reaction (PCR) which is the most sensitive method of HPV detection (as compared to others such as in situ hybridization and dot blot hybri-

Correspondence to: M. Uršič-Vrščaj, MD, MSc, Institute of Oncology, Zaloška 2, 61105 Ljubljana, Slovenia.

UDC: 618.146-006.6-022:616.988.15

dization), resulted in the isolation of over 60 different HPV genotypes. The types 6 and 11 are associated with benign changes in the uterine cervix. Their presence most probably does not represent an increased risk of cervical cancer. HPVs 16, 18, 31 and 33 are, on the other hand, considered to be oncogenic HPV types, as they can be frequently seen in intraepithelial cervical dysplasias (CIN II*), in severe dysplasias or in noninvasive squamous carcinoma of the uterine cervix (CIN III) and invasive SCC. According to some data, HPV 16 and 18 can be found in 1.5 % of healtly women, in 20–40 % of patients with squamous intraepithelial changes (CIN I), in 60–80 % of patients with changes described as CIN II and III, as well as in 80–90 % of patients with SCC.[1, 3]

The present report was aimed to explain the role of certain suspected risk factors in the sexual behavior of patients, believed to be associated with the appearance of SCC. We also wanted to establish the number of gynecological checkups performed within two years before diagnosis, as well as the number of cytological smears and cytological findings in the same period, and to determine the percentage of patients with HPV 16 and 18.

Patients and methods

The study included 31 patients younger than 40 years, who were treated for operable squamous carcinoma of the uterine cervix at the Department of Gynecology of the University Clinical Center, and at the Institute of Oncology in Ljubljana, in the period from February 1990 to February 1992.

The data were collectec by means of a questionnaire comprising general as well as specific questions related to the patient's life syle, her gynecological and reproductive history and sexual behavior (age at first sexual intercourse, the number of partners in the last two years), and the type and duration of contraception used. We also collected the data on patients' imminent gynecological problems just before diagnosis and on the number of cytological smears taken during the last two years before diagnosis.

Each patient had cervical smear for the determination of HPV 16 and 18 taken on gynecological checkup. Tests for the presence of HPV 16 and 18 ware done at the institute of Microbiology in Ljubljana. The serum levels of vitamin A and beta-carotene were also determined in each patient in order to establish possible correlation between a decrease in these values and the appearance of SCC metastases.

The patients were followed up for 12 to 36 months after the diagnosis.

Sample processing

Smear samples were immersed in 2 ml of phosphate buffer saline (PBS) at 7.4 pH, and immediately taken to the laboratory for further processing. After the PBS immersed smears are well shaken on a vortex, the smears alone are removed while PBS with cells in centrifuged at 2000 rpm for 10 min. Using glass slides, two smears from the cell sediment are made for HPV-16 and HPV-18 determination. The slides are then air-dried and fixed in cold acetone for 7–10 min. Thus prepared samples can be stored at –20 °C for a longer period of time till hybridization, or the hybridization procedure can be started immediately.

Hybridization in situ *by means of biotinilated DNA probes*

Control slides for negative and positive check were included in eash test. The samples were first immersed in 0.3 % H_2O_2 in methanol for 15–30 min. in order to stop the activity of endogenous peroxydase; 3–5 ul of biotinilated

* It seems that the international classification of intraepithelial cervical neoplasms (CIN), which was accepted in 1973, will be replaced by a new classification from Bethesda, where CIN I stands for "low grade" squamous intraepithelial lesion, whereas CIN II and III denote "high grade" squamous intraepithelial lesion; this classification system is based on the degree of probability to develop cancer.

DNA probe were added to the smears, which were after wards covered with slips and heated at 100–105 °C on a metal plate for 10 min. with the aim to unbind the double-stranded target DNA.

The procedure is followed by 2-hr incubation in a humid chamber at 37 °C (the incubation can be continued overnight).

Afterwards, the slides are held vertically and rinsed in 2 × SSC with 0.1 % SDS addes until the slips fall off. The rinsing in repeated several times, finally with PBS.

Each smear is covered with 10 ul of streptavidin-peroxydase complex and left to incubate for 30 min. at 37 °C before being rinsed with PBS three times.

To obtain staining reaction, a drop of diamynobenzidine with addition of H_2O_2 substrate is put onto each smear. Thus prepared samples are incubated for 15 min. in dark at a room temperature.

The reaction is stopped by immersing the slides into distilled water. After contrast staining with Mayer's hematoxilin for 1–2 min, the samples weree rinsed in running water.

The slides were then dehydrated in growing concentrations of ethanol (to 100 %), and immersed in xylol; after adding a drop of PBS and glycerine (1 : 10), the slides were covered with cover slips.

Microscopic examination is done by means of a light microscope. We used the reagents produced by Epignost company.

Positive reaction is evident from brown-stained cell nuclei (Figure 1, image 30). There is no brown precipitate in the nuclei seen in negative reaction (Figure 2, image 28).

Results

The studied patients were younger than 40 years, their mean age being 33 years. The youngest patients was 20 years old.

As to education, 40 % of our patients had primary and vocational school; 55 % of their partners had equal educatioon (the same level of education).

Most patients did not suffer from defficiency of vitamin A in their food either during childhood or adolescence period. Over a half of the patients (58 %) were smokers; they smoked 20 cigarettes daily from 19 years on average.

The data on familial gynecological cancer burden were avialable for 3 patients only.

Most patients were married (80 %), two were divorced. Their mean age at marriage was 23 years.

Mean age at menarche was 13 years, and at the first sexual intercourse 17 years. In the last two years before diagnosis, all patients claimed having sexual relation with one partner only. Neither the data on urogenital diseases of partners nor on their past relationships SCC patients were available.

Two patients were nulliparous, whereas the rest gave birth twice at an average age of 21 years; 65 % of patients had abortions, the first one at an average age of 21 years. Only one patient had a spontaneous abortion.

65 % of patients were using hormonal contraceptives for 60 months on average, starting at 24 years of age. A half of the patients got IUD protection at an age of 26 years and were using if for 70 months on average. One third of the patients (32 %) were not gynecologically examined within the last two years before the diagnosis, though a majority of them (77 %) claimed that they attended regular annual checkups. In the last two years before the diagnosis, 73 % of the patients underwent one or two, and the rest more than two gynecological examinations.

Before the onset of disease, 45 % of the patients were free of any gynecological complaints while 35 % of them presented with recurrent vaginitis.

The main symptoms before diagnosis were bleeding (55 %), pain (50 %) and vaginitis (23 %). Four patients with SCC were pregnant at the time of diagnosis. 6 % of patients had no gynecological complaints.

Cytological smear (PAP) was not taken within two years before diagnosis in 35 % of patients, while 26 % had one and 32 % two smears taken. In almost a half of the patients with cytologic smear taken, this was done within the

year before diagnosis; 35 % of the smears were classified as negative.

The disease was diagnosed by biopsy in 71 % of the 31 patients, whereas the remaining ones underwent conization. On admission, 90 % of patients had Stage I, 81 % of these stage Ib of the disease.

81 % of patients were treated by surgery, and two received preoperative Ra applications. One fifth of the patients were also given postoperative radiotherapy.

Treatment-related complications

Minor urological complications were noted in 4 patients; two of these were treated by surgery and irradiation.

Three patients presented with recurrence (2 local, 1 distant), all of them within 6 months after primary therapy. Two patients died within the first year after diagnosis.

Normal vitamin A values were established in 84 %, and normal β-caroten in 44 % of patients.

The presence of HPV-16 was confirmed in 67 %, and of HPV-18 in 22 % of patients. Further, HPV-16 was found in 2 of three patients with uncontrollable disease, whereas HPV-18 presenmce was not established in any of those patients.

Discussion

According to the data of the Cancer Registry of Slovenia, in 1986 cervical cancer was still the sixth most frequent cancer in Slovene female population. From 1977 on, the crude incidence (15/100,000) has remained basically unchanged. A moderate increase (5.3 %) can be observed only among women of 60–64 year age group. Also the relevant mortality rates (5.6/100,000) in the past few decades have been virtually the same.

In 1960 a systematic screening for cervical cancer (CC) was started throughout Slovania. However, according to the data from 1966, such organized screening for precancerous changes and intraepithelial cervical cancer was available in some of the Slovene communes only. One of the criteria for the evaluation of the effectiveness of cervical cancer detection is the rate of established intraepithelial vs. invasive cancers; for Slovenia, this rate is 1.2. The small number of patients with intraepithelial CC and the high number or those with invasive CC, as well as concequentially high mortality due to this type of cancer call for a systematic screening for CC, supported by additional investigations, particularly in the litoral communes of Izola, Koper and Piran, and in Maribor. We presume that the poor results of screening for precancerous and early forms of CC in these regions are attributable to the so-far unexplained risk factors such as HPV, as well as to the specific life style believed to be associated with the etiology of CC.

Numerous studies have long been supporting the belief that the risk of SCC is in correlation with woman's sexual behavior (e.g. the first sexual relation before 18 yrs of age, numerous sexual partners), as well as with education level, marriage before the age of 18 yrs, a higher number of births and abortions, smoking, less frequent use of mechanical contraceptives, and oral contraceptive use.[4, 5] However, considering the results of multivariate analyses, any conclusion based solely on the presumed association of CC morbidity and sexual behavior is not convincing.[4–6] Our data are consistent with the reported as to the age at first sexual relation, education, smoking, number of abortions and the use of contraceptives. The fact that one third of patients fail to undergo a gynecological examination within the last two years before diagnosis points at the deficient organization of our gynecological service and monitoring of female population at risk, particularly since two thirds of cytological smears are confirmed as pathologic.[7]

According to the results of numerous studies, the two most relevant risk factors associated with the etiology of SCC are 1) the degree of dysplasia of the squamous epithelium of the uterine cervix, and 2) the presence of HPV infection.

Apart from their relevance for diagnosis,

HPVs – particularly HPV-18 – are also considered increasingly important for their prognostic value. It seems that HPV-18 is more virulent than other oncogenic HPVs, and that the fast-growing CC are presumably associated with the presence of HPV-18.[8–9]

It has been found that in adenocarcinoma HPV-18 is present in 30–60 % whereas HPV-16 is found in only 20 %. In SCC this proportion is just the opposite.[11–15]

Endocervical smear taking, which should be an integral part of every routine gynecological examination, together with testing for HPV-16/18 infection, might – at least to some extent – help to reduce the incidence of SCC. According to our data, the presence of HPV-16 was established much more frequently than the presence of HPV-18.

Contrary to our expectations, HPV-18 could not be found in patients with recurrent disease, which might be attributable to the lesser reliability of the methods used. Perhaps, this is also why the results are somewhat disappointing.

A new study using more advanced methods might help to resolve several interesting questions on possible association between HPV infection and gynecological neoplasms.

References

1. Helmerhorst TJM, Kenemans P, Walboomers JMM, Meijer CJLM, Lammes FB. Is HPV screening beneficial in the fight against cancer of the cervix uteri? *ECC Newslett* 1992; **1**: 15–6.
2. Jarrell, MA, Heintz N, Howard P et al. Squamous cell carcinoma of the cervix: HPV 16 and DNA ploidy as predictors of survival. *Gynecol Oncol* 1992; **46**: 361–6.
3. Ambros RA, Kurman RJ. Current concepts in the relationship of human papillomavirus infection to the pathogenesis and classification of precancerous squamous lesions of the uterine cervix. *Semin Diagn Pathol* 1990; **7**: 158–72.
4. Lorincz AT, Reid R. Association of human papillomavirus with gynecologic cancer. *Curr Opin Oncol* 1989; **1**: 123–32.
5. Nuovo GJ, Blanco JS, Lepzig S, Smith D. Human papillomavirus detection in cervical lesions nondiagnostic for cervical intraepithelial neoplasia: correlation with Papanicolau smear, colposcopy, and occurrence of cervical intraepithelial neoplasia. *Obstet Gynecol* 1990; **75**: 1006–11.
6. Pasetto N, Sesti F, de Santis L, Piccione E, Novelli G, Dallapiccola B. The prevalence of HPV16 DNA in normal and pathological cervical scrapes using the polymerase chain reaction. *Gynecol Oncol* 1992; **46**: 33–6.
7. Pompe Kirn V, Kovačič J, Primic Žakelj M. Epidemiological evaluation of cervical cancer screening in Slovenia up to 1986. *Eur J Gynecol Oncol* 1992; **13**: 75–82.
8. Kjaer SK, Engholm G, Teisen C et al. Risk factors for cervical human papillomavirus and herpes simplex virus infections in Greenland and Denmark: a population-based study. *Am J Epidemiol* 1990; **131**: 669–82.
9. Murthy NS, Sehgal A, Satyanarayana L et al. Risk factors related to biological behaviour of precancerous lesions of the uterine cervix. *Br J Cancer* 1990; **61**: 732–6.
10. Jones CJ, Brinton LA, Hamman RF et al. Risk factors for in situ cervical cancer: results from a case-control study. *Cancer Res* 1990; **50**: 3657–62.
11. Burnett AF, Barnes WA, Johnson JC et al. Prognostic significance of polymerase chain reaction detected human papillomavirus of tumors and lymph nodes in surgically treated stage IB cervical cancer. *Gynecol Oncol* 1992; **47**: 343–7.
12. Hording U, Stubbe Teglbjaerg C, Visfeldt J, Bock JE. Human papillomavirus types 16 and 18 in adenocarcinoma of the uterine cervix. *Gynecol Oncol* 1992; **46**: 313–6.
13. Macri CI, Cook NS, Walker JL, Berman M, Patton TJ, Wilczynski SP. Analysis of fine-needle aspirates for HPV by PCR may be useful in diagnosis of metastatic gynecologic malignancies. *Gynecol Oncol* 1992; **46**: 372–6.
14. Mandelblatt J, Richart R, Thomas L et al. Is human papillomavirus associated with cervical neoplasia in the elderly? *Gynecol Oncol* 1992; **46**: 6–12.
15. Palmer L, S Falkow. Selection of DNA probes for use in the diagnosis of infections disease. In: Kinsbury DT, S Falkow eds. *Rapid detection and identification of infectious agents*, New York, Academic Press, Inc., 1985: 211–8.

Radiol Oncol 1994; 28: 205-8.

Malignant lymphoma mimicking metastatic adenocarcinoma

Rastko Golouh and Andreja Zidar

Institute of Oncology, Ljubljana, Slovenia

We report a case of malignant lymphoma of the inguinal lymph node exhibiting gland-like structures and abundant fibrillary matrix, mimicking cytologically and histologically a metastatic adenocarcinoma. The only clue to the possible lymphomatous nature of the lesion was immunohistochemical study proving that this represented a B-cell non-Hodgkin's lymphoma, staining positively for leukocyte common antigen, L26(CD20), IgG and kappa light chain, supported by ultrastructural findings of filiform cytoplasmatic processes on the surface of tumor cells. We conclude that the possibility of malignant lymphoma should not be disregarded even when a tumor shows gland-like structures or cohesive growth pattern.

Key words: lymphoma, non-Hodgkin's; adenocarcinoma, diagnostic pitfall

Introduction

An unexpected malignant process in the lymph nodes, especially in instances where microscopic changes are not sufficiently informative to decide whether the malignant cells show epithelial, mesenchymal or lymphoid phenotype, is a frequent problem facing surgical pathologist. The presence of glandular formations in metastatic tumors is strongly suggestive of the diagnosis of metastatic adenocarcinoma. When rosette-like formations and abundant fibrillary matrix in poorly differentiated tumors are dominant, the diagnosis of neural tumors such as neuroblastoma or ganglioneuroblastoma are favored. In this report we describe a unique case of a malignant lymphoma with gland-like structures and abundant fibrillary matrix.

Correspondence to: Rastko Golouh, MD, PhD, Department of Pathology, Institute of Oncology, Zaloška 2, 61115 Ljubljana, Slovenia. Tel: 386 61 1322 099, Fax: 386 61 1314 180

UDC: 616.428-006.442-079:616-006.66

Case report

A 63-year-old female was observing a slowly growing lump in her left groin for 11 months. The swelling was interpreted by a surgeon as a hernia. Due to the acute pyelonephritis and transient renal insufficiency, the patient was admitted to a general hospital, where an aspiration biopsy of the inguinal tumor was performed and interpreted as a metastatic process of unknown origin. After admission to the Institute of Oncology, Ljubljana, an additional, 5.5 cm infiltrate of the left retroperitoneum was disclosed by laparoscopy. An excisional biopsy of a left inguinal lymph node was performed.

Materials and methods

Formalin and methacarn-fixed, paraffin embedded tissue sections were stained with hematoxylin and eosin, Giemsa, periodic acid Shiff and Kreyberg.

Immunohistochemical staining was carried out on paraffin-embedded sections using the avidin-biotin-peroxidase complex technique with antibodies to keratin wide spectrum, vimentin, alpha-smooth muscle actin, S-100 protein, leukocyte common antigen(LCA), T-markers CD3, CD43, CD45RO, B-markers CD 20, CD22, MB2, Ig, kappa and lambda light chains, and activation marker CD30. The immunohistochemical staining was done with appropriate positive controls.

For electron microscopic analysis, wet tissue fixed in 10% neutral formalin was used. It was washed in phosphate buffer at Ph 7.2, postfixed in buffered osmium tetroxide, and embedded in Epon LX-112. Thin sections were stained with uranyl acetate and lead citrate and examined with an Opton 9 electron microscope.

Results

The resected tissue was a solitary, enlarged lymph node, measuring $4.5 \times 4.0 \times 3.0$ cm. On the cut surface, the tissue was homogenous, pink, partially nodular. Necrosis was not evident.

Histologically, most of the lymphoid tissue was replaced by tumor cells forming cords, nests, several layers thick, with some solid areas and gland-like structures within the myxoid stroma (Figure 1). The residual small germinal centers were surrounded by neoplastic cells, with their mantles often infiltrated. In some areas tumor cells were dissociated in between prominent capillaries. The tumor cells were round to oval, with eosinophilic or clear cytoplasm. The nuclei were irregular, pleomorphic, sometimes multilobated, with one to several distinct nucleoli. In the cells of gland-like structures, the nuclei were situated peripherally.

The overall impression of the tumor resembled that of a metastatic, poorly differentiated adenocarcinoma with poorly developed myxoid stroma. However, stains for mucin and keratin were negative. In contrast, the tumor cells showed definite membrane positivity for LCA (Figure 2) and CD20 (Figure 3). The cells also showed monotypic staining pattern for IgG with a definite kappa ligh chain excess, thus confirming their B lineage. Staining for CD 22 and MB2 was negative. The fibrillar matrix, expressed mostly within gland-like spaces, also stained strongly with LCA and CD20. T-Cell

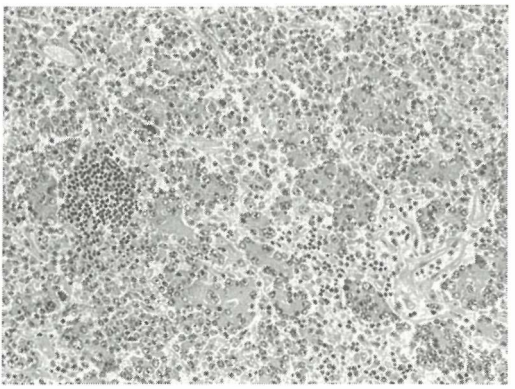

Figure 1. Lymph node almost diffusely replaced by solid and gland-like tumor cell clusters, separated by pale hypocellular areas with distinct capillaries.

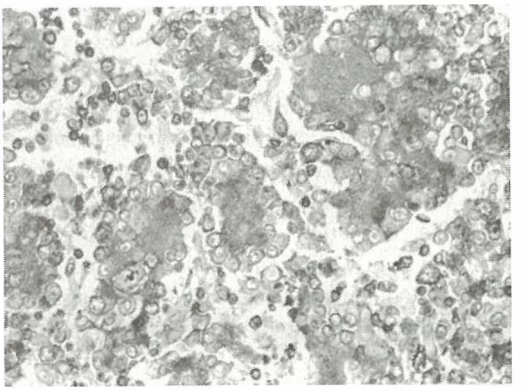

Figure 2. Clusters of tumor cells show membrane staining for leukocyte common antigen (CD 45 RB). Deeply stained central fibrillary matrix additionally supports the wrong impression of gland-like formations.

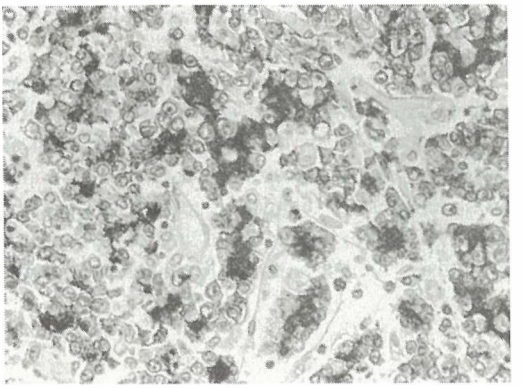

Figure 3. Tumor cells demonstrating strong reactivity for B-cell marker L26 (CD 20).

markers, actin, vimentin, S-100 protein and CD30 were all negative. Thus, the immunohistochemical studies clearly showed that the initial impression of metastatic carcinoma had been incorrect, and proved the condition to be a large cell non-Hodgkin's malignant lymphoma of B-cell lineage.

Ultrastructurally, the large lymphoid tumor cells displayed long, interdigitating cytoplasmic processes (Figure 4). These thin, filiform, branching projections filled intercellular spaces, but also a solitary intracytoplasmic lumen filled with the same type of projections was found within a lymphoma cell. Intercellular junctions were absent.

Follow-up

The patient was treated by chemotherapy according to CHOP regimen, followed by regional radiotherapy (TD 2100 cGy). A complete remission was achieved. The patient is alive and well 9 months after the diagnosis.

Discussion

Malignant non-Hodgkin's lymphomas can occasionally exibit unusual histological patterns, such as sinusoidal growth in anaplastic large cell lymphoma (ALCL), CD30 positive, resembling metastatic carcinoma,[1] spindle cells with

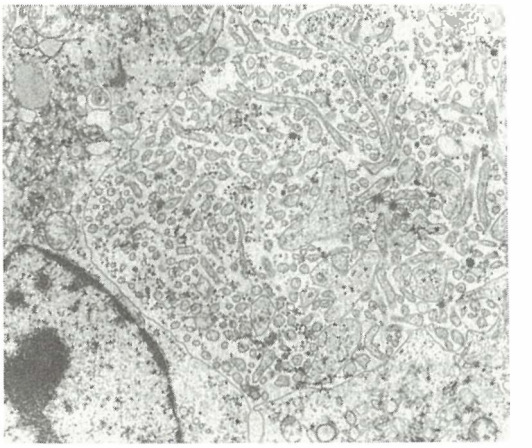

Figure 4. Lymphoid cell characterized by round nucleus, few organelles and profuse interdigitating villopodial projections along the cell surface (x 5000).

storiform pattern similar to that seen in sarcoma or malignant melanoma,[2] myxoid stromal changes and cord like cellular arrangement not unlike that in myxoid chondrosarcoma[3] or even signet cell differentiation simulating metastatic mucoid cell carcinoma.[4]

The gland-like structures with solid areas in a myxoid, vascularized stroma exhibited in this case were cytologically and histologically thought to be a poorly differentiated carcinoma metastatic to the lymph node, but negative stainings for mucins and cytokeratins ruled out this possibility.

The immunological studies proved fruitful in demonstrating the lymphoid nature of this neoplasm with definite membrane positivity for LCA and L26 (CD20) with IgG and kappa light chain clonality in the tumor cells.

Adenocarcinoma-like change is a previously unrecognized pattern of malignant lymphoma. It is well known, however, that ALCL, CD 30 positive, characterized sometimes with varying degrees of sinusoidal and subcapsular infiltration by large bizarre neoplastic cells might simulate other neoplasms, such as metastatic carcinoma,[5] but adenocarcinomatous pattern in such cases has not been observed so far.

The presence of an abundant extracellular mucoid matrix has not been considered to sup-

portive in the diagnosis of lymphoma until the reports by Chan[2] and Tse.[3] They described a case of anaplastic large cell Ki-1 lymphoma with myxoid matrix showing unusual sarcomatoid appereance and a case of B-cell malignant lymphoma in the soft tissue exhibiting prominent myxoid stromal changes. These authors claim that lymphoma tumor cells can elicit an exuberant myxoid change, probably by stimulating stromal cells. Contrary to their case of sarcomatoid lymphoma, where tumor cells were situated predominantly around the blood vessels, in the present case well defined perivascular cuffs were absent. Groups of tumor cells were situated randomly without any evidence of angiotropism lacking appereance that would suggest the diagnosis of lymphoma.

Histologically, the cytoplasm of the tumor cells merged into an abundant fibrillary matrix filling the central parts of gland-like and pseudo-rosette-like structures, but which was absent outside them. Similarly to the tumor cells, the fibrillary matrix stained with LCA and B-cell marker. Immunohistochemically and ultrastructurally, this case represents a type of filiform or anemone B-cell lymphoma which is characterized by multiple cytoplasmic projections on the cell surface.[6] It is interesting that in the current case, the cytoplasmic processes of the lymphoma cells were present almost exclusively in the center of cell groups thus forming the condensed eosinophilic fibrillary matrix which, seen on conventional histologic sections, was partially responsible for diagnostically misleading organoid histological picture. As most of the matrix was made of cell membrane material, it readilly stained with membrane leukocyte markers.

Given the wide range of histological appearances that malignant non-Hodgkin's lymphoma can assume, it is important and of clinical relevance not to exclude malignant lymphoma from differential diagnostic consideration even when the tumor shows gland-like or rosette-like structures or an apparently cohesive growth pattern.

References

1. Stein H, Mason DY, Gerdes J, O'Connor N, Wainscoat J, Pallesen G, Gatter K, Falini B, Delsol G, Lemke H, Schwartig R, Lennert K. The expression of the Hodgkin's disease associated antigen Ki-1 in reactive and neoplastic lymphoid tissue: evidence that Reed-Sternberg cells and histiocytic malignancies are derived from activated lymphoid cells. *Blood* 1985; **6:** 848–58.

2. Chan JKC, Buchanan R, Fletcher CDM. Sarcomatoid variant of anaplastic large cell Ki-1 lymphoma. Report of a case. *Am J Surg Pathol* 1990; **14:** 983–8.

3. Tse CCH, Chan JKC, Yuen RWS, NG CS. Malignant lymphoma with myxoid stroma: a new pattern in need of recognition. Histopathology 1991; **18:** 31–5.

4. Kim H, Dorfman RF, Rappaport H. Signet ring cell lymphoma. A rare morphologic and functional expression of nodular (follicular) lymphoma. *Am J Surg Pathol* 1978; **2:** 119–32.

5. Penny RJ, Blaustein JC, Longtine JA, Pinkus GS. Ki-1-positive large cell lymphomas, a heterogenous group of neoplasms. Morphologic, immunophenotypic, genotypic, and clinical features of 24 cases. *Cancer* 1991; **68:** 362–73.

6. Bernier V, Azar HA. Filiform large-cell lymphomas. An ultrastructural and immunohistochemical study. *Am J Surg Pathol* 1987; **11:** 387–96.

Radiol Oncol 1994; 28: 209-20.

Physical parameters for patient dose reduction with X-ray filtration in diagnostic radiology

L. John Schreiner, Noël Blais, J.-P. Bissonnette and Ervin B. Podgoršak

Department of Oncology (Radiation Oncology) and Medical Physics Unit, McGill University, Canada

Although radiographic techniques have been established for clinical diagnostic studies, research continues in the reduction of patient dose through various technical modifications. However, dose savings from the adoption of different techniques are often reported using a variety of exposure or dose parameters. In this paper the evaluation of patient dose reduction in terms of surface doses and integral doses is analyzed. The review is performed using a specific example of dose reduction with various x-ray filter materials in order to illustrate the limitations of the various parameters for assessing risk reduction. The x-ray techniques required for each filter material to give a similar radiographic quality as the standard technique are established. The surface dose reductions, integral dose reductions, tube loading increases relative to the standard techniques are reported for the beams filtered with different materials. To clarify the differences between surface dose and integral dose savings, the integral doses are determined from depth dose data. An analysis of the relationship of effective dose equivalents to surface doses and integral doses indicates that the use of integral dose ratios more accurately specifies the risk reduction to the patient.

Key words: radiation protection; patient dose; x-ray filters

Introduction

The aim of diagnostic radiology is to make an accurate diagnosis with the lowest possible radiation risk to the patient. Whereas standard radiographic techniques have been established over the years to achieve this goal, research to reduce the patient dose without compromising image quality continues. The effects of x-ray beam filtration on patient dose have been investigated for a range of radiological techniques, however, to date no standard dose parameter has been adopted for reporting the risk reduction to the patient achieved with modifications of x-ray techniques.[1–11] In typical vendor literature describing the benefits of commercial x-ray filters (and often in the scientific literature);[2, 5, 6, 7] the dose savings to the patient are described in terms of entrance exposure or surface dose reductions only. Dose reductions have also been reported in terms of the measured or calculated integral doses absorbed by a phantom or patient.[1, 3, 8, 10, 11] The reported integral dose reductions by various approaches are usually less dramatic than the reductions in the surface doses or entrance exposures.[3, 8, 11]

Correspondence to: L. John Schreiner PhD, Department of Oncology and Medical Physics Unit, McGill University, 1650 avenue des Cèdres, Montréal, Québec, Canada. H3G IA4

UDC: 616-073.75:614.876

There has been little discussion of the relevance of these differences. Only one group[9] has reported dose comparisons with different filters using effective dose equivalents[12] or effective doses,[13] which are the parameters considered to indicate patient risk in medical radiation dosimetry.[14, 15] Thus, the evaluation of the efficacy of using different x-ray beam filtration for patient risk reduction has been confounded by reports using different dose reduction parameters.

The issue of x-ray beam filtration arises because clinical x-ray units produce a continuous spectrum of photons, with energies from ~10 keV to the energy corresponding to the kVp of the radiographic technique. The low energy photons in this spectrum are absorbed in the patient, contributing significantly to the absorbed dose, and give no diagnostic information since they do not reach the imaging device. The high energy photons of the spectrum, on the other hand, cause a decrease in radiographic contrast because the attenuation coefficients of different tissues are more similar at higher photon energies. The clinical x-ray spectrum can be improved by placing attenuating materials, referred to as x-ray filters, between the x-ray source and the patient. These filters effectively narrow the x-ray spectrum by preferentially attenuating the low, and perhaps the high, photon energy regions of the x-ray spectrum. Ideally this results in a decrease in patient dose without any loss of diagnostic information. While there has been no conclusive determination as to which material makes an optimum filter, aluminum has been the standard filter material in most x-ray units, while molybdenum and copper are often used in low kVp and high kVp radiography, respectively.

The literature on x-ray filters presents the results of a large number of experimental measurements and computer calculations for many different filter materials under a variety of clinical conditions. It is apparent from these results that the choice of filter material depends strongly on the clinical situation and that for any given situation there may not be a unique choice of filter. While the measure of the dose reduction achieved with the different filter materials is obviously critical in evaluating patient risk, there has been no concensus on which dose parameter best combines practical utility with useful information. This note is intended to establish the adoption of one variable, the integral dose, as the practical parameter of choice.

Materials and methods

Experiments were performed on a clinical x-ray unit consisting of a Picker GX600 3 phase 12 pulse generator together with a ceiling mount Machlett Dynamax 62U tube containing a 69B insert with a 12° anode angle. The unit's performance specifications were well established. The coefficient of variation of the output reproducibility and the linearity of exposure coefficient of less than 0.004 and 0.05, respectively, were well below the acceptable upper limits (0.05 and 0.1, respectively; ref. 16). All studies were done with the large (nominal 1.2 mm) focal spot to minimize stress on the anode. Four x-ray filter materials were studied and the results compared with those obtained with standard tube filtration consisting of 1.31 mm aluminum equivalent inherent filtration and 1.5 mm added aluminum. The commercial 0.05 mm *niobium* foil (Niobix Filter, North American Health Care Products Inc., Oakville, Ontario) and *R-Filter* (RSP Incorporated, San Carlos, California) filters were used as obtained from the manufacturer. The *samarium* (with a K edge at 46.8 keV) and *holmium* (with a K edge at 55.6 keV) foils (99 + % purity, Atomergic Chemetals Co., Plainsview, New York) were sealed in lacquer to retard oxidation. The niobium filter was added directly to the standard filtration in place in the x-ray tube (as per vendor's instructions). The R-filter, samarium and holmium filters were added to the inherent filtration of the tube after the 1.5 mm Al filter had been removed; that is, these materials were used in lieu of the added 1.5 mm Al.

To account for decreased x-ray tube output with the new filters the tube loading (mAs × kVp) was increased to produce radiographs similar in quality to those obtained with

the standard techniques. The film quality evaluation was performed with $25 \times 25\,cm^2$ polystyrene phantoms of 5 thicknesses from 6 cm to 25 cm. The phantoms were centered on the x-ray table under the collimator; the table top was positioned 100 cm from the x-ray source, and the x-ray film (Dupont Cronex film in a Quanta III High Resolution Modular Daylight Cassette processed with a Kodak RP-X-Omat Model M7 daylight unit) was placed 40 cm below the table top. This air gap reduced the scatter contribution to a level similar to that which would be obtained with conventional 8 : 1 or 12 : 1 grids.[17] The film was approximately 40 cm above the floor to minimize backscatter. Either aluminum or water step wedges were placed on the phantom to give contrast in radiographs obtained with the x-ray beams filtered by the different materials. The contrast was considered a sufficient indicator of image quality in this work, since the comparison was between film-screen images.[18] Also, the fact that contrast was at least almost equal implied that the image noise did not differ significantly, since the x-ray spectra from the differently filtered beams giving similar images were expected to be alike.[8, 11] The various phantom thicknesses and contrast objects permitted study of radiographic techniques over a large range of kVps. A standard film was obtained for each phantom thickness using the standard 2.81 mm aluminum filtration, the kVp and mAs were set to give a background optical density of $\sim 1.6 \pm 0.1$ OD (Table 1). Radiographs were then taken with the various filter materials substituting for the standard aluminum; the operating techniques were changed by increasing kVp until the optical densities under each step of the contrast wedge were similar to those obtained with the standard aluminum technique. A parallel plate ionization chamber (model 96035, Keithley Instruments Inc., Cleveland, Ohio) was placed on the polystyrene phantoms and connected to a digital electrometer (Keithley, Model 616) to measure surface exposures with backscatter.

Subsequent to the determination of the radiographic techniques giving equivalent film quality with the various filter materials, transmission curves through aluminum (alloy 1100) were measured to characterize the x-ray beam quality for each technique. Relative depth doses in polystyrene were also measured for the different filter – phantom combinations. The measurements were made with either an end-window ionization chamber (PTW model # 2532/3 low energy chamber, Nuclear Enterprises Ltd, Beenham, England) with the Keithley 616 electrometer or with thermoluminescent detectors (TLD-800 and TLD-100; Harshaw Chemical Co., Solon, Ohio).

The experimental results were confirmed by computer calculations on a Macintosh system (Apple Computer Inc., Cupertino, California).[19] Measured transmission data through aluminum were used to generate the x-ray photon spectrum for each filtered beam via the three parameter equivalent spectra technique (EQSPEC).[20] The spectra were based on the Birch and Marshall[21] model for x-ray spectra from an x-ray tube; this is not a limitation since the EQSPEC spectra are essentially independent of model.[22] In the determination of the EQSPEC the anode angle was fixed at 12°, the kVp was set to the measured value. The EQSPEC spectra were determined for a number of different kVp and filter combinations so that the inherent spectrum emanating from the x-ray tube before any added filtration was well determined. The spectra after the different x-ray filters were calculated by attenuating the inherent spectrum through the filter materials. The attenuation coefficients required for the calculations were based on polynomial parametrizations suitable at diagnostic energies.[22] The determination of the x-ray EQSPEC enabled the calculation of the surface doses, relative depth doses (using a ray tracing algorithm which incorporated primary and first scatter contributions.[9, 24] and integral doses (see below) for the various radiographic techniques with the different filters.

Results

In our experiments the radiographic techniques for all filters were adjusted to achieve under

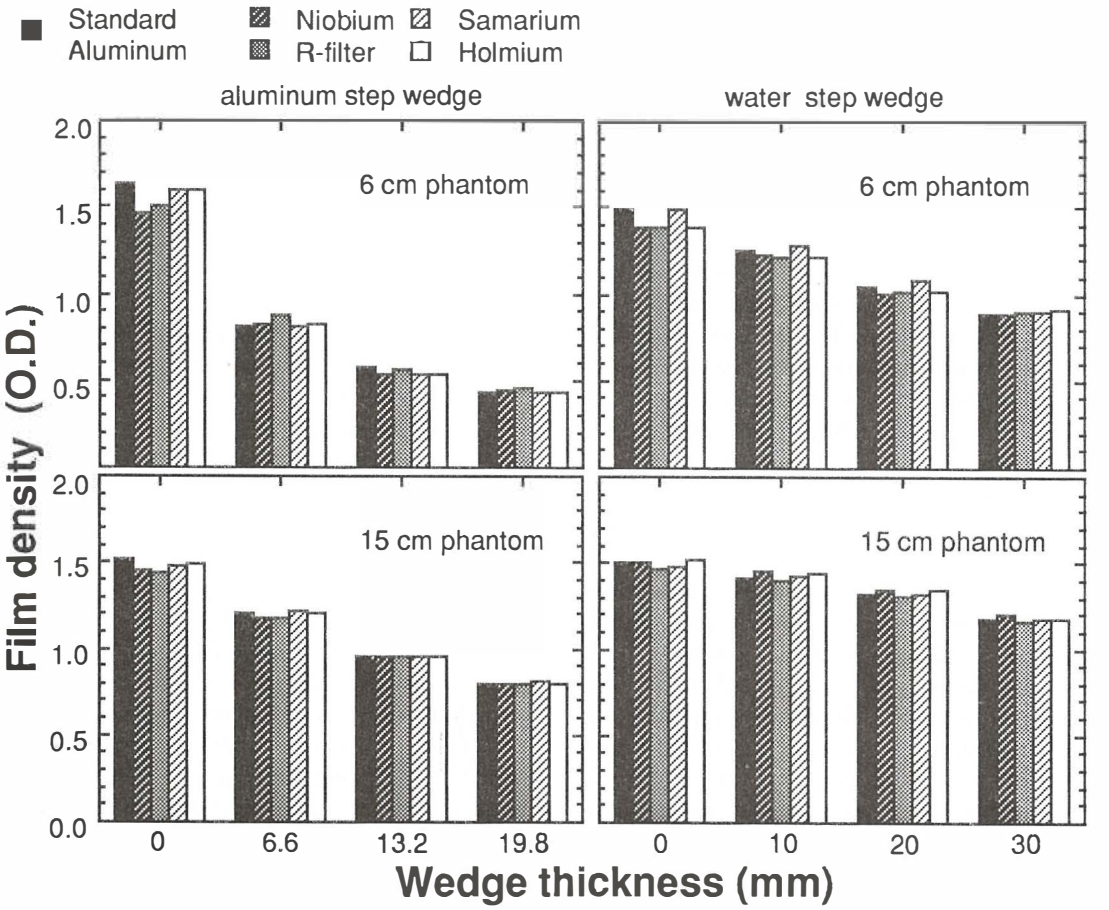

Figure 1. The variation of film density (in units of optical density) of the background of the film and under three steps of the aluminum (high contrast) and the water (low contrast) step wedges as the standard aluminum was replaced by the other filter materials. The radiographic techniques with the different filter materials were modified by increasing the kVp in order to maintain similar film densities under all wedges. The results are shown for two of the phantom thicknesses: 6 and 15 cm of polystyrene respectively. While some change in film density under the various steps of the test tool is apparent, especially for the 6 cm phantom thickness, the image quality is considered to be equivalent for the purpose of this study.

contrast step wedges film optical densities similar to those obtained with the standard technique (with 2.81 mm aluminium filtration). This film density matching was attained by increasing the kVp relative to the standard while maintaining the mAs constant. The resulting film quality did vary slightly in some tests, as apparent in Figure 1, which shows the variation in film density under aluminum and water contrast test tools for two of the phantom thicknesses investigated; the 6 cm phantom data show the worst matching experienced. The change in film quality was not considered significant enough, however, to attempt additional corrections by adjustments of mAs. Radiographic techniques which gave similar image quality, albeit with different filter materials, are called equivalent techniques in this paper.

The first half value layers (HVLs) in aluminum determined from measured transmission data through aluminum are given for selected tests in Tables 1 and 2. The x-ray beam qualities (as indicated by the HVLs) obtained with the various filters were different from those for beams filtered with the standard aluminum filt-

Table 1. The physical characteristics of the radiographic techniques used with the standard filtration (2.81 ± 0.10 mm of aluminum). These were the standard techniques against which the various filter combinations were compared over the 5 phantom thicknesses. The errors are ± 0.10 mm in the half value layers and ± 20 μGy in the surface doses. The test wedge column indicates the material of the contrast test tool: water (w) or aluminum (Al).

Phantom thickness (cm)	nominal kVp	1st HVL (mm Al)	mAs	Surface Dose (μGy)	test wedge
6	45	1.73	12.5	225	w
	60	2.32	3.2	125	Al
10	55	2.13	16	630	w
	70	2.66	4.8	340	Al
15	55	2.13	40	1505	w
	80	3.03	8.0	675	Al
20	75	2.86	20	1985	w
	100	3.96	7.5	1275	Al
25	80	3.07	30	2940	w
	120	4.85	10	2700	Al

ration. The non-standard beams were harder and more homogeneous (i.e., the ratios of the first and second HVLs are closer to unity) than the standard x-ray beams.

The tube loadings (mAs × kVp) of the equivalent techniques relative to those of the standard technique were in the range from 1.05 to 1.2 over the whole set of phantoms studied. Some representative data are given in Table 2.

The surface dose ratios for the various equivalent techniques, relative to the standard aluminum filtration, were determined from ion chamber measurements during the film studies and confirmed by subsequent relative depth dose measurements at the surface. The surface dose ratios ranged from ~0.34 (for the R-filter low contrast test with the 6 cm phantom relative to standard Al filtration at 45 kVp) to ~0.76 (for the samarium high contrast test with the 20 cm phantom relative to standard Al filtration at 100 kVp). The variation of the surface dose ratios for the various tests is reviewed for some conditions in Table 2.

Typical measured (data points) and calculated (solid curves) relative depth doses are shown in Figure 2. The depth doses are normalized to 100% for the surface dose obtained with the

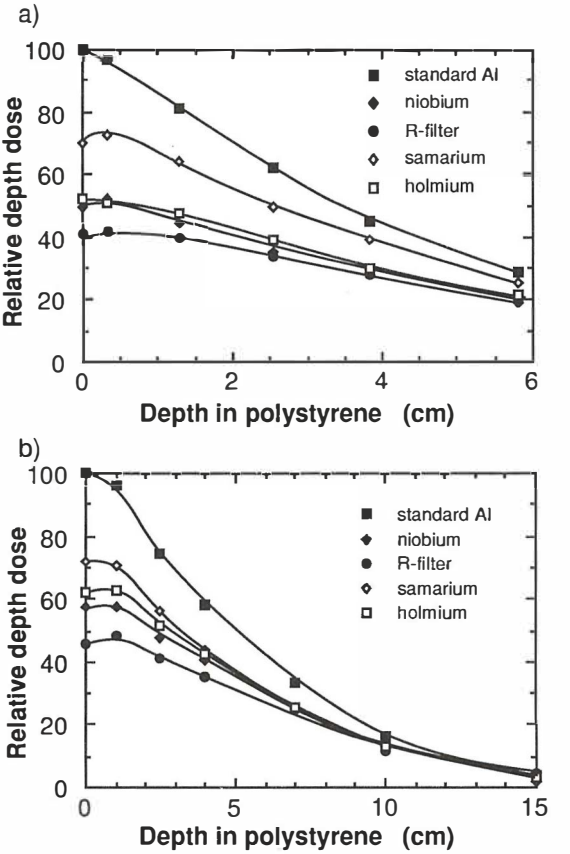

Figure 2. Relative depth doses for the radiographic techniques established in the high contrast tests with the 6 and 15 cm thick phantoms. The data are normalized to 100% at the surface dose for the x-ray beam filtered by the standard aluminum. The symbols show measured data; the curves show the results of computer calculations. While there is a large difference in the surface doses achieved with the x-ray beams filtered by the various materials, the exit doses are similar. Therefore, the differences in the integral doses (essentially the area under the depth dose curve, with corrections accounting for beam divergence) for the different beams are less than the difference in the surface doses.

standard aluminum filtration techniques. In all cases the relative doses for the different equivalent techniques approached each other with increasing depth so that the exit doses were essentially equal. The relative depth dose data were used to calculate integral dose reductions with the various filter materials relative to the standard techniques. The integral dose ratios ranged from ~0.43 (for the R-filter low con-

Table 2. Some of the characteristics of the radiographic techniques used with the different filter materials to give film quality similar to that obtained with the standard 2.81 mm of aluminum. The data are shown for the aluminum step wedge contrast tests for three phantom thicknesses. Similar results were obtained for the other conditions; the complete dose reduction data are presented in Fig. 3. The tube loading, surface dose, and integral dose ratios are normalized to the standard techniques with the aluminum filtration.

Filter material	Tube loading ratio	1st HVL (mm Al)	Surface dose ratio	Integral dose ratio
6 cm phantom				
niobium	1.10	3.81	0.53	0.64
R-filter	1.13	4.88	0.43	0.56
samarium	1.10	3.13	0.63	0.72
holmium	1.10	3.72	0.55	0.62
15 cm phantom				
niobium	1.08	4.98	0.58	0.70
R-filter	1.10	6.08	0.48	0.62
samarium	1.16	4.28	0.72	0.81
holmium	1.16	5.04	0.62	0.72
25 cm phantom				
niobium	1.04	7.14	0.70	0.84
R-filter	1.05	8.16	0.61	0.75
samarium	1.13	6.33	0.74	0.83
holmium	1.21	7.42	0.73	0.81

trast test with the 6 cm phantom relative to standard Al filtration at 45 kVp) to ~0.85 (for the holmium high contrast test with the 20 cm phantom relative to standard Al filtration at 100 kVp). The integral dose ratios for the various tests are also reviewed for some conditions in Table 2. In all cases the integral dose reductions were considerably smaller than the surface dose reductions, as apparent from Figure 3, which shows the surface dose ratios and integral dose ratios for all the different filter and phantom combinations studied. The dose ratios are plotted against the HVLs of the various equivalent techniques so that the data from the different experiments can be presented together. The measured surface and integral dose ratios were also confirmed with computer calculations using the EQSPEC spectra. In most cases, except for some results for the samarium filter (see below), the calculated results are within 5% of the measured values.

Discussion

For ionizing photon beams with energies below 3 MeV the simplest measurement of radiation quantity is the exposure X, which specifies the amount of charge created as radiation passes through a unit mass of air (in units of C kg^{-1}(SI) or roentgen R). Exposure is easily determined with an ionization chamber placed in the radiation field. If the chamber is placed on the surface of a phantom, the exposure includes backscattered radiation from the phantom and is designated surface exposure or exposure with backscatter.

A more fundamental and general quantity in radiological physics is the absorbed dose D, which is defined as the energy absorbed per unit mass of irradiated medium (i.e., a patient or a phantom material). The SI unit of dose is the gray (1 Gy = 1 joule per kilogram), although doses are still often expressed in terms of an older unit: the rad (1 erg per gram); numerically 1 Gy = 100 rads. The absorbed dose at the surface of a phantom, D_s, can be determined from the surface exposure through the use of conversion factors which account for the amount of energy required to ionize air and for the different absorption characteristics of air and the phantom material. In fact, if one is interested in comparisons between the surface doses from two different radiographic techniques, the relative surface doses will be identical to the relative surface exposures since the conversion factors are essentially equal over the range of energies encountered in radiology. Since surface dose is easily determined, it has often been the quantity of choice in specifying the 'dose' reduction achieved with different radiological techniques.

In radiation protection one must consider that the physical parameters of exposure and dose may not be sufficient, *a priori,* to quantitate biological risk.[12, 13, 14] Thus, while the probability of a given biological injury occurring (e.g., in the case of cancer induction or genetic changes) depends on the absorbed dose received, the quantification of risk requires that the dose be modified by factors which reflect the

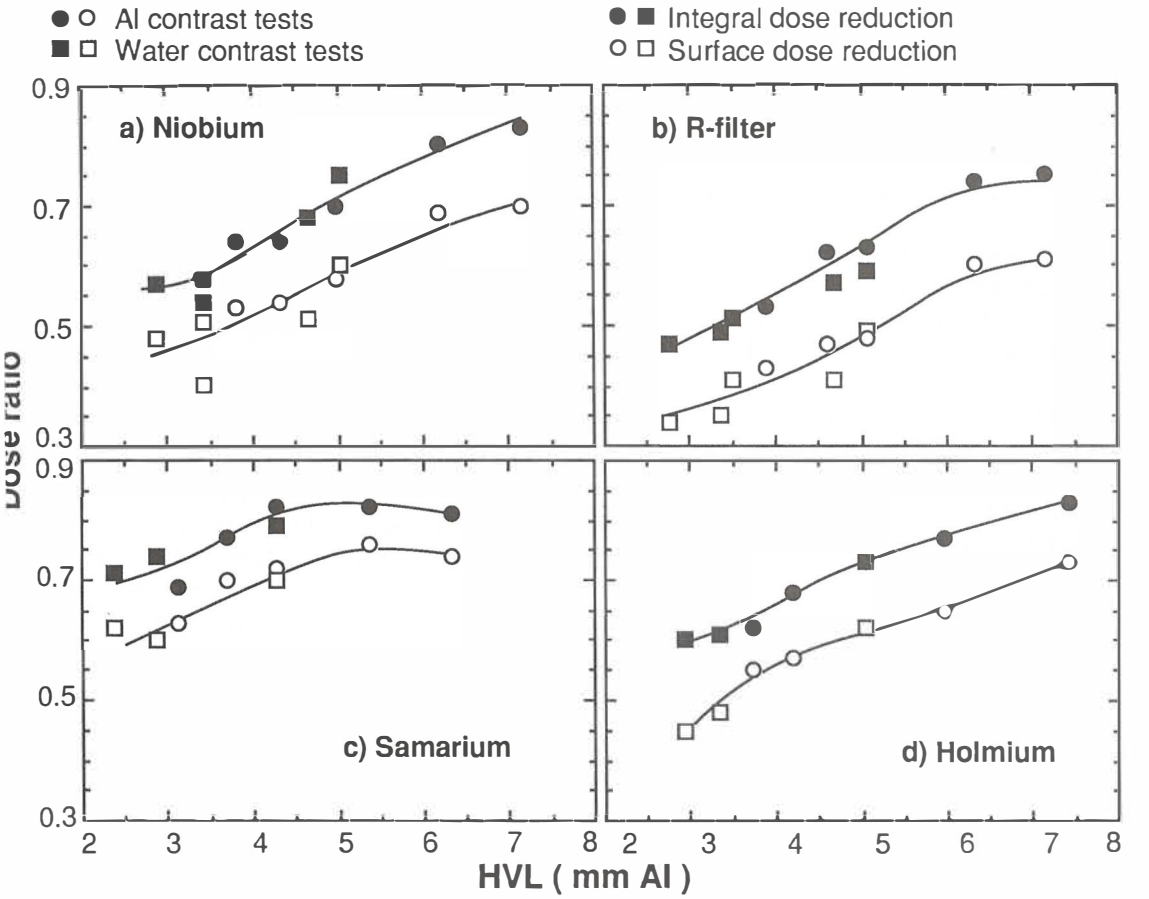

Figure 3. The integral dose and surface dose reductions determined for the x-ray beams filtered by the different materials; the dose reductions are given in terms of the ratio of the doses measured with the various filters to those determined for the standard aluminum filtration. The data for all filters, phantom thicknesses are shown by plotting the data against the aluminum half value layers for the different x-ray beams. The high and low contrast data refer to the tests performed with the aluminum and water contrast tools, respectively. In all cases the integral dose ratios are closer to 1.0 than the surface dose ratios. Therefore, the dose reductions determined from integral dose measurements are less than those determined from surface dose measurements.

wealth of human radiobiological and radioprotection data amassed in the last 50 years.[12, 13, 14] The dose parameters which are considered to be the best indicator of patient risk in medical radiation dosimetry are the effective dose E,[13] or its precursor the effective dose equivalent H_E.[9, 12–15, 25–29] These quantities take into account that the irradiation may not be uniform over the whole body. For the purposes of this paper, both E and H_E can be taken as the weighted means of the doses delivered to various irradiated body organs or tissues. The only radiations being considered here are diagnostic x-rays and one can set the equivalent dose, which accounts for differences in biological effect from different radiations, numerically equal to the dose.[13] Thus to calculate the effective dose one can sum the weighted doses absorbed by various tissues or organs:

$$E = \sum_T w_T \cdot D_T \qquad [1]$$

where D_T is the dose delivered to a particular tissue T and w_T is a weighting factor for that tissue. Both E and H_E are expressed in units

of Sieverts (1 Sv = 1 joule per kilogram) to denote that the doses have been modified by unitless weighting factors.

The differences between E and H_E are essentially differences in the weighting factors w_T and in the organs considered in the summation of Eq [1].[12, 13] While the effective dose is the more recent quantity, most evaluations to date in diagnostic radiology have been performed using H_E and this will be the quantity used in the remainder of this paper. This is quite acceptable since the ICRP itself[13] suggests that previous quantities may still be used without correction as long as the quantities are clearly specified. There are some questions about the actual significance of H_E as a risk assessment parameter for a heterogeneous population group and about its actual calculation,[9] however, for our purposes the view that H_E is a useful risk parameter for comparative use is accepted.[25]

Although H_E may be widely regarded as the best risk assessment parameter, its use in diagnostic radiology dosimetry has been limited since its evaluation requires first the determination of the three-dimensional dose distribution associated with particular radiographic examination under consideration and then the calculation of the weighted sums over all the organs of interest. This problem is illustrated somewhat by the measured depth doses shown in Figure 2. The relative doses decrease with increasing depth because of attenuation in the medium and at each depth the value depends on the beam filtration and the kVp of the technique. Thus, the relative doses absorbed by the various organs will change for different radiographic examinations or even for different views (e.g., AP, PA or Lat) in the same examination, and H_E may vary significantly for different studies even if the studies use identical x-ray beams. The practical problems associated with the determination of H_E are apparent even in reviewing the literature on x-ray filter materials; only one group[9] has evaluated effective dose equivalents for differently filtered beams and that study was restricted to a specific diagnostic examination (PA chest study) with only two different filter materials considered.

It has been suggested that another physical quantity Σ, the energy imparted or, alternately, the integral dose, be used in assessing risk, because it also takes into account the energy distribution throughout the patient or phantom.[3, 8, 26] At diagnostic photon energies the integral dose Σ is defined[29] as the difference between the incoming energy R_{in} and the energy transmited through a volume of interest R_{out}:

$$\Sigma = R_{in} - R_{out}. \qquad [2]$$

The determination of R_{out} for particular beams requires computer simulation, however, the integral dose can also be determined empirically by integrating depth dose data such as that shown in Figure 2.[30] This has been the approach used in our work. While the calculation of the integral dose is more difficult than the determination of exposure or surface dose, it is, on the other hand, considerably less labour or calculation intensive than the evaluation of H_E. Also, the integral dose depends primarily on the physics and geometry of the x-ray beam and not on other biological or clinical factors.

At this point in the discussion one is left with the following dilemma: the easily measured dose reduction quantities may not give the best indication of radiation risk reduction for the patient, while the optimal risk reduction parameter is extremely difficult to evaluate. We propose that the solution to the problem lies in the fact that most risk evaluation in diagnostic radiology is relative, e.g., for x-ray beam filtration studies risk reduction is usually referenced to risk associated with standard aluminum filtration. Therefore, in the evaluation of risk reduction with the use of different filter materials, it may not be necessary to calculate H_E if the conversion factor between surface or integral doses and H_E remains constant for the x-ray beams filtered by the different materials. With this in mind one can now consider the results obtained in the comparison of the five x-rays filters undertaken in this work.

Although the x-ray beam quality changes

with the different filter materials, the image quality (as indicated by the simple contrast test used in this study) can be maintained through the modification of the radiographic technique. This result has been reported previously.[2, 3, 5, 8, 11] The tube output decreases sufficiently with the different filtration that tube loading has to be increased in order to establish the equivalent techniques for the new filters. In our study the increases were implemented by increasing kVp with mAs kept constant. The tube loading ratios observed (from 1.05 to 1.2 over the range of techniques studied) are considerably lower than the tube loading ratios typically reported in the literature (e.g., 1.3 to 2.1,[5] ~2.0 to 4.0[2] and 1.81 to 2.45[6]) in which mAs is the varied tube loading parameter. This is not unexpected since the x-ray tube output increases with kVp raised to a power between 2 and 3, while output increases linearly with mAs. In fact this, along with reports in the literature that kVp increases could be used for some selected filters,[2, 3] was a motivating factor in using kVp increases in the search for equivalent techniques. Attempts to match the different filter techniques by increasing the mAs gave tube loading ratios which were larger than those obtained with the kVp increases. Also, the surface dose reductions with mAs increases were smaller than those obtained with the kVp changes. For example, the respective tube loading increases for the R-filter techniques with the 6 cm and 20 cm phantom studies are 2.34 and 1.33 with the mAs increase and 1.13 and 1.10 with the kVp increase. The surface dose ratios are 0.54 and 0.62 (mAs increased; 6 cm and 20 cm phantoms) and 0.42 and 0.60 (kVp increased), respectively.

That the x-ray beams filtered by the niobium filter are harder and more homogeneous than the standard filtered x-ray beam is expected since the new filters were added directly to the standard filtration. The changes in the x-ray beam quality for the other filters, which were added to the inherent filtration of the x-ray tube, cannot be attributed only to the increased kVp required to maintain the image quality with the different filters. The changes also reflect the fact that the R-filter, 0.1 mm holmium, and 0.1 mm samarium harden the beam more than the 1.5 mm Al removed from the tube before these materials were added. The HVL increase with the rare earth samarium and holmium filters is usually less than that with the commercial niobium and R-Filter filters, although for some phantom thicknesses, which require radiographic techniques with higher kVp, the HVLs of the niobium-filtered beams are less than those transmitted by the holmium filter. As has been observed previously,[5] the R-filter hardens the beam more than the other filter materials.

The surface dose reductions observed with the various filter materials are significant: the surface dose ratios range from ~0.30 to ~0.78 depending on the radiographic technique. However, since the image quality has been maintained for the equivalent techniques, the exit doses for the different beams must be similar since film is, in fact, a dosimeter. This is confirmed by relative depth dose measurements for the differently filtered x-ray beams, as shown in Figure 2. Although there are large differences in the doses from the various filtered beams at shallow depths, the doses approach each other as depth is increased until the exit doses, especially for the thicker phantoms, are essentially equal. Thus, as reported previously,[3, 8, 11] the integral dose reductions for the beams filtered by the diverse materials are consistently smaller than the surface dose reductions. As indicated in Figure 3, the integral dose reduction is typically 20 to 25 % less than the reduction established by the surface dose ratios; the minimum difference was ~10 % for the samarium filter while the maximum difference reached up to ~45 % for the niobium and R-filters. Therefore, it is necessary to determine which dose reduction parameter, the surface dose reduction or the integral dose reduction, gives a more reliable measure of the risk reduction experienced by the patient.

Recently, there have been a number of reports in the literature giving conversion factors for surface dose and/or integral dose to H_E for

various radiographic examinations. In particular the dependence of the conversion factors on such parameters as the half value layer or the kVp of the x-ray beam have been investigated. In an attempt to assess the reliability of surface dose reduction as the parameter of risk reduction in x-ray filter studies, Shrimpton et al.[27] evaluated the conversion factor from surface dose to H_E (i.e., the ratio H_E/D_s) for PA chest studies for different x-ray beam filtrations over a range of kVp. Alm Carlsson and Carlsson[26] had earlier reported the conversion factors $H_E/\overline{D}$ for mean absorbed dose $\overline{D}$ (which is the energy imparted divided by the mass of the irradiated volume)[28] to H_E for a large number of diagnostic x-ray examinations including PA chest studies. Most recently Huda et al.[28] have reported measured and calculated conversion factors H_E/Σ and H_E/D_s for x-ray chest examinations.

The data for PA chest radiographic techniques are reviewed in Figure 4a; the half value layers for the data from Shrimpton et al.[27] were taken from the reported kVp and total mm filtration assuming a constant potential generator; the $H_E/\overline{D}$ from Huda's data[28] were calculated from his effective dose equivalent to energy imparted conversion factors assuming a patient mass of 70 kg. The conversion factor $H_E/\overline{D}$ for the PA chest examinations is ~ 1 Sv Gy^{-1} over the whole range of HVLs investigated, approximately in the middle of the range from 0.4 to 2.2 Sv Gy^{-1} typical for most radiographic techniques.[28] The conversion factor from surface dose to effective dose equivalent ranges from 0.05 to 2.0 Sv Gy^{-1}.

The relative behavior of the conversion factors H_E/Σ and H_E/D_s as the HVL changes is more clearly illustrated by Figure 4b in which the values have been (arbitrarily) normalized to 1.0 at a HVL of 2 mm of aluminum. Note that the normalized values of H_E/Σ are identical to the normalized $H_E/\overline{D}$. The conversion factor H_E/Σ changes by less than 10% over the range of HVLs shown. On the other hand, the conversion factor H_E/D_s increases by ~ 430% as the HVL is increased from 1.0 to 7.0 mm of aluminum. Therefore, for x-ray filter investigations, in which HVLs of x-ray beams filtered by different materials may change considerably, the relative surface dose reduction is not a true

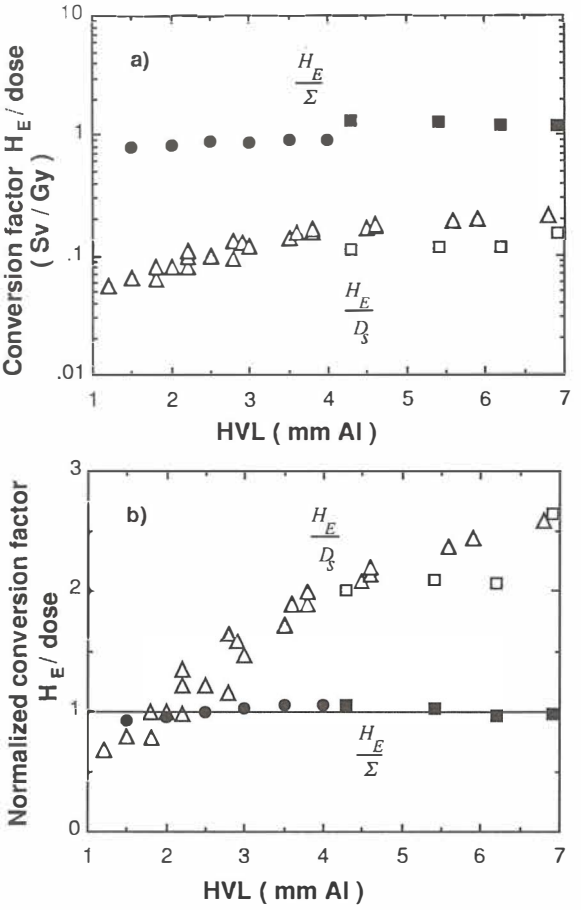

Figure 4. The variation of the relationship of the effective dose equivalent H_E to the integral dose Σ, mean absorbed dose $\overline{D}$, and surface dose D_S with the HVL of the radiographic technique for PA chest radiography. The data are taken from measurements and calculations reported by Alm Carlsson and Carlsson (•) Shrimpton et al. (Δ), and Huda et al. (■, □). These data are presented since they cover a range of HVLs similar to that covered in the present study.

a) The conversion constants for determining H_Es from mean absorbed dose and surface dose measurements.

b) The same data as above normalized to 1.0 at a HVL of 2.0 mm of aluminum. This plot shows the relative change in the conversion factors as the HVL of the radiographic technique is increased. The solid line at a normalized conversion factor of 1.0 indicates the behaviour expected for a conversion factor which is independent of HVL.

indication of the effective dose equivalent since the conversion factor H_E/D_s may not be constant. Rather, the integral dose should be used for the risk reduction evaluation since the conversion factor H_E/Σ remains essentially constant with changing HVL. With the results reported earlier, it is apparent that the risk reduction achieved by the use of novel x-ray filtration schemes is exaggerated by 10 to 45 per cent, if only surface dose or entrance exposure reductions are quoted.

One further point can be made. The results for the samarium filter confirm a caveat[31] often overlooked in filter discussions. As the experiments progressed the parameters measured empirically and determined by the computer calculations no longer agreed. The empirical results for the dose reductions began to be less than those predicted by calculations. Visual examination of the 0.1 mm samarium foil used in the experiments indicated that the foil had cracked. Therefore, the use of thin foils for practical x-ray filtration has an additional quality assurance aspect which must be considered in the choice of optimal filtration.

Conclusions

While the measure of the dose reduction achieved with modifications of diagnostic radiographic techniques (for example, by the use of different x-ray filters) is obviously critical in evaluating changes in patient risk, to date no standard dose parameter has been adopted for reporting the risk reduction. In this paper an evaluation of the physical parameters used to describe the risk reduction resulting from the use of a variety of x-ray filter materials is presented. Various physical parameters for the x-ray beams filtered by different materials have been established. The radiographic techniques with the various filters were modified by increasing the tube kVp to equalize image quality to that obtained with the standard techniques. The integral dose reductions relative to the standard techniques achieved with the different filters are significantly less dramatic than the reductions seen in surface dose. Furthermore, in all cases the x-ray beams filtered by the new filter materials had HVLs thicker than beams filtered by the standard aluminum. An analysis of previously reported data indicates that the conversion factors for integral dose to effective dose equivalent, the parameter of choice in evaluating patient risk, are essentially independent of x-ray beam quality (i.e., HVL). However, the factors for converting surface dose to effective dose equivalent increase dramatically as the HVL increases. This analysis clearly indicates that integral dose ratios more accurately specify the reduction in the patient radiation risk attained with different radiographic techniques. Descriptions of risk reduction based on surface doses or entrance exposures considerably overestimate the benefit to the patient.

Acknowledgements

The authors would like to thank Ms. Marina Pla for her assitance with the TLD measurements.

References

1. Yamaguchi C, Yamamoto T, Terada H, Akisada M. Effect of tungsten absorption edge filter on diagnostic x-ray spectra image quality and absorbed dose to the patient. *Phys Med Biol* 1983; **28:** 223–32.
2. Burgess AE. Physical measurements of heavy metal filter performance. *Med Phys* 1985; **12:** 225–8.
3. Koedooder K, Venema HW. Filter materials for dose reduction in screen-film radiography. *Phys Med Biol* 1986; **31:** 585–600.
4. Jennings RJ. A method for comparing beam-hardening filter materials for diagnostic radiology. *Med Phys* 1988; **15:** 588–99.
5. Kohn ML, Gooch AW, Keller WS. Filters for radiation reduction: a comparison. *Radiology* 1988; **167:** 255–7.
6. Wesenberg RL, Amundson GM, Mueller DL, Coupland SG. Ultra-low dose routine pediatric radiography utilizing a rare-earth filter. *J Can Assoc Radiol* 1987; **38:** 158–64.
7. Horner K, Lawinski CP, Smith NJD. Erbium filtration for dose reduction in dental radiology. *Brit J Radiol* 1988; **61:** 609–12.

8. Nagel HD. Comparison of performance characteristics of conventional and K-edge filters in general diagnostic radiology. *Phys Med Biol* 1989; **34:** 1269–87.

9. Thierens H, Kunnen M, Van der Plaetsen A and Segaert O. Evaluation of the use of niobium filter for patient dose reduction in chest radiography. *Brit J Radiol* 1991; **64:** 334–40.

10. Carrier R, Beique RA. Analogous filters for beam shaping in diagnostic radiology. *Phys Med Biol* 1992; **37:** 1313–20.

11. Regano LJ, Sutton RA. Radiation dose reduction in diagnostic x-ray procedures. *Phys Med Biol* 1992; **37:** 1773–88.

12. International Commission on Radiological Protection: *Recommendations of the International Commission on Radiological Protection*, ICRP Publication 26, Pergammon Press London, 1977.

13. International Commission on Radiological Protection: 1990 *Recommendations of the International Commission on radiological Protection,* ICRP Publication 60, Pergammon Press London, 1991.

14. UNSCEAR: *United Nations Scientific Committee on the Effects of Atomic Radiation Ionizing Radiation: Sources and Biological Effects Report to the General Assembly.* United Nations New York NY 1982.

15. Huda W, Lentle B, Sutherland JB. The effective dose equivalent in radiology. *J Can Ass Radiol* 1989; **40:** 3–4.

16. Hendee WR and Rossi P. Performance specifications for diagnostic x-ray equipment. *Radiology* 1976; **120:** 409–12.

17. Sorenson JA, Floch J. Scatter rejection by air gaps: An empirical model. *Med Phys* 1985; **12:** 308–16.

18. Fahrig R, Maidment AD, Yaffe MJ. Optimization of peak kilovoltage and spectral shape for digital mammography. *SPIE* 1992; **1651:** 74–83.

19. Bissonnette J-P. Percent Depth Doses for Diagnostic Radiology. M.Sc. thesis, McGill University 1991 (unpublished).

20. Boone JM. The three parameter equivalent spectra as an index of beam quality. *Med Phys* 1988; **15:** 304–10.

21. Birch R, Marshall M. Computation of bremsstrahlung x-ray spectra and comparison with spectra measured with a Ge(Li) detector. *Phys Med Biol* 1979; **24:** 505–17.

22. Bissonnette J-P, Schreiner LJ. A Comparison of Semiempirical Models for Generating Tungsten Target X-ray Spectra. *Med Phys* 1992; **19:** 579–82.

23. Ouellet R, Schreiner LJ. A Parametrization of the Mass Attenuation Coefficients for Elements with $Z = 1$ to $Z = 92$ in the Photon Energy Range from $\sim$ 1 to 150 keV. *Phys Med Biol* 1991; **36:** 987–99.

24. El-Khatib EE, Podgoršak EB, Pla C. The effect of lead attenuators on dose in homogeneous phantoms. *Med Phys* 1986; **13:** 928–35.

25. Dunster HJ. Effective dose equivalent and risk. *Radiol Prot Bull* 1984; **59:** 14–5.

26. Alm Carlsson G, Carlsson CA. Relations between effective dose equivalent and mean absorbed dose (energy imparted) to patients in diagnostic radiology. *Phys Med Biol* 1986; **31:** 911–21.

27. Shrimpton PC, Jones DG, Wall BF. The influence of tube filtration and potential on patient dose during x-ray examinations. *Phys Med Biol* 1988; **33:** 1205–12.

28. Huda W, Sandison GA, Palser RF, Savoie D. Radiation doses and detriment from chest x-ray examinations. *Phys Med Biol* 1989; **34:** 1477–92.

29. International Commission on Radiation Units and Measurements: *Radiation Quantities and Units,* ICRU Report 33, ICRU Washington, 1980.

30. Carlsson C. Determination of integral absorbed dose from exposure measurements: *Acta Radiol Ther Phys Biol* 1963; **1:** 433–58.

31. Meridith WJ, Massey JB. *Fundamental Physics of Radiology,* 2nd ed., John Wright & Sons Ltd., Bristol, 1972.

Radiol Oncol 1994; 28: 221-5.

Pre-treatment verification of high dose rate Ir-192 treatment plans

Matthew B. Podgoršak, Claudio H. Sibata, Anthony K. Ho, and Kyu H. Shin

Department of Radiation Medicine, Roswell Park Cancer Institute, Buffalo, New York 14263, USA

A computer program that enables a pre-treatment verification of high dose rate iridium-192 dose distributions calculated by any treatment planning system has been developed. The software is first used to verify that the potential dwell positions determined by the planning system from localizing radiographs coincide with the applicators implanted within the patient. It then calculates the dose at user-defined points based on the source dwell position coordinates and dwell times reported by the treatment planning system. A comparison of the dose values at several verification points to the isodose distribution calculated by the planning system provides an independent check of the treatment plan that could prevent large errors in dose delivery.

Key words: brachytherapy: radiotherapy planning, computer-assisted, iridium radioisotopes

Introduction

The remote afterloading of small, high activity radioactive sources into pre-implanted applicators is an effective treatment modality for both intracavitary and interstitial radiation therapy. The dose rates associated with these sources are several orders of magnitude greater than those in conventional brachytherapy implants made with manually-loaded sources of much lower activity. Hence, the high activity sources have come to be known as high dose-rate (HDR) sources, and the treatment itself is referred to as HDR brachytherapy.

Correspondence to: Matthew B. Podgorsak, Ph.D., Department of Radiation Medicine, Roswell Park Cancer Institute, Elm and Carlton St., Buffalo, New York 14263, USA.

UDC 615.849.5

The advantages and disadvantages of HDR brachytherapy compared to standard brachytherapy delivered with conventional low dose rate (LDR) sources have been well documented in the literature.[1, 2] Presently, the most commonly used HDR remote afterloader is the Microselectron (Nucletron Corporation, Leersum, Holland). This unit houses a single iridium (Ir-192) source with a nominal activity of 370 GBq (10 Ci). The source is attached to a stainless steel cable and is driven by remote control between the storage safe located at the unit and user-programmed positions within the lumen of applicators implanted inside a patient. The source dwell positions coupled with the length of time that the source sits at each position define an HDR implant.

Treatment planning algorithms calculate the dose distribution for these implants using a formalism which includes several variables that

describe the radiation properties of the HDR Ir-192 source.[3] In view of the potentially serious consequences of a misadministration of an HDR brachytherapy procedure, an independent verification of each treatment plan before treatment is not only highly recommended, but has already or will in the near future become a requirement in many jurisdictions. A program which performs such a verification was recently described by Young and Witbeck.[4] In their system, dose calculations are made using the dose point and dwell position coordinates and dwell times extracted from a planning system. These doses are then compared to the treatment plan. It is not sufficient, however, to only verify the dose calculated by a treatment planning system using source and dose point coordinates reported by the same planning system. This is because the accuracy of the implant geometry used in the dose calculation algorithm is limited by the accuracy of the digitization of the source localization films. A complete verification of an HDR Ir-192 treatment plan must therefore start with a check of the fidelity of the dwell position and dose point coordinates reported by the planning system to the actual implant, and conclude with a verification of the dose calculation.

The HDR brachytherapy verification program developed at our institution is a menu-driven stand-alone application that runs on any Macintosh (Apple Computer, Inc., Cupertino, CA) computer. The first step in using the software involves entering the patient name and medical record number. The source activity on the day of treatment is automatically calculated based on the calibrated activity of the source, the time elapsed since the last source calibration, and a half-life for HDR Ir-192 source decay of 73.83 days.[5] Next, the user enters the Cartesian (x, y, z) coordinates of each dwell position along with each corresponding dwell time, as reported by the planning system. Once the data for all dwell positions has been entered, the user selects the option *Review Dwell Positions and Times* from the main menu. A listing of the dwell positions and times as well as a scaled diagram of the implant appear in two separate windows on the screen. Each point in the two-dimensional implant diagram represents a dwell position projected onto the z = 0 plane. The diameter of each point is proportional to the value of the z-coordinate of the corresponding dwell position in the actual implant. Even though the diagram does not provide a quantitative geometrical description of the implant, it is still useful to examine a scaled, projected image of the planned source dwell positions relative to each other. Since source movement is constrained to an applicator with a known geometry, all source dwell positions in a correct representation of the implant should conform to the expected shape of the applicators used. Assuming there were no typographical errors in the input of the dwell position coordinates into the verification software, any misplaced dwell positions would be the result of an error in the digitization of the dummy source positions from the localization films.

Verification of localizing radiograph digitization

If no obvious errors are found based on a cursory examination of the implant diagram, a more quantitative evaluation of the digitization can be performed. With the mouse, the user can click in the vicinity of any dwell position in the window displaying the implant diagram. The coordinates of the closest dwell position are marked in the list by an asterisk and the dwell position itself is highligted in the diagram. The user then selects a second dwell position which also in highlighted. The software draws a solid line between the two selected dwell positions in the diagram and then calculates and displays the distance between these two dwell positions in the actual implant. If there were no errors in the digitization of the localization films, this distance will be very close to a multiple of the source step size (2.5 mm in most Microselectron HDR Ir-192 implants). A distance significantly different is probably the result of an error in the digitization of the source localizing films. Possible errors include

incorrect determinations or transcriptions of localizing film magnification, or an inaccurate digitization of the dummy source positions. The user now has the option of checking the distance between any two other dwell positions in the implant diagram, quitting the program if an error in digitization is found, or continuing to the next part of the program to verify the dose calculation in the treatment plan. We recommend verifying the distance between several consecutive and non-consecutive dwell positions before making a judgment on the accuracy of the film digitization.

Verification of dose calculation

After establishing the accuracy of the implant geometry determined by the planning system, the user can proceed to the option *Input Dose*

** RPCI HDR BRACHYTHERAPY VERIFICATION **

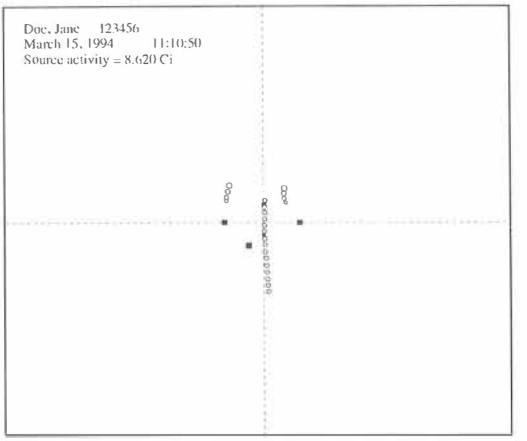

Figure 1. Sample printout from the verification program. In this case, the HDR Ir-192 implant is comprised of a tandem and two ovoid applicators. In the implant diagram, the open circles and filled squares represent source dwell positions and dose verification points, respectively. The source dwell position coordinates and dwell times as well as the dose the each verification point are listed beneath the implant diagram.

Doe, Jane 123456
March 15, 1994 11:10:50
Source activity = 8.620 Ci

RPCI HDR BRACHYTHERAPY VERIFICATION

Dwell Position (mm)	Dwell Time (s)	Dose Point	Coordinates (mm)	Dose (Gy)
(–18.9, 14.6, –3.2)	12.7	bladder	(–7.5, –14.7, 11.2)	8.306
(–18.5, 16.9, 0.4)	14.2	rectum 1	(–0.1, 13.1, –23.6)	3.162
(–18.0, 19.8, 3.7)	15.2	rectum 2	(0.5, –7.5, –32.8)	2.223
(–17.4, 23.4, 6.9)	15.4	left »m«	(–20.0, 0.0, 0.0)	5.328
(10.4, 15.3, –3.5)	13.4	right »m«	(20.0, 0.0, 0.0)	4.821
(10.1, 18.0, 0.2)	13.1			
(9.9, 21.0, 3.9)	13.3			
(9.8, 24.3, 7.3)	13.6			
(1.9, –51.6, 7.4)	20.5			
(1.9, –46.9, 6.4)	20.7			
(2.0, –42.3, 5.5)	21.3			
(1.7, –37.4, 4.3)	21.9			
(1.4, –32.5, 3.2)	22.3			
(1.1, –27.6, 2.6)	22.2			
(0.8, –22.7, 1.9)	21.5			
(0.7, –17.5, 1.4)	20.0			
(0.5, –12.3, 0.8)	17.8			
(0.4, –7.7, 0.5)	15.2			
(0.2, –3.0, 0.1)	12.5			
(0.4, 2.3, 0.0)	10.2			
(0.5, 7.5, 0.0)	8.5			
(0.4, 12.0, 0.1)	7.4			
(0.3, 16.4, 0.2)	6.9			

Points and Calculate Dose from the main menu. In this module, the software calculates and displays the dose at user-defined points in the implant. The dose calculation algorithm assumes that each source dwell position represents a point source radiating isotropically. Corrections for photon scatter and attenuation in the patient are made using the Nucletron Planning System (NPS) dose buildup model, however, exposure rate anisotropy around the HDR Ir-192 source is ignored. The coordinates of the verification points entered into the program are those determined by the planning system based on identification and digitization of applicator and anatomical landmarks from the localization films. Typically, the points chosen for verification include the prescription point and several dose-limiting structures, such as the rectum and bladder in gynecologic implants and the spinal cord in endobronchial treatments.[6,7] Once all verification points have been entered, the software displays an image of the implant, again projected onto the $z = 0$ plane, with all dwell positions and dose points marked individually by circles and squares, respectively. The dose and coordinates at each verification point are listed in a second window to permit comparison with the treatment plan. A hardcopy printout showing a scaled two-dimensional diagram of the implant and all relevant patient identification can be requested. An example of the printout for an implant using a tandem and two ovoid applicators is shown in Figure 1. In addition to the implant diagram, the printout gives a listing of the dwell positions and times along with the name, coordinates, and calculated dose at each verification point. This printout can become part of the patient chart and demonstrates an independent check of the treatment plan before initiation of treatment.

In our practice, the discrepancy in the isodose plan and the dose evaluated using the verification software is typically less than 4% for implants where the localizing film digization was done properly. A large fraction of this discrepancy can be attributed to the brachytherapy planning system (NPS) accounting for the exposure rate anisotropy of the HDR Ir-192 source whereas our verification software does not. Evidence supporting this explanation is the increasing dose discrepancy as the dose calculation points get closer to an applicator longitudinal axis. In the implant shown in Figure 1 the greatest difference in the calculated dose occurs at the dose point labeled *rectum 1,* where the exposure rate anisotropy has the largest effect. The smallest error occurs at *right »m«,* the furthest point from an applicator axis. As expected, if the treatment plan is recalculated using an isotropic source model (no corrections for source anisotropy) and the same dwell positions and times, the dose discrepancy disappears. Unfortunately, recalculating each treatment plan using an isotropic source model is time-consuming and cannot be done before the initiation of treatment. Moreover, incorporating source anisotropy correction factors into the verification algorithm is not a trivial proposition and is beyond the scope of this present software. Therefore, a difference of 4% in the doses calculated by a planning system (using source anisotropy correction factors) and the verification software, with the latter dose being higher, is considered acceptable. Dose discrepancies larger than 4%, however, cannot be attributed to differences in the dose calculation algorithm and should be investigated before a treatment procedure is initiated.

Conslusion

The verification software described above allows an independent check of an HDR brachytherapy treatment plan calculated by any treatment planning system. The program first checks the accuracy of the implant geometry determined by the planning system based on the digitization of source localizing radiographs. The software then verifies that the calculated dwell positions and times will deliver the prescribed dose to the prescription point and, also, that they will not result in a serious overdose to any sensitive structure. Use of this software does not considerably increase the time between applicator insertion and the beginning of treat-

ment for most implants and, furthermore, could prevent a dangerous dose misadministration.

References

1. Chenery SGA, Pla M, Podgorsak EB. Physical characteristics of the Selectron high dose rate intracavitary afterloader. *Br J Radiol* 1985; **58**: 735–40.
2. Fu KK, Phillips TL. High dose-rate versus low dose-rate intracavitary brachytherapy for carcinoma of the cervix. *Int J Radiat Oncol Biol Phys* 1990; **19**: 791–6.
3. Killian H, Baier K, Loeffler E, Sussenbach K, Dorner K. A comparison of different planning algorithms used in interstital radiotherapy with iridium-192 wires. In: Mould RR ed. *Brachytherapy 2*. Nucletron, 1989: 92–100.
4. Young RD, Witbeck KA. Dose verification in HDR remote afterloading. *Activity – International Selectron Brachytherapy Journal* 1993; **7**: 12–13.
5. Podgorsak MB, DeWerd LA, Paliwal BR. The half-life of high dose rate Ir-192 sources. *Med Phys* 1993; **20**: 1257–9.
6. Stitt JA, Fowler JF, Thomadsen BR, Buchler DA, Paliwal B, Kinsella TJ. High dose rate intracavitary brachytherapy for carcinoma of the cervix: the Madison system: I. Clinical and radiobilogical considerations. *Int J Radiat Oncol Biol Phys* 1992; **24**: 335–48.
7. Mehta M, Petereit D, Chosy L, Harmon M, Fowler J, Shahabi S, Thomadsen B, Kinsella T. Sequential comparison of low dose rate and hyperfractionated high dose rate endobronchial radiation for malignant airway occlusion. *Int J Radiat Oncol Biol Phys* 1992; **23**: 133–9.

Radiol Oncol 1994; 28: 226-30.

Development of treatment planning at X-ray, telecobalt and betatron units between 1936 and 1978

László Gyarmathy, László Bozóky, György Reischl, Tibor Major

National Institute of Oncology, Budapest, Hungary

Authors report the treatment planning modalities (at X-ray, telecobalt and betatron) developed in the Radium Hospital and later at the National Institute of Oncology from 1936 till 1978. The technical advance and trends of dosimetry used for this purpose is briefly outlined.

Key words: radiotherapy-history; history of megavolt and rotation therapy; dosimetry; treatment planning

Beginning

The precursor of our Institute was the capital's "Eötvös Lóránd Radium and Roentgen Institute" established in 1936. For the therapy of deep situated tumors it had a 3 g Ra unit and a 400 kV roentgen apparatus, representing the highest energy at that time.[1] The physics laboratory constructed a slowly turning platform with a chair, for 200 kV rotation therapy of sitting patients, at horizontal beam direction. By choosing the parameters, (axis of rotation, field size, etc.) it was possible to measure appropriate dose distributions with Bozóky's little condenser ionisation chambers in a trunk shaped, tissue-equivalent phantom. This method of therapy was then used for routine treatment.

In 1944 a bomb fell in front of the building. Some equipment and instruments were hidden in the cellars of the St. Stephen cathedral and the Ra-source was put into the rock-treasury of National Bank in Veszprém. Later it was carried away to Bavaria. En route, the lorry was hit by a fire-bomb and burnt down. The molten lead container including Ra fused with the wreckage and the pavement of the highway. Only two – thirds of the Ra were regained later. William Czunft, director and the leading light of our research – a man of outstanding character – sacrified his life, having hidden personally the Ra needles and tubes in wartime. He had suffered radiation injury.

Correspondence to: Dr. László Gyarmathy, Kisköre u. 16, III. Lépcsó 7, H-1116 Budapest, Hungary.

UDC: 615.849.1 (091)

National Institute of Oncology

In 1953 the Radium Hospital was reorganized and completed with different departments and the new "National Institute of Oncology" occupied its recent location in Buda. At that time the Ra-units were replaced by telecobalt ones all over the world, the latter having three times higher order of magnitude considering the radiation intensity. Our physics laboratory constructed a special cobalt unit "Gravicet" (Figure

1) providing much better protection for the staff, than the conventional ones.[2] On completion of treatment the source immediately left the head and slid into a lead container imbedded in the concrete wall. The movement of the source was carried out by gravitation with the help of two weights. This unique machine was

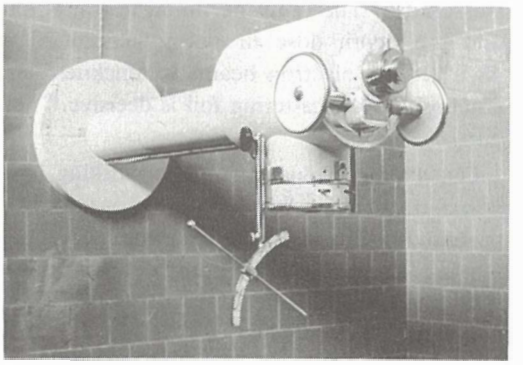

Figure 1. The primordial Gravicert, constructed in our Department of Physics.

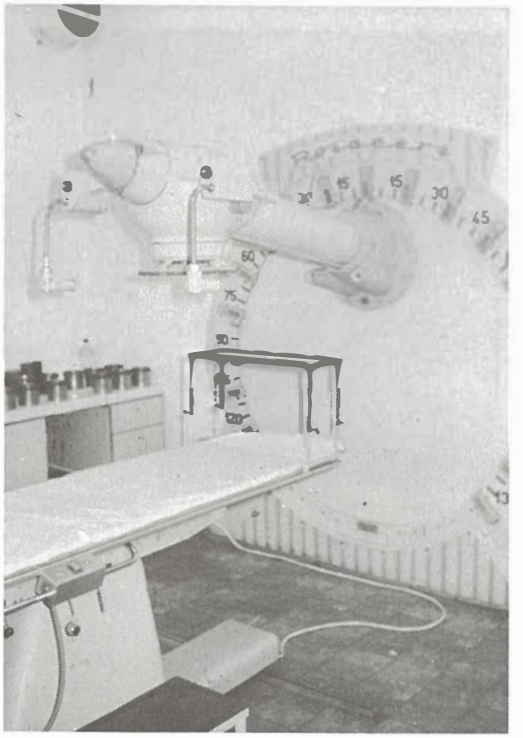

Figure 2. The Rotacert, made by Medicor Co., working with gravicert principle.

then manufactured by Medicor Co. for home and foreign use. The therapy with our in the home made Gravicert began in 1958. Soon the planning of an arc therapy machine, co-operating with Medicor, based on Gravicert principle started as well. The »Rotacert« was installed in 1965 (Figure 2). It is still operating, but only for stationary field therapy.[3] The movement of the source here is also made by the same manner: gravitation and two weights. The only difference is that the neck of Gravicert is situated horizontally, but that of the Rotacert and the axis of rotation form an acute angle (Figure 3) and the container in the wall is fixed in a steel cylinder, revolving simultaneously with the head directed by machine. Such cobalt units, with similar excellent radiation protection were constructed nowhere else. In the last years the ICRP lowered again the professional dose limits, nearly to the hundredth of the old Mutscheller's tolerance dose. Therefore it proved to be very favourable for the staff to work with a machine, having outstanding radiation protection, reducing the risk of carcinogenic and genetic mutation or other injury.[2–4] The Gravicert had been removed and its wooden maquette is now exhibited in the Museum of Technics. A 10-MeV Neptun-10p linac is operating there instead of it.

The radioprotective measurements, depth dose data and isodoses were done by our Physics Department[2–5] in accordance with the international rules and practice.[7–11] As till 1969 the telecobalt division had no resident physicist, the treatment planning was made by the physician through graphical summation of our isodo-

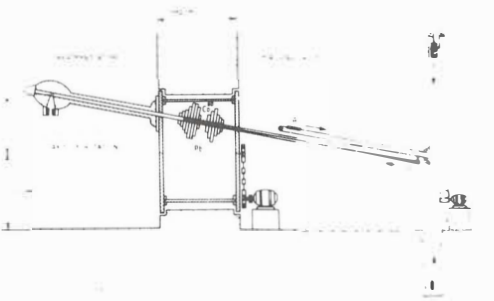

Figure 3. Cross-section of the Rotacert.

ses in the actual cross-section.[12] Special measuring procedures, necessary for the rotation therapy (TAR, absorption of treatment couch, etc.) were done as well. Later, for the calculation of the absolute dose instead of TAR we used the Tissue-Normaldose Ratio (TNR), i.e. the dose at the center of the field, measured in the axis of rotation at any depth, related to the dose received in the same place, at 5 cm depth in water. For the determination of dose distribution we adapted the effective absorption coefficient method, described by Jones et al,[13] modified to Rotacert.[14] A number of typical plans were calculated for different cross-sections, rotation centers, field size and pendulum angles. If the latter exceeded 180° a correction was made for the treatment coach. Years later comparing the isodoses obtained by this method and that of van de Geijn's we found the difference in the central zone was negligible, peripherally the values of van de Geijn method were lower.

The next step was the installation of a soviet B5M-25 betatron (Figure 4). It was located under the garden in the place of an old air-raid shelter. It was the first piece of a new series and hadn't measured exactly enough.[15–17] For example, we did not obtain any isodose chart or energy diagram. The original monitor proved not to be reliable for electron therapy, so we had to construct a new pair of these. After studying the current literature.[7,8,10,11,18–20] we started a complete measurement procedure in 1970/71. Our current guide was the protocol of NACP, as professor Svensson kindly sent us a lot of their publications on betatron dosimetry, the earlier versians having been published in the Acta Radiologica.[21–25]

The X-ray therapy began in March, 1971, the electron irradiation at the end of 1973. The energy calibration was done by threshold analysis, detecting the (γ,n) reactions of Cu-63, O-16 and C-12, (10.8, 15.7 and 18.7 MeV respectively), using copper sheets, water and n-heptane. Extrapolating the maximum energy was derived 28 MeV at X-ray. For electrons the practical range (Rp) was measured in water. This quality was utilizable from 7 to 26 MeV.

The deep- and izo-ionisation curves were measured with Siemens Sondenfingerhut, PTW normal and microchambers in water. Later we used self-manufactured little cylindrical chambers of 15–50 mm^3 as well. At X-ray the changing of flattening filter together with field size influenced the depth dose less, but the positioning of the former, in respect of homogeneity was critical. The dose maximum lies in 4.5 cm and the depth dose in 10 cm 86.5 in 20 cm 58.5 %.[14] At electron beam the thickness and composition of scattering foil is decisive.[16] (Figure 5).

Our Physics Department was working as a dosimetric center,[1,6] In this period our dosimetry based mainly in Co-60 exposure calibration. Among others such measurement was made with National Office of Measurements (NOM) and with IAEA, Vienna in 1971 and 1972.[6,26] The second was completed with calorimetry as well. In the meantime a comparative measurement was also done with 20 MeV electron beam

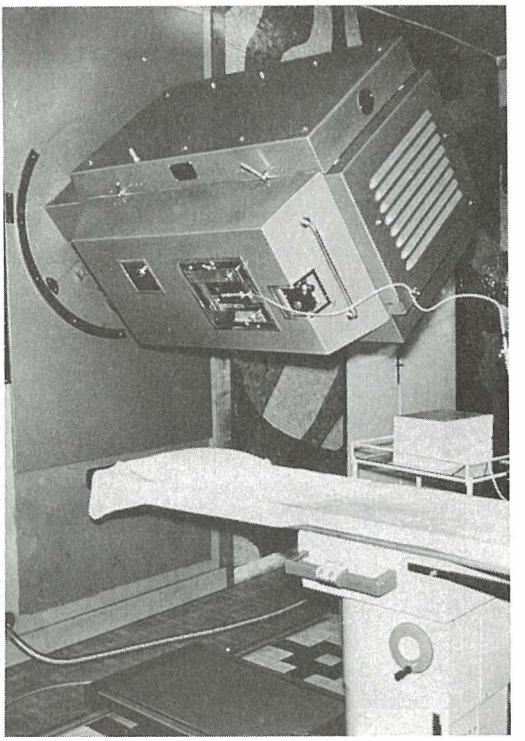

Figure 4. The B5-M25 betatron.

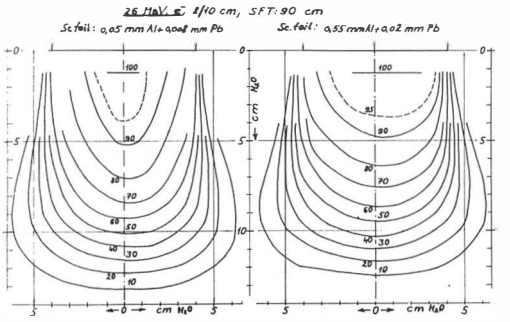

Figure 5. Isodoses of 26 MeV electron irradiaton with different scatter-foils.

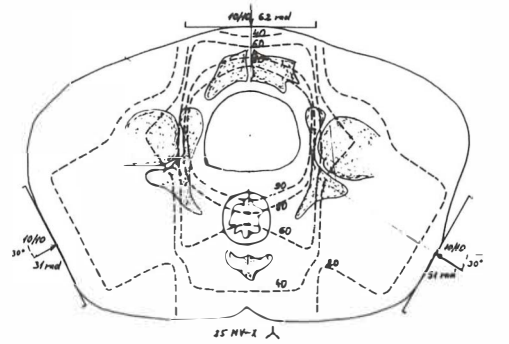

Figure 6. 25MV X-rays; treatment plan with 3 fields (vesica urinaria).

in water and plexi-phantom. The participants were NOM, our Physics Department and the betatron division. On this occasion ferrous-sulphate dosimetry was also used (Toperczer). Later $FeSO_4$ and LiF samples were irradiated and sent to IAEA, Vienna.

The treatment planning was made by graphical addition (Figure 6). In some case electron therapy was combined with telecobalt gamma, or betatron X-radiation. In 1978 the Computerized Treatment Planning Network came into being in Hungary by the organisation of the Physics Department of our Institute, but this is an another story.

References

1. Bozóky L, Toperczer J. Progresin radiophysics. In: Vikol J, Sellei C, State Oncol Inst ed. *Twenty-five Years in the Fight Against Cancer.* Budapest: Acad Press, 1966: 79–89.
2. Bozóky L. Ein Telekobaltgerät mit vollständigem Strahlenschutz. *Strahlentherapie* 1960; **112**: 629–31.
3. Bozóky L. The new rotational cobalt unit of our Institute (In Hungarian). *Magy Onkol* 1966; **10**: 189–92.
4. Bozóky L. New technique for full radiotation protection of personnel in telecobalt treatment. In: Snyder WS ed. *Proceedings of the First Internat Congr of Radiation Protection Rome.* Vol II. Oxford: Pergamon Press, 1968; 1597-601.
5. Bozóky L. Single field isodose charts for high energy radiation. *IAEA Techn Rep Ser* (Vienna) 1962; **8**: 55.
6. Bozóky L, Zsdánszky K, Hizó J. Standard dosimetry in Hungary and international dose intercomprison since 1938. In: *Biomedical Dosimetry. Proceedings of a Symposium.* Vienna 10–14 March 1975; IAEA 1975: 405–15.
7. Hospital Physicists Assotiation HPA. A code of practice for the dosimetry of 2 to 35 MV x-ray Caesium-137 and Co-60 gamma ray beams. *Phys Med Biol 1969;* **14**: 1–8.
8. Hospital Physicists Association HPA. A review of Suppl. 10. Depth dose tables for use in radiotherapy. *Brit J Radiol* 1968; **41**: 932–6.
9. International Commission on Radiological Units and measurements ICRU: Report No. 10d. *Clinical dosimetry.* NBS handbook 87. Washington D.C.: 1968.
10. International Commission on Radiological Units and Measurements ICRU: Report No. 14. *Radiation dosimetry:* X-rays and gamma rays with maximum photon energies between 0,6, and 50 MeV, Washington D.C.: 1969.
11. Johns HE, Cunnigham JR. *Physics of radiology.* 2nd ed. Charles C Thomas, Springfield, 1968.
12. Gyarmanth L. Dose distribution in stationary field telecobalt irradiation. In Vikol J, Sellei C, State Oncol Inst ed. *Twenty-five Years in the Fight Against Cancer.* Budapest: Acedemic Press, 1966; 65–73.
13. Jones DEA, Gregory C, Birchall I. Dosage distribution in rotational Cobalt-60 therapy. *Brit J Radiol* 1956, **29**: 196–201.
14. Gyarmanthy L. Clinical application of moving beam telecobalt irradiation with Rotacert unit (In Hungarian). *Magy Onkol* 1966; **10**: 228–31.
15. Bozóky L. 25 MeV betatron (In Hungarian). *Fiz Szle* 1969; **19**: 352–5.
16. Gyarmathy L, Reischl Gy. Some characteristics of electron beam therapy (In Hungarian). *Magy Radiol* 1973; **25**: 355–61.
17. Gyarmathy L, Reischi Gy. Characteristics of betatron therapy (In Hungarian). Tigyi J, Rontó Gy. ed. Yearbook of the Hungarian Biophysics Society. 1975: 26–9.

18. Johns HE, Laughlin JS. Interaction of radiation with matter. In: Hine GJ, Brownell ed. *Radiation Dosimetry*. New York: Academic Press, 1958: 50–126.

19. Harder D. Energiespektren schneller Elektronen in verschiedenen Tiefen. In: Zuppinger A, Poretti G ed. *Symposium on high energy electrons*. Berlin: Springer Verlag, 1971: 26–31.

20. Sub-committee on Radiation Dosimetry of American Association of Physcists in Medicine (SCRAD): Protocol for dosimetry of high energy electrons. *Phys Med Biol* 1966; **11**: 505.

21. Pattersson C, Hettinger G. Dosimetry of high energy electrons based on ferrous-sulphate dosemeter. *Acta radiol Ther Phys Biol* 1967; 6: 160–76.

22. Svensonn H, Hettinger G. Dosimetric measurements at the Nordic medical accelerators I. Characteristics of the radiation beam. *Acta radiol Ther Phys Biol* 1971; **10**: 369–84.

23. Svensson H, Pettersson C, Hettinger G. Commercial thimble chambers for absorbed dose measurements at high energy electron radiation. *Acta radiol Ther Phys Biol* 1971; **10**: 504–9.

24. Svensson H. Dosimetric measurements at the Nordic medical accelerators, II. Absorbed dose measurements, *Acta Radiol Ther Phys Biol* 1971; **10**: 631–54.

25. Nordic Association of Clinical Physicists (NACP). Procedures in radiation therapy dosimetry 5 to 50 MeV electrons and roentgen and gamma rays with maximum photon energies between 1 and 50 MeV. *Acta radiol Ther Phys Biol* 1971; **11**: 603–24.

26. Bozóky L, Nagl J, Haider J. Consideration of factors for determination of absorbed dose from exposure measurements in the beam of Co-60 teletherapy units. *Acta Phys Sci Hung* 1974; **35**: 105–12.

Notices

Notices submitted for publication should contain a mailing address, phone and/or fax number of a contact person or department.

Good clinical practice

The ESO teaching course will be held at *October 18–20, 1994.*

Contact Miss Gollubics, ESO-Vienna-Office, Arztekammer für Wien, Fortbildungsreferat Weihburggasse 10-12, A-1010 Vienna, Austria; or call +43 1 51501 293; fax +43 1 51501 240.

Radiotherapy

ESTRO teaching course "Role of Radiotherapy in the Management of Cancer" will take place in Athens, *October 23–27, 1994.*

Contact the ESTRO Secretariat, Radiotherapy Department, University Hospital St Rafael, B-3000 Leuven, Belgium; or call +32 16 33 64 13; fax +32 16 33 64 28.

Nuclear medicine

The 6th World Congress of The World Federation of Nuclear Medicine & Biology will be held in Sydney, Australia, *October 23–28, 1994.*

Contact The Secretariat, 6th World congress of The World Federation of Nuclear Medicine and Biology, GPO Box 2609, Sydney, NSW Australia; or call +61 2 241 1478; fax +61 2 251 3552.

IAEA Scientific meeting

The international conference on radiation, health and society: comprehending radiation risks will be offered in Paris, France, *October 24–28, 1994.*

Contact International Atomic Energy Agency, P.O. Box 100, Vienna International Centre, A-1400 Vienna, Austria.

Radiology

The 45th annual general and scientific meeting organised by Royal Australiasian College of Radiologists will be held in Christchurch, New Zealand, *October 28–31, 1994.*

Contact Dr. P. Scally, Brisbane, Australia; or call +61 7 840 8111; fax +61 7 844 8755.

Cancer

The 16th international cancer congress will be held in New Delhi, India, *October 30 – November 5, 1994.*

Contact UICC Congress Secretariat, XVI International Cancer Congress, Tata Memorial Centre, Parel, Bombay 400 012, India; or call +91 22 41 29 399/ +91 22 41 46 685; fax +91 22 41 39 318/ +91 22 41 46 927.

Oncology

The 11th Austrian annual meeting "ÖGRO-Jahrestagung (Österreichische Gesellschaft für Radioonkologie, Radiobiologie und Radiophysik)" will be offered in Wiena, Austria, *November 4–5, 1994.*

Contact ÖGRO-Jahrestagung Secretariat, Universitaetsklinik für Strahlentherapie und Strahlenbiologie, Währing Gürtel 18<20, A-1090 Wien, Austria; or call + 43 1 40 400 27 00 (Frau Juller); fax + 43 1 40 400 27 01.

Medical oncology

The 19th European Sociaty for Medical Oncology (ESMO) Congress will take place in Lisbon, Portugal, *November 18–24, 1994.*

Contact ESMO Central Secretariat, Via Soldino 22, 6903 Lugano, Switzerland; or call +41 91 575 411; fax + 41 91 575 744.

Radiation protection

The 2nd symposium of Croatian Radiation Protection Association will be held in Zagreb, Croatia, *November 23–25, 1994.*

Contact Dr. Kubellia, Institute for Medical Research and Occupational Health University of Zagreb, Meštrovićev trg 16; 41000 Zagreb, Croatia; or call +38541 674 572; fax + 38541 274 572.

Gastrointestinal diseases

The "1st Croatian Gastroenterology Congress with the International Contribution" will be held in Zagreb, Croatia, *November 24–26, 1994.*

Contact Dr. Rajko Ostojić, Clinic for Internal diseases, KBC Rebro, Kišpatićeva 12, 41000 Zagreb, Croatia.

Radiology

The "80th Scientific Assembly and Annual Meeting of the Radiological Society of North America (RSNA)" will take place in McCormick Place, Chicago, USA, *November 27–December 2, 1994.*

Contact RSNA, 2021 Spring Road, Suite 600, Oak Brook, IL 60521, USA; or call + 1 708 571 2670; Fax + 1 708 571 7837.

Therapeutic endoscopy

The 9th international workshop will be offered in Hong Kong, *December 6–8, 1994.*

Contact Dr. Sydney Chung, Endoscopy Ctr., CUKHK, Prince of Wales Hosp., Shatin, N. T. Hong Kong; or call + 852 636 2233.

Endocurietherapy

The 17th Annual Mid-Winter Meeting of American Society will take place in McCormick Place, Fort Myers, Florida, USA, *December 7–10, 1994.*

Contact Office of the Secretariat, American Endocurietherapy Society, 1101 Market Street, Philadelphia, PA 19107, USA; or call + 1 215 574 13158.

Pulmonary disease

The 3rd International Postgraduate Course "New Trends in the Diagnostic of Respiratory Disorders" will be offered in Trieste, Italy, *December 12–13, 1994.*

Contact Organising Secretariat, Trieste Traduzioni Congressi, Via C. Battiosti 1, 34125 Trieste, Italy; or call + 39 40 371 678; + 39 40 370 634.

Oncogenes

The symposium "Oncogenes: 20 Years Later" will be offered in Keystone, Colorado, USA, *January 5–11, 1995.*

Contact "Keystone Symposia", Deawer 1630, Silverthorne, CO 80498, USA; or call + 1 303 262 1230.

Gastrointestinal malignancies

Tne 2nd International Conference on Biology, Prevention, and Therapy of Gastrointestinal Malignancies will be held in Koeln, Germany, *January 9–12, 1995.*

Contact H. Wilke, Essen Univ. School, Essen, Germany; or call + 49 201 72231; fax: + 49 201 723 5924.

Pediatric oncology

The evolving role of radiation in pediatric oncology "Controversies and Consensus" will be offered in Philadelphia, USA, *January 19–21, 1995.*

Contact Office of Continuing Medical Education, University of Pennsylvania School of Medicine, 134-R Nursing Education Building, 420 Guardian Drive, Philadelphia, PA 19104-6020, USA; or call + 1 215 898 8005; Fax: + 1 215 898 1888.

Dietetics

The "2nd International Conference on Dietary Assessment Methods" will take place in Boston, USA, *January 22–24, 1995.*

Contact Kathryn Lord, Harvard School of Public Health, Office of Cont. Educ., 677 Huntington Ave., LL-23, Boston, MA 02115-6023, USA; or call + 1 617 432 1171.

Oncology

The "4th European Winter Oncology Conference" will be held in Meribel, France, *January* 22–27, 1995.

Contact Mrs A. M. Vangindertael, EWOC-4 Secretariat, Department of Radiotherapy, University Hospital St Rafael, Kapucijnenvoer 33, B-3000 Leuven, Belgium; or call + 32 16 33 64 27; Fax: + 32 16 33 64 23.

Medical oncology

The 5th International Congress on Anti-Cancer Chemotherapy will take place in Paris, France, *January 31–February 3, 1995.*

Contact 5th CICAC Secretariat; or call + 45 70 22 37; Fax: + 45 70 28 36.

Colorectal cancer

The seminar, entitlet "Colorectal Cancer: from Gene to Cure" will be held in Amsterdam, The Netherlands, *Februry 9–11, 1995.*

Contact R. F. M. Van Bokhoven, Head Educational Dept. IKA, Plesmanlaan 125, 1066CX Amsterdam,

The Netherlands; or call + 31 20 617 2903; Fax: + 31 20 615 5904.

Breast cancer

A meeting, entitled "Adjuvant Therapy of Primary Breast Cancer" will be held in St Gallen, Switzerland, *March 1–4, 1995.*

Contact Mrs B. Nair, ABC-95, C/o Prof H. J. Senn, Department C of Internal Medicine, Kantonsspital, Building 09, Room 202, CH-9007, St Gallen, Switzerland; or call + 41 71 261 097; Fax: + 41 71 256 805.

Radiology

The 9th European Congress of Radiology ECR'95 will be held in Vienna, Austria, *March 5–10, 1995.*

Contact ECR-Office, European Congress of Radiology, Neutorgasse 9/2a, A-1010 Vienna, Austria; or call + 43 1 533 40 64; Fax: + 43 1 533 40 649.

As a service to our readers, notices of meetings or courses will be inserted free of charge.

Please send information to the Editorial office, Radiology and Oncology, Vrazov trg 4, 61105 Ljubljana, Slovenia.

1995 OECI CONFERENCE ON CANCER AND QUALITY OF LIFE

will be organized by the Organization of European Cancer Institutes (OECI), the Institute of Oncology in Ljubljana and Istituto Nazionale per la Ricerca sul Cancero Genova.

The conference will be held from **May 12 to 14, 1995, in Bled,** Slovenia.

Informations: M. Zwitter, MD, Institute of Oncology, 61105 Ljubljana, Slovenia.
Phone: + 386 61 1314 225.
Fax: + 386 61 1314 180.

Dr. J. Cholewa

FONDACIJA

FONDACIJA DOC. DR. J. CHOLEWA

v skladu s pravilnikom za financiranje študija in znanstveno raziskovalnega dela za leto 1995, razpisuje

1. ***štipendije za večmesečni študij s področja onkologije doma in v tujini,***

2. ***denarno podporo 1,000.000 SIT za znanstveno raziskovalno delo s področja onkologije.***

Na razpis se lahko prijavijo zdravniki specialisti onkologi ali zdravniki drugih specializacij z onkološko usmeritvijo.

Prijave s kratkim opisom predvidenega študija ali raziskovalnega dela, skupaj z življenjepisom in bibliografijo, pošljite do 15. novembra 1994 na naslov:

FONDACIJA DOC. DR. J. CHOLEWA -
Komisija za štipendije in nagrade, 61000 Ljubljana, Mesesnelova 9.

Kandidati bodo o izboru pisno obveščeni 14 dni po zaključenem razpisu.

FONDACIJA DOC. DR. CHOLEWA
Upravni odbor

OMNIPAQUE™

joheksol

NYCOMED

neionsko kontrastno
sredstvo
gotovo za upotrebu

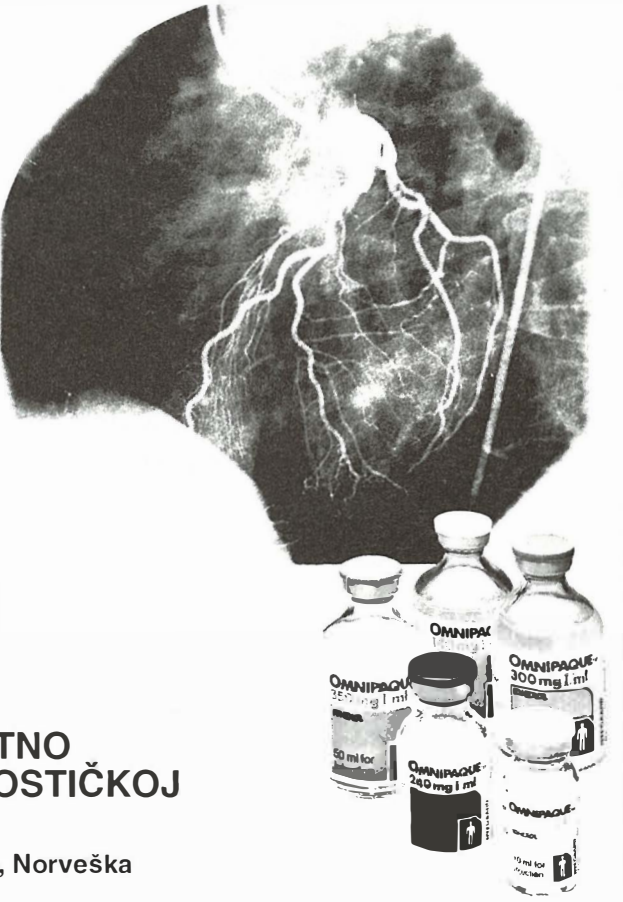

Glavne prednosti Omnipaquea

- dobra opća i lokalna podnošljivost
- vrlo niska opća toksičnost
- vrlo niska neurotoksičnost
- značajno smanjena učestalost i težina nuspojava u usporedbi s ionskim kontrastnim sredstvima
- izuzetno rijetka pojava alergijskih reakcija
- visokokvalitetni radiogrami

IZ NYCOMEDA-INOVATORA U PODRUČJU KONTRASTNIH SREDSTAVA

Omnipaque je zaštićeno ime

SIGURNIJE KONTRASTNO SREDSTVO U DIJAGNOSTIČKOJ RADIOLOGIJI

Proizvođač Nycomed A/S Oslo, Norveška

Isključiva prava prodaje u Hrvatskoj ima firma
"EWOPHARMA AG"
CH-8200 Schaffhausen/Švicarska

"EWOPHARMA AG"
Predstavništvo za Hrvatsku
Znanstveno -stručni savjetnik
Mr ph. ALFRED SENEČIĆ
41000 Zagreb, Mandićeva 29
Tel/fax: (041) 318 034

Iopamiro®

Iopamidol

150 - 200 - 300 - 370 mgI/ml

FOR ALL RADIOLOGICAL EXAMINATIONS

MYELOGRAPHY
ANGIOGRAPHY
UROGRAPHY
C.T.
D.S.A.

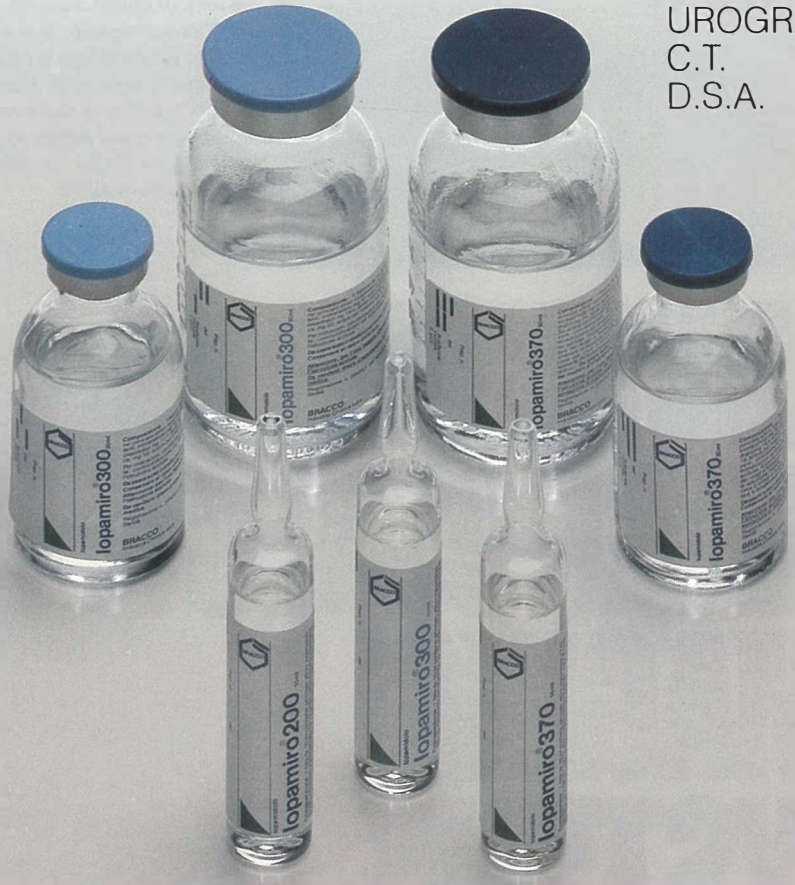

THE FIRST WATER SOLUBLE READY TO USE NON-IONIC CONTRAST MEDIUM

Manufacturer:

Bracco s.p.a.
Via E. Folli, 50
20134 - Milan - (I)
Fax: (02) 26410678
Telex: 311185 Bracco I
Phone: (02) 21771

BRACCO

Distributor:

Agorest s.r.l.
Via S. Michele, 334
34170 - Gorizia - (I)
Fax: (0481) 20719
Telex: 460690 AF-GO I
Phone: (0481) 21711

© Eastman Kodak Company, 1990

Kodak systems provide dependable performance for advanced diagnostic imaging. Our quality components are made to work together from exposure to viewbox.

Kodak X-Omat processors are the most respected in the field. Kodak X-Omatic cassettes are known the world over for unexcelled screen-film contact and durability. Kodak multiloaders have earned an enviable reputation for reliability. The Kodak Ektascan laser printer is changing the look of digital imaging. The list goes on. There are quality Kodak products throughout the imaging chain.

Equally important, they are made to work together to achieve remarkable performance and diagnostic quality. Contact your Kodak representative for more information.

ADVANCED DIAGNOSTIC IMAGING SYSTEMS. KODAK

Quality imaging worldwide

Kodak

POOPERATIVNA SLABOST IN BRUHANJE

NELAGODJE IN STISKA
OGROŽATA USPEH OPERATIVNEGA POSEGA

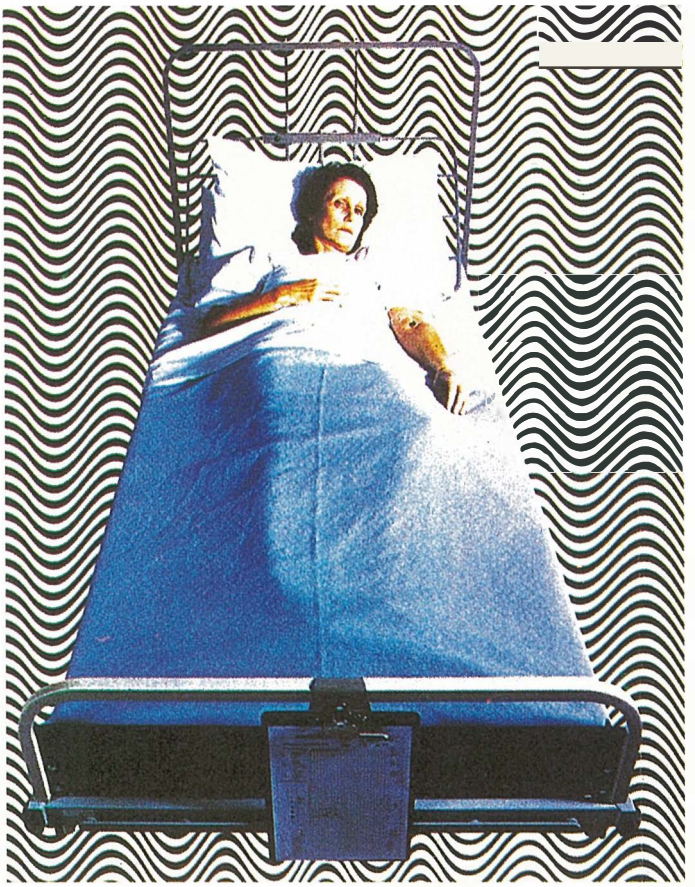

PREPREČEVANJE
Ena sama intravenska injekcija po 4 mg pri uvajanju v anestezijo

ZDRAVLJENJE
Ena sama intravenska injekcija po 4 mg

Zofran
ondansetron

Glaxo

Podrobnejše informacije dobite pri: Glaxo Export Limited
Predstavništvo v Ljubljani, Cesta v Mestni log 55, 61115 Ljubljana, p.p. 17, Slovenija
Telefon: (386 61) 123 10 70, 123 20 97, 123 23 19
Telefax: (386 61) 123 25 97

Slovenia's Bank for Global Business

SKB BANKA d.d. is an independent joint-stock company and the second largest Slovenian bank in terms of branch network and capital.

The large amount of capital on its balance sheet and its foreign currency reserves guarantee customers security and excellent prospects for further expansion.

SKB BANKA d.d. offers a wide range of banking services including:

- International payments and account services
- Non-resident account services, private and corporate
- Trade finance services
- International finance services
- Treasury and foreign exchange services
- Securities services
- Real estate financing, trading and renting

SKB BANKA d.d. has a network of first-class foreign correspondents on all five continents.

The range of services offered by the bank, is complemented by the services offered through its three bank-owned companies:
SKB Real Estate and Leasing Ltd.,
SKB Investment Company Ltd.,
SKB Aurum- Trade in precious metals, works of art, antiques and safekeeping of valuables and securities Ltd.

SKB BANKA D.D.

SKB BANKA d.d.
International Division
Ajdovščina 4
61000 Ljubljana, Slovenia
Tel.: (386 61) 312-396
Fax: (386 61) 302-808
SWIFT Code: SKBA SI 2X

SKB BANKA D.D.
Representative Office London,
37-39 Eastcheap,
London EC3M 1 DT,
United Kingdom
tel.: (44 71) 929-2174,
fax: (44 71) 929-2175

SIEMENS

Vaš partner v ultrazvočni diagnostiki:

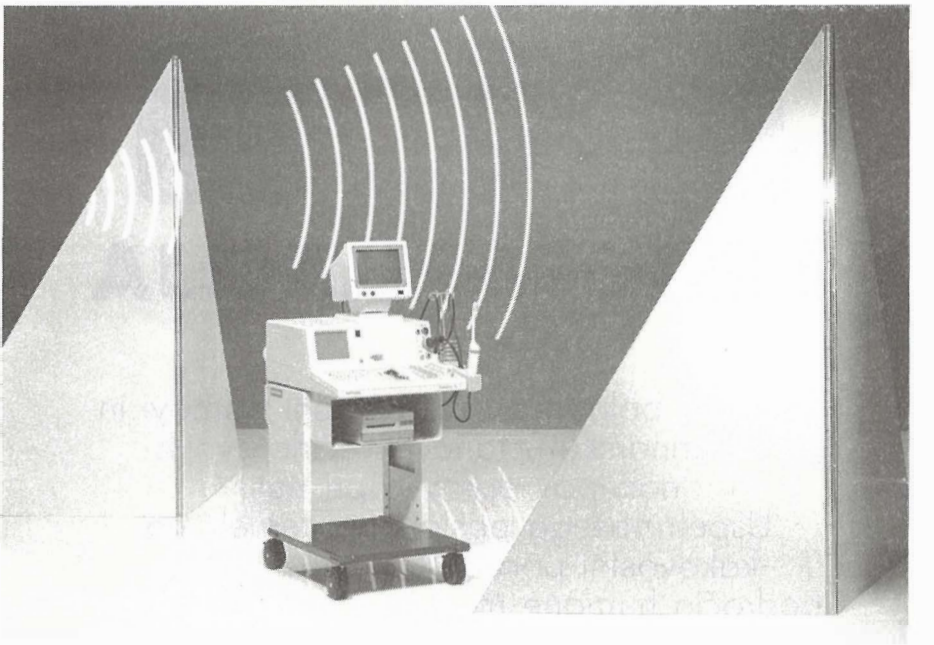

SIEMENS * SONOLINE SL-1

* **Možnost priključka sektorskega, linearnega, endo-p in endo-v aplikatorja**
* **Izredno ugodna cena (možnost kredita ali leasing-a)**
* **Servis v Sloveniji z zagotovljenimi rezervnimi deli in garancijo**
* **Izobraževanje za uporabnike**

SIEMENS D.O.O.
Dunajska 47, Ljubljana
Tel. 324-670
Fax. 132-4281

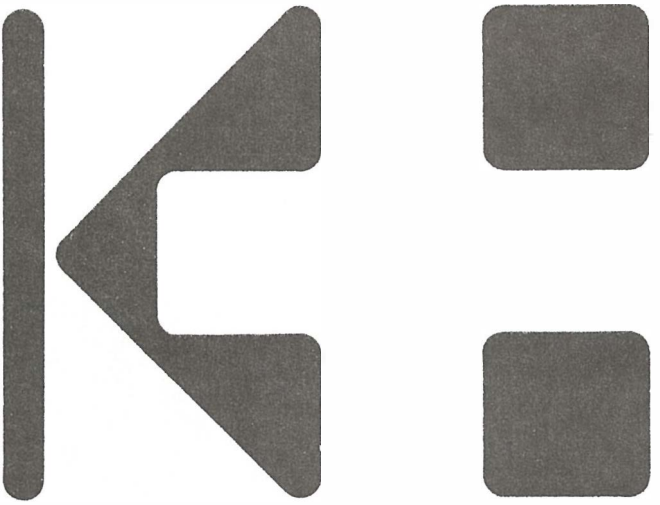

KEMOFARMACIJA

Lekarne, bolnišnice, zdravstveni domovi in veterinarske ustanove večino svojih nakupov opravijo pri nas.
Uspeh našega poslovanja temelji na kakovostni ponudbi, ki pokriva vsa področja humane medicine in veterine, pa tudi na hitrem in natančnem odzivu na zahteve naših kupcev.

KEMOFARMACIJA – VAŠ ZANESLJIVI DOBAVITELJ!

KEMOFARMACIJA
Veletrgovina za oskrbo zdravstvo, p.o. / 61001 Ljubljana, Cesta na Brdo 100
Telefon: 061 268-145 / Telex: 31334 KEMFAR / Telefax 271-362

PHILIPS

BV 29

INTEGRIS C 2000

DIAGNOST 76 +

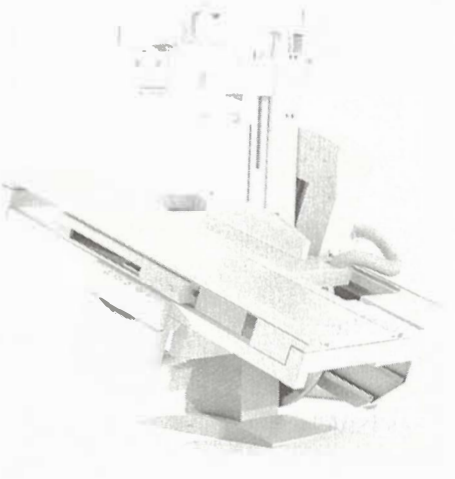

DIAGNOST 93

NOV ČLAN DRUŽINE PHILIPSOVIH TELEDIRIGIRANIH RENTGENSKIH STATIVOV, KI JIH ODLIKUJE KVALITETNA MODULARNA IZDELAVA, VISOKA ZANESLJIVOST, ENOSTAVNA UPORABA IN IZREDNA KVALITETA SLIKE.
APARAT JE MOGOČE OPREMITI S SISTEMOM ZA DIGITALNO RADIOGRAFIJO PREKO SVETLOSTNEGA OJAČEVALNIKA (DSI), KI OLAJŠA DELO UPORABNIKOM, MANJŠA DOZE, NIŽA STROŠKE IN KRAJŠA PREISKAVE.

ZA VSE DODATNE INFORMACIJE SE OBRNITE NA ZASTOPNIKA PHILIPS MEDICAL SYSTEMS V SLOVENIJI:

skupina
avtotehna d.d.

AVTOTEHNA d.d. Ljubljana, Slovenska 54, tel.: (061) 320 767, faks: (061) 322 377

SANOLABOR

za ljudi v belem

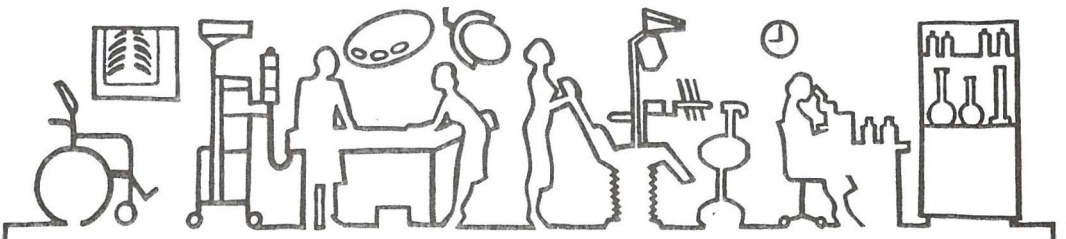

Pri nas dobite vse za rentgen!

▫ KODAK ▫ AGFA GEVAERT ▫ POLAROID ▫ 3M ▫ PHILIPS ▫
▫ GENERAL ELECTRIC ▫ SIEMENS ▫ TOSHIBA ▫ HITACHI ▫
▫ NICHOLAS ▫ BYK GULDEN ▫ MAVIG ▫ CAWO ▫

- rentgenski filmi in kemikalije
- kontrastna sredstva
- rentgenska zaščitna sredstva
- rentgenski aparati, aparati za ultrazvočno diagnostiko, stroji za avtomatsko razvijanje in druga oprema za rentgen

SANOLABOR Cigaletova 9, 61000 LJUBLJANA
☎ 061/1333231 FAX: 061/325 - 395

Your Partner in Radiology

ACTIVA International Sri
Via di Prosecco, 2
34016 Opicina – Trieste
Italy

Tel. 040-212856
Telefax 040-213493
Telex 460250 I

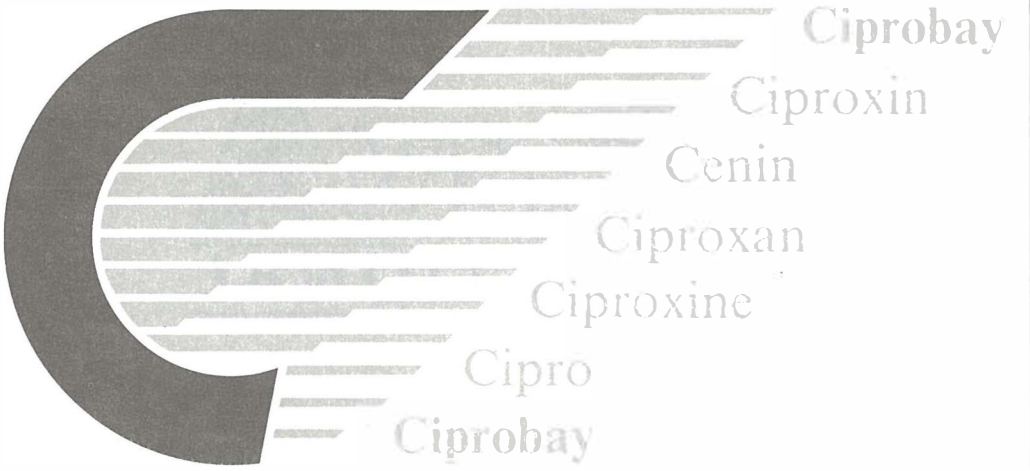

- **Fluorirani kinolon, danes najuspešnejši v svoji skupini**
- **Zdravljenje, ki ustvarja zaupanje (preizkušen pri 100 miljonih bolnikov)**
- **Začetno parenteralno zdravljenje je moč učinkovito nadaljevati peroralno (doma)**

Ciprobay®

ciprofloksacin — Bayerjeva kakovost v 57 državah (tudi v ZDA, Veliki Britaniji, Japonski in Rusiji)

Ciprobay: ciprofloksacin: 10 tablet 250/500 mg; infuzijski raztopini (50 ml, 100 ml) 100/200 mg. **Doziranje:** Peroralni odmerek Ciprobaya je 125—750 mg dvakrat na dan ali 100—400 mg (i.v.) dvakrat na dan. Polovični odmerek je priporočljiv kadar je očistek kreatinina manjši od 20 ml/min. **Kontraindikacije:** preobčutljivost za ciprofloksacin in druge kinolone; otroci in mladi v obdobju rasti, nosečnost, dojenje dokler ni dovolj izkušenj o možnih poškodbah sklepnega hrustanca med rastjo, posebej previdno dajemo zdravilo starejšim bolnikom in pri tistih s poškodbami osrednjega živčevja.

Bayer

Bayer Pharma d.o.o.
Ljubljana

OSKRBA ZDRAVSTVA JE NAŠA NALOGA

SALUS

L J U B L J A N A d. d.

ZAUPAJO NAM NAŠI KUPCI IN DOBAVITELJI, ZNANI PROIZVAJALCI IZ TUJINE PA SO NAM ZAUPALI TUDI ZASTOPSTVA IN KONSIGNACIJE

ZASTOPSTVA IN KONSIGNACIJE:

- BAXTER EXPORT CORPORATION
- BOEHRINGER INGELHEIM
- NOVO NORDISK
- ORTHO DIAGNOSTIC SYSTEMS
- SCHERING & PLOUGH – ESSEX CHEMIE
- HOECHST AG
- HOFFMANN LA ROCHE
- SANDOZ
- COMESA
- EWOPHARMA

SALUS LJUBLJANA d. d. – 61000 LJUBLJANA, MAŠERA SPASIĆEVA 10, TELEFON: N.C. (061) 168-11-44, TELEFAX: (061) 168-10-22

Instructions to authors

The journal **Radiology and Oncology** publishes original scientific papers, professional papers, review articles, case reports and varia (reviews, short communications, professional information, ect.) pertinent to diagnostic and interventional radiology, computerised tomography, magnetic resonance, nuclear medicine, radiotherapy, clinical and experimental oncology, radiobiology, radiophysics and radiation protection.

Submission of manuscript to Editorial Board implies that the paper has not been published or submitted for publication elsewhere: the authors are responsible for all statements in their papers. Accepted articles become the property of the journal and therefore cannot be published elsewhere without written permission from the Editorial Board.

Manuscripts written in English should be sent to the Editorial Office: Radiology and Oncology, Institute of Oncology, Vrazov trg 4, 61000 Ljubljana, Slovenia; Phone: + 386 61 1320 068, Fax: + 386 61 1314 180.

Radiology and Oncology will consider manuscripts prepared according to the Vancouver Agreement (N Engl J Med 1991; 324: 424-8.; BMJ 1991; 302: 6772.).

All articles are subjected to editorial review and review by two independent referees selected by the Editorial Board. Manuscripts which do not comply with the technical requirements stated here will be returned to the authors for correction before the review of the referees. Rejected manuscripts are generally returned to authors, however, the journal cannot be held responsible for their loss. The Editorial Board reserves the right to require from the authors to make appropriate changes in the content as well as grammatical and stylistic corrections when necessary. The expenses of additional editorial work and requests for reprints will be charged to the authors.

General instructions: Type the manuscript double spaced on one side with a 4 cm margin at the top and left hand side of the sheet. Write the paper in grammatically and stylistically correct language. Avoid abbreviations unless previously explained. The technical data should confirm to the SI system. The manuscript, including the references may not exceed 15 typewritten pages, and the number of figures and tables is limited to 4. If appropriate, organise the text so that it includes: Introduction, Material and methods, Results and Discussion. Exceptionally, the results and discussion can be combined in a single section. Start each section on a new page and number these consecutively with Arabic numerals. Authors are encouraged to submit their contributions besides three typewritten copies also on diskettes (5 1/4") in standard ASCII format.

First page:

– name and family name of all authors,

– a brief and specific title avoiding abbreviations and colloquialisms,

– complete address of institution for each author,

– in the abstract of not more than 200 words cover the main factual points of the article, and illustrate them with the most relevant data, so that the reader may quickly obtain a general view of the material.

Introduction is a brief and concise section stating the purpose of the article in relation to other already published papers on the same subjects. Do not present extensive reviews of the literature.

Material and methods should provide enough information to enable experiments to be repeated.

Write the **Results** clearly and concisely and avoid repeating the data in the tables and figures.

Discussion should explain the results, and not simply repeat them, interpret their significance and draw conclusions.

Graphic material (figures and tables). Each item should be sent in triplicate, one of them marked original for publication. Only high–contrast glossy prints will be accepted. Line drawings, graphs and charts should be done professionally in Indian ink. All lettering must be legible after reduction to column size. In photographs mask the identities of patients. Label the figures in pencil on the back indicating author's name, the first few words of the title and figure number: indicate the top with and arrow. Write legend to figures and illustrations on a separate sheet of paper. Omit vertical lines in tables and write the next to tables overhead. Label the tables on their reverse side.

References should be taped in accordance with Vancouver style, double spaced on a separate sheet of paper. Number the references in the order in which they appear in the text and quote their corresponding numbers in the text. Following are some examples of references from articles, books and book chapters:

1. Dent RG, Cole P. *In vitro* maturation of monocytes in squamous carcinoma of the lung. *Br J Cancer* 1981; **43:** 486-95.

2. Chapman S, Nakielny R. *A guide to radiological procedures.* London: Bailliere Tindall, 1986.

3. Evans R, Alexander P. Mechanisms of extracellular killing of nucleated mammalian cells by macrophages. In: Nelson DS ed. *Immunobiology of macrophage.* New York: Academic Press, 1976: 45-74.

For reprint information in North America Contact: International reprint Corporation 968 Admiral Callaghan Lane, # 268 P. O. Box 12004, Vallejo, CA 94590, Tel.: (707) 553 9230, Fax: (707) 552 9524.

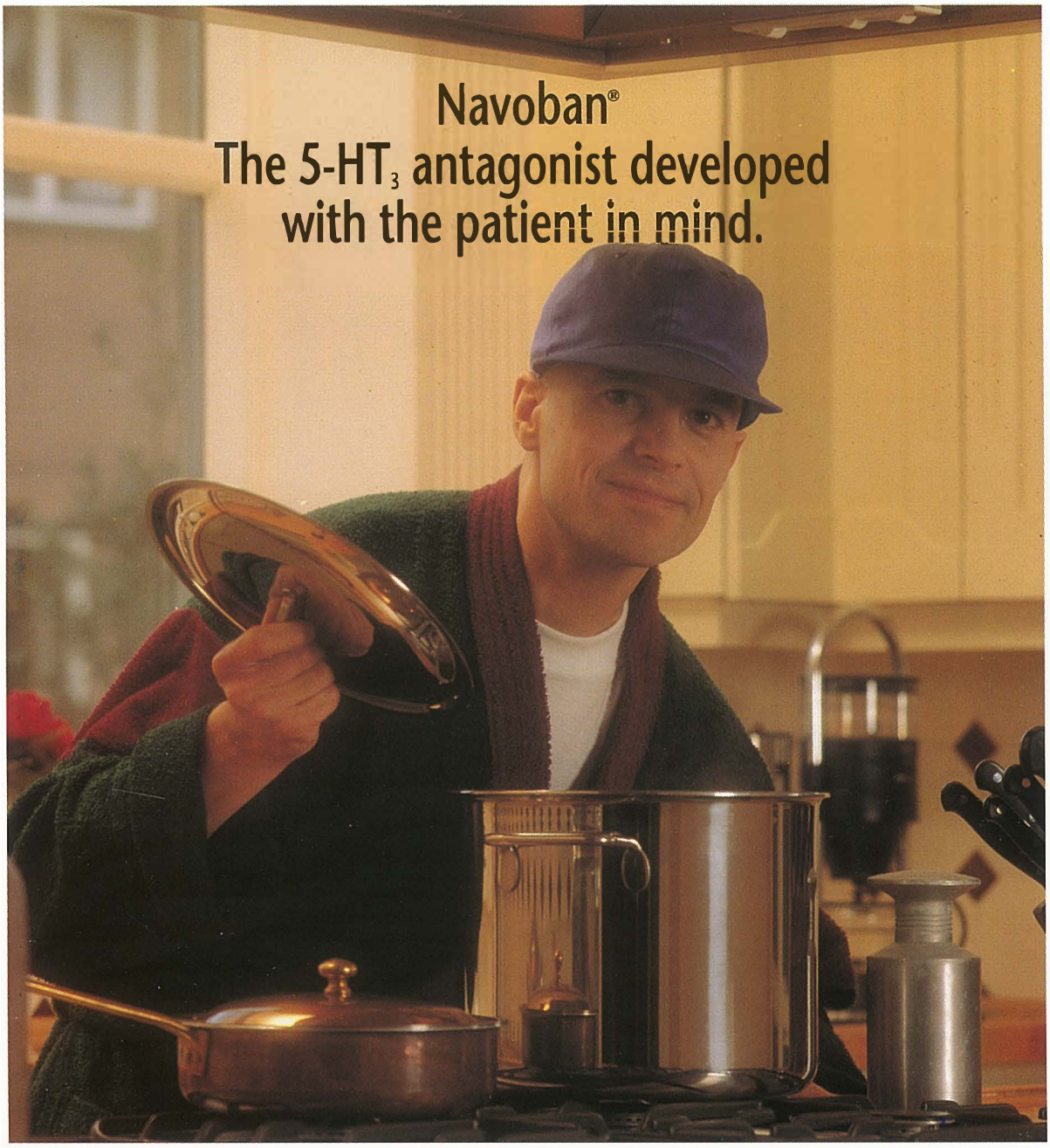

Navoban® (tropisetron)

Always once a day. Always 5 mg.

SANDOZ

Sandoz Pharma Ltd, Pharma Basle Operations, Marketing & Sales, CH 4002 Basle/Switzerland